

27
11/2/86
RB

①

I-24527

PNL-5708
UC-70

⑨

DR-1487-7

Research Report
for Rockwell Hanford Operations

**Laboratory Studies of Shear/
Leach Processing of Zircaloy Clad
Metallic Uranium Reactor Fuel**

J. L. Swanson C. L. Matsuzaki
L. A. Bray S. G. Pitman
H. E. Kjarmo J. H. Haberman
J. L. Ryan

December 1985

Prepared for the U.S. Department of Energy
under Contract DE-AC06-76RLO 1830

Pacific Northwest Laboratory
Operated for the U.S. Department of Energy
by Battelle Memorial Institute



MASTER

PNL-5708

DISCLAIMER

This report was prepared as an account of work sponsored by an agency of the United States Government. Neither the United States Government nor any agency Thereof, nor any of their employees, makes any warranty, express or implied, or assumes any legal liability or responsibility for the accuracy, completeness, or usefulness of any information, apparatus, product, or process disclosed, or represents that its use would not infringe privately owned rights. Reference herein to any specific commercial product, process, or service by trade name, trademark, manufacturer, or otherwise does not necessarily constitute or imply its endorsement, recommendation, or favoring by the United States Government or any agency thereof. The views and opinions of authors expressed herein do not necessarily state or reflect those of the United States Government or any agency thereof.

DISCLAIMER

Portions of this document may be illegible in electronic image products. Images are produced from the best available original document.

PNL--5708

DE86 005100

RESEARCH REPORT FOR
ROCKWELL HANFORD OPERATIONS

LABORATORY STUDIES OF SHEAR/LEACH
PROCESSING OF ZIRCALOY CLAD METALLIC
URANIUM REACTOR FUEL

J. L. Swanson
L. A. Bray
H. E. Kjarmo
J. L. Ryan
C. L. Matsuzaki
S. G. Pitman
J. H. Haberman

December 1985

DISCLAIMER

This report was prepared as an account of work sponsored by an agency of the United States Government. Neither the United States Government nor any agency thereof, nor any of their employees, makes any warranty, express or implied, or assumes any legal liability or responsibility for the accuracy, completeness, or usefulness of any information, apparatus, product, or process disclosed, or represents that its use would not infringe privately owned rights. Reference herein to any specific commercial product, process, or service by trade name, trademark, manufacturer, or otherwise does not necessarily constitute or imply its endorsement, recommendation, or favoring by the United States Government or any agency thereof. The views and opinions of authors expressed herein do not necessarily state or reflect those of the United States Government or any agency thereof.

Prepared for the
U.S. Department of Energy
Under Contract DE-AC06-76RLO 1830

Pacific Northwest Laboratory
Richland, Washington 99352

SUMMARY

This report presents the results of studies addressing several aspects of the shear/leach processing of N-Reactor fuel elements. The safety aspects addressed centered on understanding and explaining the undesirable reactions, "fires", observed in a few instances during earlier processing of such fuel at the Nuclear Fuels Services (NFS) plant at West Valley, New York.

Consideration of the dissolver fires that occurred at NFS leads to the conclusion that they resulted from rapid reactions with uranium metal, rather than with zirconium metal or with sensitized weld beads. The fires observed at NFS during hulls handling operations may have involved sensitized weld beads as suggested by earlier investigators, but current results suggest that these fires also could have been caused by reactions involving uranium metal.

Very little pyrophoric activity was observed in leached cladding hulls, indicating a very low probability for safety problems resulting from the U-Zr intermetallic zone in N-Reactor fuel. Consideration of the potential role of hydrides in the fires observed at NFS indicates that they were also not important factors.

Consideration was also given to protective atmospheres to be used during shearing to prevent excessive reaction during that operation. A water deluge during shearing will likely provide adequate safety while meshing well with other process considerations.

Studies on the dissolution of metallic uranium in nitric acid show an initial slower reaction followed by a faster reaction that proceeds at a sustained rate for a prolonged period of time. At solution concentrations typical of those encountered in practical uranium dissolver conditions, this sustained rate is governed by an equation such as:

$$\text{Dissolution rate} = K (\text{surface area}) ([\text{HNO}_3] + 2[\text{U}])^{2.6}.$$

Little difference was found in dissolution rates of as-fabricated and of irradiated fuel.

The transuranic element content of leached cladding hulls was found to be ~400 nCi/g. This is too high to allow disposal as low-level waste.

CONTENTS

| | |
|--|------|
| SUMMARY..... | iii |
| 1.0 INTRODUCTION..... | 1.1 |
| 1.1 REFERENCES FOR SECTION 1.0..... | 1.2 |
| 2.0 SUMMARY AND CONCLUSIONS..... | 2.1 |
| 2.1 REFERENCES FOR SECTION 2.0..... | 2.3 |
| 3.0 DISSOLUTION RATE OF URANIUM METAL IN NITRIC ACID..... | 3.1 |
| 3.1 DISSOLUTION RATE PROCEDURES..... | 3.1 |
| 3.2 DISSOLUTION RATE RESULTS AND DISCUSSION..... | 3.4 |
| 3.2.1 Effect of Fuel Irradiation Level on Dissolution Rate..... | 3.5 |
| 3.2.2 Foaming During Dissolution..... | 3.11 |
| 3.2.3 Effect of Nitric Acid Concentration on Uranium Dissolution Rate..... | 3.12 |
| 3.2.4 Effect of Uranyl Nitrate Concentration on Uranium Dissolution Rate..... | 3.14 |
| 3.2.5 Effect of Temperature on Uranium Dissolution Rate..... | 3.17 |
| 3.2.6 Effect of Nitrous Acid Concentration..... | 3.18 |
| 3.2.7 Surface Roughening During Dissolution..... | 3.23 |
| 3.2.8 Complete Dissolution Experiments..... | 3.25 |
| 3.3 REFERENCES FOR SECTION 3.0..... | 3.33 |
| 4.0 TRANSURANIC ELEMENT CONTENT OF LEACHED FUEL HULLS..... | 4.1 |
| 5.0 RESIDUAL UNDISSOLVED SOLIDS..... | 5.1 |
| 6.0 SHEAR COVER-GAS EVALUATION..... | 6.1 |
| 6.1 HIGHLIGHTS OF THE LITERATURE REVIEW..... | 6.3 |
| 6.2 BIBLIOGRAPHY FOR SECTION 6.0..... | 6.5 |
| 7.0 EVALUATION OF POTENTIAL FOR RUNAWAY REACTIONS DURING DISSOLUTION OF SHEARED N-REACTOR FUEL..... | 7.2 |

| | | |
|------|--|------|
| 7.1 | POTENTIAL U METAL REACTIONS AND REACTIONS ENERGETICS..... | 7.1 |
| 7.2 | U AND Zr METAL REACTION RATES..... | 7.4 |
| 7.3 | NFS DISSOLVER ENERGY BALANCE..... | 7.8 |
| 7.4 | POSSIBLE CONTRIBUTIONS OF IRRADIATION LEVEL TO RUNAWAY DISSOLVER REACTIONS..... | 7.10 |
| 7.5 | REFERENCES FOR SECTION 7.0..... | 7.13 |
| 8.0 | SENSITIZATION AND PASSIVATION OF WELD BEADS..... | 8.1 |
| 8.1 | WELD BEAD CHEMICAL STUDIES..... | 8.1 |
| 8.2 | WELD BEAD METALLOGRAPHY STUDY..... | 8.5 |
| 8.3 | REFERENCES FOR SECTION 8.0..... | 8.10 |
| 9.0 | STUDIES OF U/Zr INTERMETALLIC ZONE..... | 9.1 |
| 9.1 | METALLURGICAL STUDIES OF U/Zr INTERMETALLIC ZONE..... | 9.1 |
| 9.2 | PYROPHORICITY OF U/Zr INTERMETALLIC ZONE..... | 9.8 |
| 9.3 | REFERENCES FOR SECTION 9.0..... | 9.11 |
| 10.0 | PYROPHORICITY OF METALLIC URANIUM..... | 10.1 |
| 11.0 | URANIUM AND ZIRCONIUM HYDRIDE STUDIES..... | 11.1 |
| 11.1 | HYDRIDING OF URANIUM AND ZIRCONIUM..... | 11.1 |
| 11.2 | METALLOGRAPHIC STUDY OF HYDRIDES IN RUPTURED FUEL..... | 11.2 |
| 11.3 | REFERENCES FOR SECTION 11.0..... | 11.9 |
| 12.0 | ACKNOWLEDGMENTS..... | 12.1 |

FIGURES

| | | |
|------|--|------|
| 3.1 | Initial Dissolution Rates of Polished Specimens of Irradiated and Unirradiated Fuel..... | 3.6 |
| 3.2 | Dissolution Rates of As-Cut specimens of Irradiated and Unirradiated Fuel in 3.0 <u>M</u> HNO ₃ | 3.7 |
| 3.3 | Dissolution Rates of Samples from Three Unirradiated Fuel Elements in 7.8 <u>M</u> HNO ₃ | 3.8 |
| 3.4 | Dissolution Rates of Irradiated and Unirradiated Uranium in Complete Dissolution Experiments..... | 3.9 |
| 3.5 | Foam Volumes During Dissolution..... | 3.11 |
| 3.6 | Uranium Dissolution at Different HNO ₃ Concentrations..... | 3.13 |
| 3.7 | Dependence of Sustained Dissolution Rate on HNO ₃ Concentration and Activity..... | 3.14 |
| 3.8 | Dissolution Rate Data in Uranyl Nitrate + HNO ₃ Solutions..... | 3.16 |
| 3.9 | Dependence of Uranium Dissolution Rate on Nitrate Concentration..... | 3.17 |
| 3.10 | Uranium Dissolution at Different Temperatures..... | 3.18 |
| 3.11 | Effect of Temperature on Uranium Dissolution Rate..... | 3.19 |
| 3.12 | Effect of Hydrazine Addition (to Destroy Nitrous Acid) on Uranium Dissolution Rate..... | 3.20 |
| 3.13 | Nitrous Acid and Uranium Concentrations During Dissolution at Different Acidities..... | 3.21 |
| 3.14 | Nitrous Acid and Uranium Concentrations During Dissolution at Different Temperatures..... | 3.22 |
| 3.15 | Uranium Dissolution Rates in Successive Leachings of One Specimen..... | 3.23 |
| 3.16 | Dissolution Rates of As-Cut and of Partially Dissolved Uranium Specimens..... | 3.25 |
| 3.17 | Complete Dissolution Experiment with Two Uranium Sections and 9.5 <u>M</u> HNO ₃ | 3.26 |
| 3.18 | Complete Dissolution Experiment with Two Uranium Sections and 8.1 <u>M</u> HNO ₃ | 3.28 |
| 3.19 | Complete Dissolution Experiment with Five Uranium Sections and 8.1 <u>M</u> HNO ₃ | 3.29 |

| | | |
|------|---|------|
| 3.20 | Complete Dissolution of Thicker Uranium Section and 9.5 M HNO ₃ | 3.30 |
| 3.21 | Total Nitrate Correlation of Incremental Dissolution Rate Data from Complete Dissolution Runs..... | 3.31 |
| 3.22 | Early Complete Dissolution Experiment with Updraft Condenser.. | 3.32 |
| 8.1 | Optical Micrographs of End Cap Weld Sections..... | 8.7 |
| 8.2 | SEM Micrographs of Reaction Layers and EDS Analysis Locations.. | 8.9 |
| 9.1 | Zirconium-Uranium Constitutional Diagram..... | 9.2 |
| 9.2 | Specimen Locations from As-Fabricated and Spent Fuel Rods..... | 9.3 |
| 9.3 | Representative Optical Micrographs of Fuel Sections..... | 9.5 |
| 9.4 | Representative SEM Micrographs of the As-Fabricated Fuel Section..... | 9.6 |
| 9.5 | Uranium/Zircaloy Composition Profile Through Diffusion Zone.... | 9.7 |
| 11.1 | Side View of Ruptured Inner Element..... | 11.3 |
| 11.2 | Micrographs of Fuel Element Adjacent to Failed Cladding..... | 11.4 |
| 11.3 | Cross Section of Cladding in Non-Failed Area Showing Typical Hydride Distribution..... | 11.5 |
| 11.4 | Micrographs of Outer Cladding at Cladding Failure..... | 11.6 |
| 11.5 | Cross Section of Outer Cladding Near Cladding Failure..... | 11.8 |

TABLES

| | | |
|-----|--|------|
| 3.1 | Other Elements in N-Reactor Uranium Fuel..... | 3.3 |
| 3.2 | Dissolution Rate Data in High U Solutions..... | 3.15 |
| 4.1 | Alpha- and Gamma-Emitting Radionuclides in N-Reactor Fuel Cladding Hulls..... | 4.3 |
| 8.1 | Comparison of Rinse Solutions in Reducing Pyrophoricity of Sensitized Weld Beads..... | 8.4 |
| 8.2 | Comparison of Pyrophoric Nature of Various Unrinsed Weld Bead Samples..... | 8.6 |
| 8.3 | Pyrophoricity of Irradiated Weld Beads after Nitric Acid Leaching..... | 8.8 |
| 8.4 | Elemental Concentration from SEM/EDS Analysis..... | 8.10 |
| 9.1 | Diffusion Zone Thickness Measurements..... | 9.4 |
| 9.2 | Ratio of Diffusion Zone to Total Uranium..... | 9.8 |
| 9.3 | Results on the Pyrophoric Nature of the U/Zr Intermetallic Zone of Leached Hulls..... | 9.10 |

1.0 INTRODUCTION

Fuel irradiated in the Hanford N-Reactor contains a metallic uranium core that is clad in Zircaloy-2. Current processing of this fuel employs chemical decladding (the Zirflex process) followed by nitric acid dissolution of the exposed core. The decladding process produces a large volume waste stream that may also be difficult to process to a waste form suitable for final disposal. Thus, a considerable incentive could exist for processing this fuel by a shear/leach process, in which the fuel is mechanically segmented, and the core then dissolved by nitric acid so that the cladding is left as a metallic, readily disposable waste form having a low volume.

Shear/leach processing of N-Reactor fuel is currently planned in the Process Facility Modifications (PFM), which is being designed for addition to the PUREX facility at Hanford. This facility was initially planned for the processing of Fast Flux Test Facility (FFTF) fuel, which has a mixed UO_2 - PuO_2 core and stainless steel cladding.

Some N-Reactor fuel was processed by a shear/leach technique from 1966 to 1971 at the Nuclear Fuels Services plant in West Valley, New York. During this processing there were several observations of undesirable reactions, "fires", which have been described by Schulz (1972). Such reactions, which occurred in only a small fraction of the batches processed, were markedly reduced by empirically-derived modifications/additions to operating procedures and conditions. A major objective of this research project was to develop understanding of the causes of these reactions and of the mechanisms by which the modifications/additions were successful in eliminating their occurrence.

Another objective of this project was to obtain data needed to better define process operating conditions in two areas. One area was the dissolution rate of uranium, where data were needed to accurately predict dissolver time cycles and off-gas generation rates, and the other area was the transuranic element concentration of the leached cladding hulls, where data were needed to define what type of disposal would be required for this waste stream.

1.1 REFERENCES FOR SECTION 1.0

Schulz, W. W. 1972. Shear-Leach Processing of N-Reactor Fuel -- Cladding Fires. ARH-2351, Atlantic Richfield Hanford Company, Richland, Washington.

2.0 SUMMARY AND CONCLUSIONS

This report presents the results of studies addressing several safety aspects of the shear/leach processing of N-Reactor fuel elements and also several process operating aspects. The safety aspects centered on understanding and explaining the undesirable reactions, "fires", observed in a few instances during earlier processing of such fuel at the Nuclear Fuels Services (NFS) plant at West Valley, New York, as described by Schulz (1972).

Detailed consideration of the mechanisms that might have led to the dissolver fires at NFS leads to the conclusion that they resulted from rapid reactions with uranium metal, rather than with zirconium metal or with sensitized (Zr-Be) weld beads. From this consideration, it appears that key factors in assuring the safety of plant-scale dissolution of uranium from sheared N-Reactor fuel include controlling uranium particle size and minimizing exposure of metallic uranium to reactive vapors, which includes water vapor. Other important factors include those important to uranium dissolution rate, principally nitrate concentration, and the heat removal capacity of the dissolution equipment.

The fires observed at NFS during hulls handling operations may have involved sensitized weld beads as proposed by Schulz, but our studies suggest that these hulls handling fires also could have been caused instead by reactions involving uranium metal. Our tests with sensitized Zr-Be weld beads failed to show as high a degree of pyrophoricity as was observed earlier by Schulz (1972). The reason for this difference is not known. Passivation of sensitized (Zr-Be) weld beads by rinsing with water or sodium hydroxide solution appears to simply involve removal of nitrate ion from the residual Zr matrix, rather than an actual passivation of a reactive Zr surface.

Very little pyrophoric activity was observed in leached cladding hulls, indicating a very low probability for safety problems resulting from the U-Zr intermetallic zone in N-Reactor fuel. This was true with irradiated fuel as well as as-fabricated fuel, and with ruptured as well as intact irradiated fuel.

Consideration of the potential role of hydrides in the fires observed at NFS indicates that they were not important factors. Zirconium hydride is present in the cladding of all irradiated fuels, but it is dispersed and not likely to contribute significantly to pyrophoricity. Uranium hydride is formed by reaction with water in ruptured elements. Most of this hydride is converted to uranium oxide by further reaction with water, but some unreacted hydride may be present in localized areas inside the failed elements. Both the unreacted hydride and the finely divided uranium oxide formed by further reaction will react rapidly with HNO_3 , and could thus contribute to runaway reactions if they are present in sufficient quantity.

Consideration was also given to protective atmospheres to be used during shearing to prevent excessive amounts of reaction during that operation. Different atmospheres provide varying degrees of safety, the problem lies in defining how safe is safe enough. A water deluge during shearing will likely provide adequate safety while working well with other process considerations.

Studies on the dissolution of metallic uranium in nitric acid show an initial slower reaction followed by a faster reaction that proceeds at a sustained rate for a prolonged period of time. This sustained rate prevails after penetrations of ~ 0.005 cm and thus is the rate of primary interest in complete dissolution predictions. At solution concentrations typical of those encountered in practical uranium dissolver conditions, this sustained rate is governed by an equation such as:

$$\text{Dissolution rate} = K (\text{surface area}) ([\text{HNO}_3] + 2[\text{U}])^{2.6}.$$

With the units of mg/h for the rate, of cm^2 for the area, and of molarity for the concentrations, the rate constant was found to be approximately 4.6 at 103°C based on the calculated geometric area. A more fundamental treatment of data obtained at low uranium concentrations indicates that uranium dissolution rate is proportional to the first power of the free nitrate ion (or hydrogen ion) activity. The effect of nitrous acid on dissolution rate was not quantified; slower reactions were observed in experiments where hydrazine was added to eliminate or minimize nitrous acid, but there appeared to be little variation of dissolution rate when nitrous acid was present at different macro concentrations.

Little practical difference was found in dissolution rates of different batches of as-fabricated N-Reactor fuel or between as-fabricated and irradiated fuel, on a surface area basis. However, irradiated fuel may break into smaller pieces during shearing than does unirradiated fuel; the higher resultant surface area would give higher initial reaction rates.

The transuranic element content of HNO₃-leached cladding hulls will be too high to allow disposal of these wastes as low-level waste. A content of 420 nCi/g was found after leach conditions simulating those planned for plant operation; an additional, more vigorous, HNO₃ leach reduced this amount, but only to 280 nCi/g.

Near the end of HNO₃ leaching of N-Reactor fuel element sections, black solids flake off the cladding at what had been the U/Zr interface. These solids appear to be a U/Zr intermetallic mixture, but exhibited little, if any, pyrophoric activity. The quantity of solids is low ($\sim 1 \times 10^{-4}$ g/g U), but provisions for dealing with such material should be included in plant design.

2.1 REFERENCES FOR SECTION 2.0

Schulz, W. W. 1972. Shear-Leach Processing of N-Reactor Fuel -- Cladding Fires. ARH-2351, Atlantic Richfield Hanford Company, Richland, Washington.

3.0 DISSOLUTION RATE OF URANIUM METAL IN NITRIC ACID

Although there is an abundance of practical experience in dissolving uranium metal in nitric acid, a literature survey performed by A. L. Pajunen, et al. (1984) failed to provide sufficient data for adequate modeling of dissolver time cycles and off-gas generation rates. Plant data were also insufficient for several reasons. With aluminum clad reactor fuels the common practice has been to leave a heel of undissolved metal behind; thus the reacting uranium surface area is unknown. When N-Reactor fuel is processed by decladding in ammonium fluoride solution, followed by HNO_3 dissolution of the uranium, the reacting uranium surface area is unknown because of uncertainties in the extent of cladding removal. Also, in this case, the dissolvent contains variable concentrations of fluoride carried over from the decladding operation plus aluminum nitrate added to minimize fluoride-induced corrosion of the dissolver; thus the dissolvent composition is not the same as will be used in shear/leach processing of N-Reactor fuel. For these reasons, uranium dissolution rate data were measured as part of this project.

3.1 DISSOLUTION RATE PROCEDURES

Most of the present dissolution rate experiments were performed in vessels fitted with a simple updraft condenser, and with no air sparge through the solution or air sweep through the vapor space. However, one set of complete dissolution experiments was performed with a downdraft condenser and both air sweep and sparge; these conditions are closer to those planned for use in the plant, and they lead to a lower consumption of HNO_3 . All of the experiments employed magnetic stirring to keep the solution well mixed.

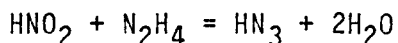
In nearly all of the dissolution rate experiments with unirradiated uranium, the course of dissolution was followed by liquid scintillation counting of solution samples taken as a function of time. The specific activity was determined for each experiment from counting of the final solution coupled with solution volume and specimen weight loss measurements. The measured activities evidently included beta activity from daughter isotopes as well as alpha activity from the uranium itself because measured values were higher than those calculated for alpha activity alone. The

specific activity varied somewhat from one fuel element to another, but was quite constant for sections cut from a given fuel element. Dissolution rate results obtained in this manner were verified in a few experiments by measuring uranium concentrations directly by pulsed laser fluorimetry. The scintillation counting method was generally used because of its simplicity.

Irradiated uranium dissolution rate experiments were generally followed by pulsed laser fluorimetry analyses for uranium and by gamma counting the fission product ^{137}Cs content. The direct uranium analyses were generally more reliable, as they did not involve several uncertainties attendant in the ^{137}Cs method (e.g., final volume, weight loss, and ^{137}Cs concentration measurements).

Nitric acid analyses were done by titration after oxalate complexing of uranium so that uranium hydrolysis would not interfere. The samples from the first complete dissolution experiment (Section 3.2.8) were analyzed using manual buret control and end-point determination. Samples from the series of four complete dissolution experiments done with a downdraft condenser were analyzed using a modified procedure with an automatic titrator (Ryan et al. 1985).

Because of the instability of nitrous acid in nitric acid solutions, an indirect method was used to determine HNO_2 concentrations in dissolution rate experiments. Solution samples were rapidly added to solutions containing a substantial excess of hydrazine; the HNO_2 in the samples was thus converted essentially quantitatively to hydrazoic acid:



The hydrazoic acid thus formed was stable for at least several days, during which time its concentration was determined colorimetrically as the ferric azide complex (Dukes and Wallace 1961).

The quantities of other elements present in the uranium used in N-Reactor fuel is given in Table 3.1. Most of the dissolution rate experiments used half-rings of portions cut from as-fabricated N-Reactor fuel elements, although some of the early work was done with mounted and polished specimens

TABLE 3.1 Other Elements in N-Reactor Uranium Fuel

| <u>Element</u> | <u>Concentration, ppm</u> |
|----------------|---------------------------|
| Aluminum | 650 - 945 |
| Carbon | 330 - 735 |
| Iron | 280 - 440 |
| Silicon | 60 - 130 |
| Beryllium | < 10 |
| Boron | < 0.25 |
| Cadmium | < 0.25 |
| Chromium | < 65 |
| Copper | < 75 |
| Hydrogen | < 2 |
| Manganese | < 25 |
| Magnesium | < 25 |
| Nickel | < 100 |
| Nitrogen | < 75 |
| Zirconium | < 65 |

and some of the later work involved whole rings. These half-rings contained two types of uranium surfaces, "end grain" surfaces on the faces of the rings and "side grain" surfaces where the rings were cut in half. In a typical 1.3-cm thick half-ring cut from an inner element, the end grain uranium surfaces amounted to ~73% of the total uranium surface area. Little difference was noted between the dissolution rates of these two types of surface. For example, in one case of extensive dissolution the penetration on the side grain surfaces was measured as being ~80% of that on the end grain surfaces.

Sections cut from several fuel elements were used in this study. Many of the figures to be shown later contain letters identifying the batch of fuel sections used in the comparison shown. CF and CJ sections were cut from different inner elements and CL sections were from an outer element.

Grain size is known to have a pronounced effect on uranium dissolution rate in HNO_3 (Bement and Swanson 1957). One of the as-fabricated specimens used in this work was determined by UNC Nuclear Industries personnel to have an average grain diameter of 0.17 mm. Attempts to measure grain size on mounted and polished specimens were not very fruitful; no sizes could be precisely determined, but it did appear that the grain sizes of irradiated ($12\% \text{}^{240}\text{Pu}$) and unirradiated specimens were roughly comparable.

Except for the sections cut from ruptured fuel elements, no evidence of crumbling or cracking was observed in any of the irradiated fuel element sections.

3.2 DISSOLUTION RATE RESULTS AND DISCUSSION

The effects of the following factors on the dissolution rate of N-Reactor fuel uranium in HNO_3 were investigated: irradiation level, nitric acid concentration, uranyl nitrate concentration, nitrous acid concentration, temperature, and surface roughening during dissolution. Data were also obtained on the extent of foaming during dissolution and on the times required for complete dissolution of specimens of different sizes.

Little if any effect of irradiation on dissolution rate was observed. A low concentration of nitrous acid is required to attain rapid dissolution, but higher concentrations give little additional rate increase; these results suggest a finite, but low, dependence of dissolution rate on nitrous acid concentration. Nitric acid concentration, on the other hand, has a strong effect on uranium dissolution rate; the rate is proportional to the second power of HNO_3 concentration from 3 to 8 M HNO_3 , at least. Application of HNO_3 activity coefficients to these data indicates that uranium dissolution rate is proportional to the first power of nitrate (or hydrogen) ion activity. The effect of uranyl nitrate concentration on dissolution rate appears to be one of contributing to the total nitrate concentration. In nitric acid/uranyl nitrate mixtures typical of those encountered in practical uranium dissolver conditions, uranium dissolution rate is proportional to the total nitrate concentration raised to the 2.6 power.

These results indicate that the basic mechanism of uranium dissolution in nitric acid can be expressed by an equation such as:

$$\text{Dissolution Rate} = K (\text{surface area}) (\text{NO}_3^-)_f (\text{HNO}_2)^x$$

where $(\text{NO}_3^-)_f$ is the free nitrate ion activity, (HNO_2) is the nitrous acid activity, and x is a small number. On a less basic level, the data obtained at nitric acid and uranyl nitrate concentrations typical of those obtained at practical uranium dissolver conditions are correlated quite well at a given temperature by the equation:

$$\text{Dissolution Rate} = K (\text{surface area}) ([\text{HNO}_3] + 2 [\text{U}])^{2.6}$$

where $[\text{HNO}_3]$ and $[\text{U}]$ are the molar stoichiometric concentrations. The value of K in this equation is ~ 4.6 at 103°C , with dissolution rate expressed as $\text{mg}/\text{cm}^2\text{-h}$ and using the initial geometric surface area.

Comparison of initial and sustained dissolution rates indicates that surface roughening during dissolution increases the surface area by a factor of approximately three over the geometric surface area. This degree of roughening appears to remain essentially constant after a penetration of ~ 0.005 cm has occurred.

Uranium dissolution rates increase with temperature up to a temperature a few degrees below the boiling point, and then decrease slightly. This effect may be due to a marked decrease in nitrous acid concentration near the boiling point. The activation energy for uranium dissolution in 7.8 M HNO_3 at 71 to 105°C was found to be ~ 11 kcal.

3.2.1 Effect of Fuel Irradiation Level on Dissolution Rate

The initial portions of the uranium dissolution rate studies of this project employed mounted and polished specimens so that the surface areas would be accurately known. This turned out to be an unwise decision, but that fact was not appreciated until after several experiments had been performed with such specimens.

Among these experiments were several aimed at determining the effect (if any) of irradiation on the rate at which uranium dissolves in HNO_3 . Qualitative statements have been made (Schulz 1972) to the effect that irradiated metal dissolves more rapidly than unirradiated, but no data were presented. In our studies we found little effect of irradiation on dissolution rate. If there was an effect, it was to decrease, rather than increase, the dissolution rate.

Figure 3.1 contains the results of experiments in which mounted and polished specimens from four different fuel elements (two irradiated and two unirradiated) were exposed to boiling 3.0 M HNO_3 and the initial dissolution rates were measured. These results indicate that the dissolution rate of uranium irradiated to an exposure giving 6% of the Pu as ^{240}Pu is the same as

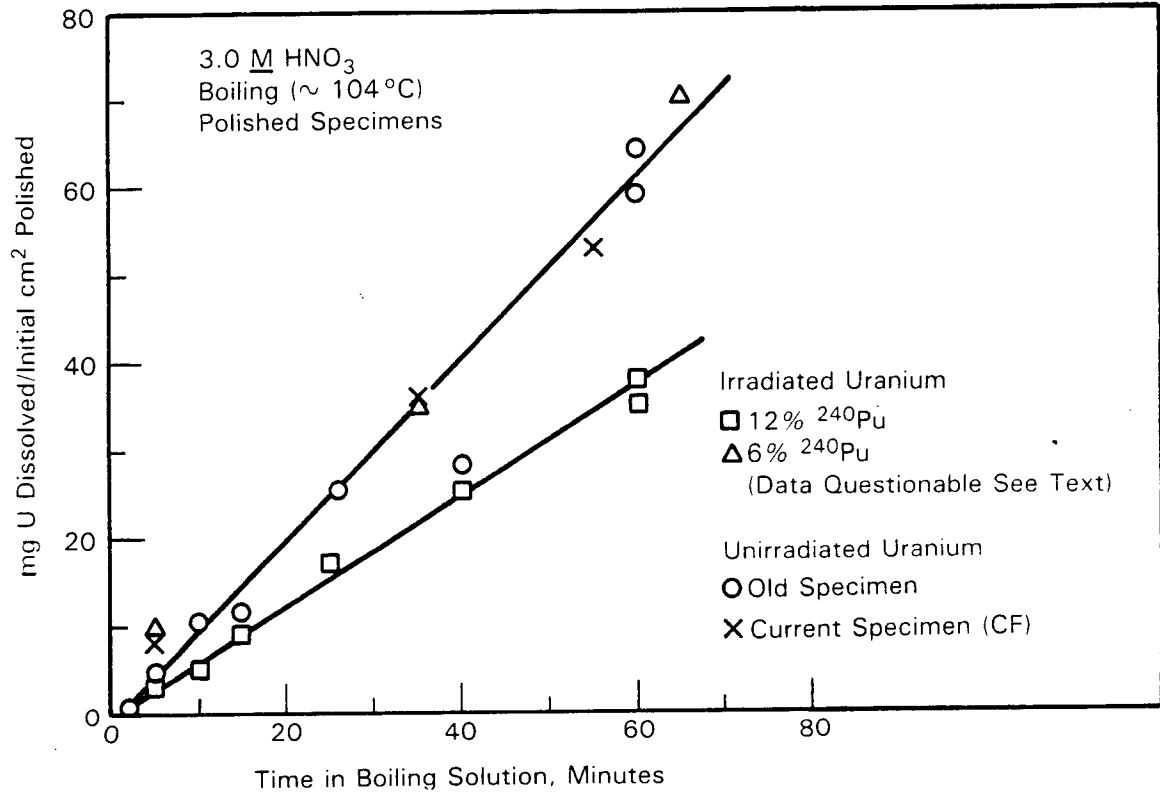


FIGURE 3.1. Initial Dissolution Rates of Polished Specimens of Irradiated and Unirradiated Fuel

that of unirradiated uranium, while uranium irradiated to a higher exposure giving 12% of the Pu as ²⁴⁰Pu dissolves about 80% as rapidly. However, this comparison is of questionable validity because of uncertainties in the actual reacting areas resulting from cracks in the plastic material in which the specimens were mounted. For example, a crack was observed in the mount holding the 6% ²⁴⁰Pu specimen shortly after these data were obtained; the crack was such that the ends of the cut section were also exposed to the solution, along with the polished surface. If this crack occurred when the specimen was first introduced into the solution, the dissolution rate of the 6% ²⁴⁰Pu specimen was actually only about 50% of that indicated by the data of Figure 3.1 (because the surface area of the ends was approximately equal to the area of the polished surface). This possibility is substantiated by data obtained later with unmounted specimens. This uncertainty is one reason why further studies were done with as-cut specimens rather than mounted and polished specimens.

A dissolution rate comparison of as-cut specimens from different fuel elements in boiling 3.0 M HNO₃ is shown in Figure 3.2. In this case, the 6% ²⁴⁰Pu irradiated uranium specimen dissolved only about half as fast as did two of the unirradiated specimens; this suggests that the crack in the mount discussed in the preceding paragraph did indeed occur early in the experiment, to give an erroneously high apparent dissolution rate. A specimen from a third unirradiated element dissolved initially at about the same rate as the irradiated element but then dissolved more rapidly.

A comparison of the dissolution rates of sections from the three unirradiated elements at a higher (7.8 M) HNO₃ concentration is shown in Figure 3.3. These sustained rates differ by only 16% between the fastest and the slowest, showing that very little difference exists at this higher HNO₃ concentration. No irradiated uranium specimen was available to include in this comparison.

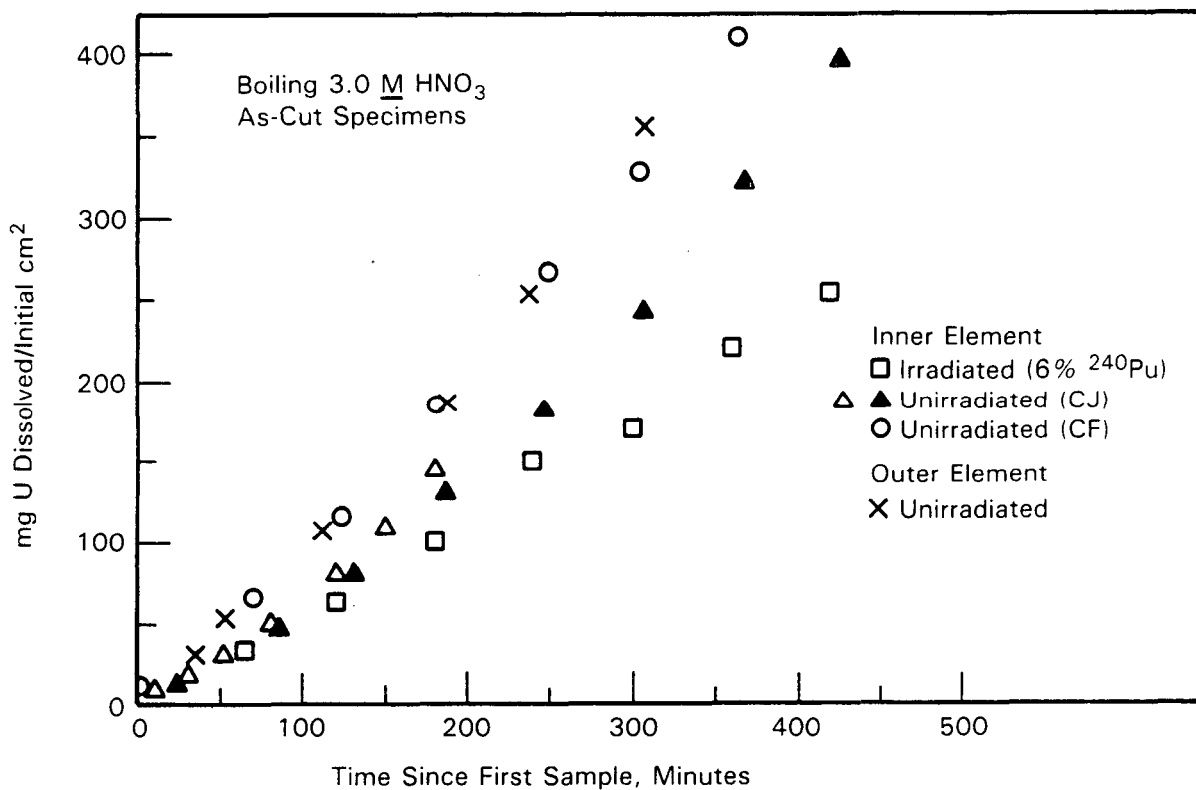


FIGURE 3.2. Dissolution Rates of As-Cut specimens of Irradiated and Unirradiated Fuel in 3.0 M HNO₃

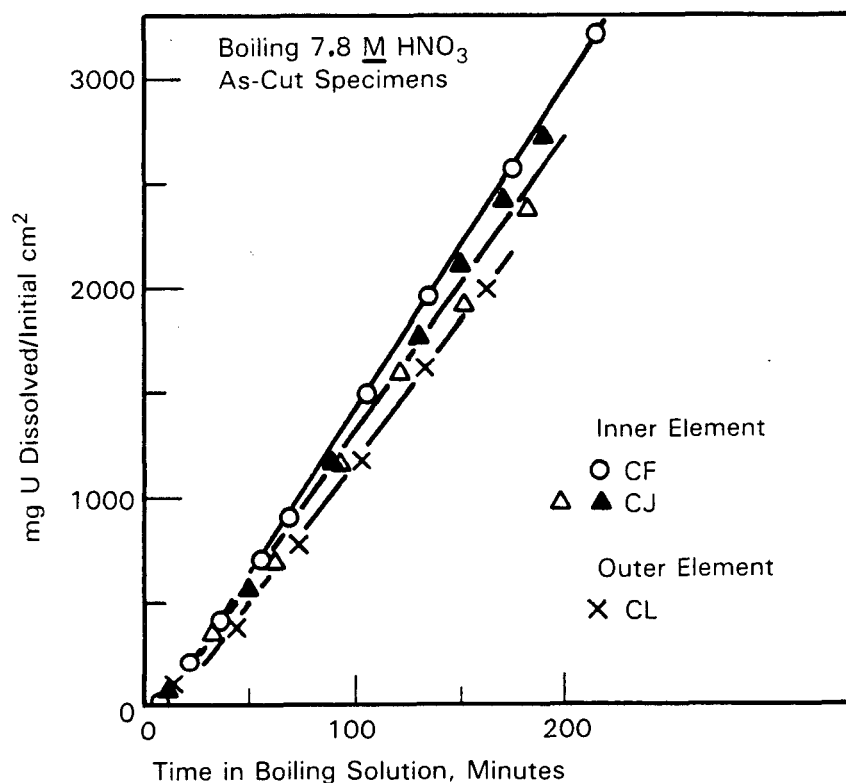


FIGURE 3.3. Dissolution Rates of Samples from Three Unirradiated Fuel Elements in 7.8 M HNO₃

Another comparison of the dissolution rates of irradiated and unirradiated fuel specimens was obtained during complete dissolutions performed preparatory to measuring the radionuclide content of spent fuel cladding hulls (Section 4.0). The procedure used in these runs was to start the dissolutions in 5.5 M HNO₃ and then periodically add increments of 15.7 M HNO₃ to supply the needed HNO₃. The initial charge of 5.5 M HNO₃ corresponded to 1.05 mole HNO₃/mole U and the total HNO₃ used amounted to 6.46 mole HNO₃/mole U. The total volume of solution used would have given a uranium concentration of 1.87 M had the volumes been additive and if no evaporative losses occurred. In a similar experiment done before the hot cell work was begun (see Figure 3.22), a HNO₃ consumption of 5.1 mole/mole U dissolved was measured; thus, the terminal HNO₃ concentration in the experiments of Figure 3.4 is calculated to have been ~2.5 M had the volumes been additive and if no evaporative losses occurred.

Figure 3.4 presents a comparison of the data collected in these two experiments, one using irradiated uranium and the other using unirradiated uranium. Values of $[(\text{mole HNO}_3 \text{ added})/(\text{L added})]$ were calculated from the known volumes and concentrations added. Values of (g U dissolved) were calculated from the uranium concentrations (measured by pulsed laser fluorimetry), and the total volume of solution that had been added at the time the samples were taken.

Each of these experiments employed two half-rings of an inner element and two half-rings of an outer element, giving an initial surface area of $\sim 45 \text{ cm}^2$ for the nominally half-inch thick rings used. The rates of dissolution of irradiated and unirradiated uranium are seen (Figure 3.4) to have been very comparable in these experiments. During the period of maximum rate, both the temperature and the added HNO_3 concentration were slightly higher in the

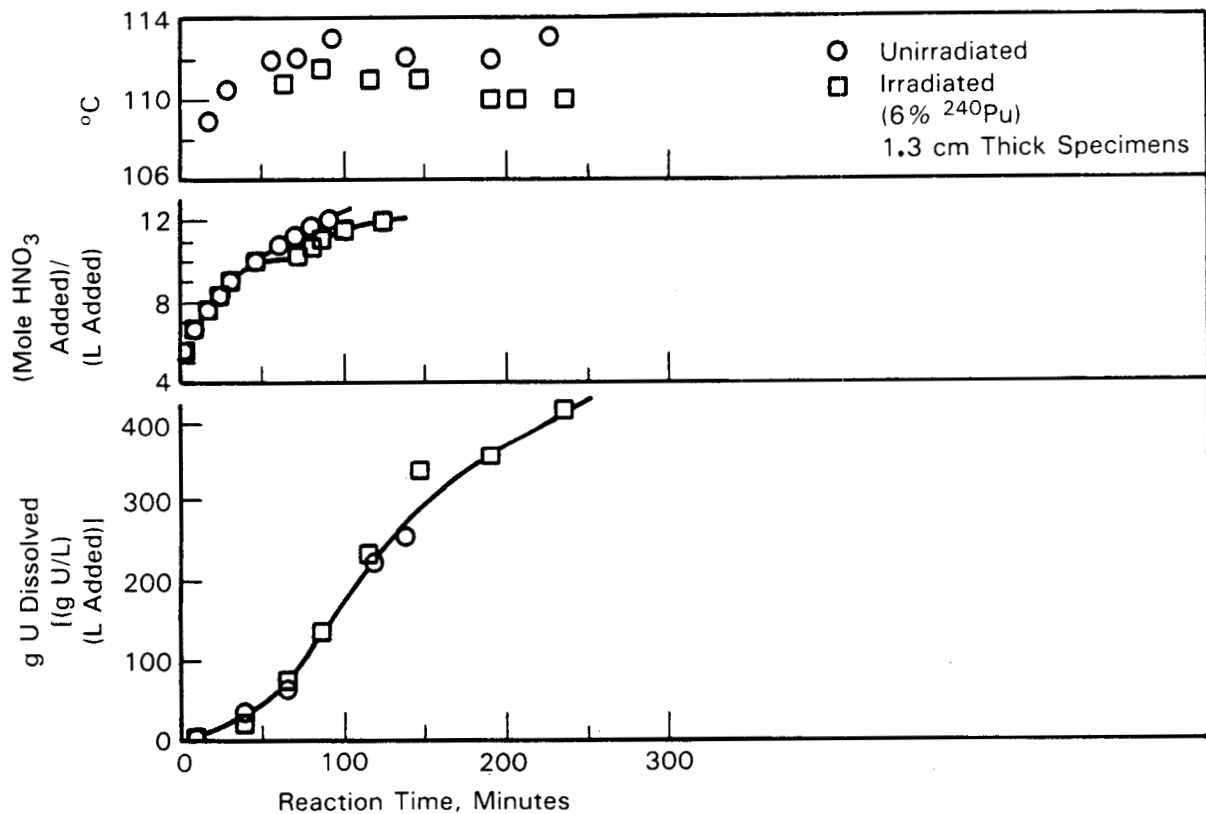


FIGURE 3.4. Dissolution Rates of Irradiated and Unirradiated Uranium in Complete Dissolution Experiments

unirradiated uranium experiment. Higher HNO_3 concentration results in more rapid dissolution, but it is not certain what effect the higher temperature would have had in the slightly sub-boiling regime in which these rate data were collected. We obtained evidence (Section 3.2.5) that the rate decreases with increasing temperature in the slightly sub-boiling regime even though it increases with increasing temperature at lower temperatures.

The times required for complete dissolution were also comparable in these two experiments; approximately 10 hours for the irradiated specimens and 8 hours for the unirradiated specimens. Based on their relative weights, the irradiated specimens were about 12% thicker than the unirradiated, which would account for about half of the 25% difference in complete dissolution times. The faster addition of acid would also contribute some to the more rapid complete dissolution observed with unirradiated fuel.

The different HNO_3 addition patterns in these two experiments resulted because of a rather severe foaming problem that occurred in the irradiated fuel experiment. In trying to keep this problem under control while maintaining a high temperature, the HNO_3 addition time was stretched out. Conversely, in trying (unsuccessfully) to duplicate this problem in the unirradiated fuel experiment, the HNO_3 addition time was shortened. It is thought that the severe foaming in this irradiated fuel experiment, and in the ruptured irradiated fuel experiment discussed in Section 3.2.8, was caused by the water soluble oil used in the cutting operation, which was not rinsed away before the dissolution experiment was performed. This contention was supported by the results of another experiment where a small amount of the cutter coolant solution was added during dissolution of unirradiated uranium; the foam level immediately increased dramatically.

The conclusion from this comparison of dissolution rates between different uranium specimens is that there is little practical difference between different batches of as-fabricated N-Reactor fuel, or between as-fabricated fuel and irradiated fuel. It should be stressed that this statement is true on a surface area basis. If, as discussed in Section 7.0, irradiated fuel breaks into smaller pieces than unirradiated fuel during the shearing operation, then markedly higher reaction rates (per unit weight) could indeed occur with irradiated fuel. Even then, however, the times

required for complete dissolution of irradiated and unirradiated fuel would be comparable if the largest irradiated uranium sheared pieces are comparable in size to the largest unirradiated uranium sheared pieces. The importance of the maximum dimension in defining the time required for complete dissolution is shown and discussed in Section 3.2.8.

3.2.2 Foaming During Dissolution

Knowledge of the degree of foaming that occurs during dissolution is important to the design of dissolution equipment. Accordingly, careful measurements of foam volume were made during the complete dissolution runs involving irradiated and unirradiated uranium discussed earlier (Section 3.2.1). The results obtained in the unirradiated uranium experiment are shown in Figure 3.5, along with the uranium dissolution and temperature measurements given earlier in Figure 3.4. As was discussed earlier, the foaming behavior

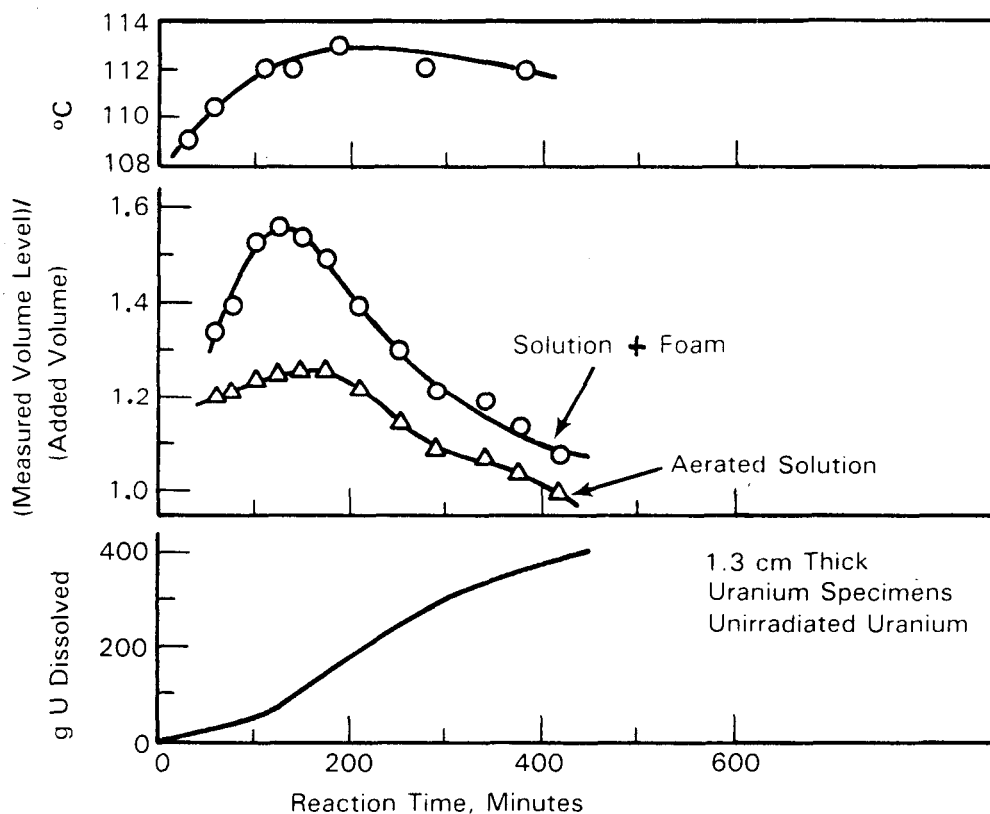


FIGURE 3.5. Foam Volumes During Dissolution

in the irradiated uranium experiments was apparently affected by cutting oil that adhered to the specimens.

The foaming results are shown in the middle of Figure 3.5, as the ratio of the measured volume level to the volume of solution added. Results are presented for two measurements: the volume reading at the top of the foam level (solution + foam) and the volume reading at the bottom of the foam level (aerated solution). The highest volume of solution + foam here corresponded to 1.56-times the volume of solution that had been added at that time, and 1.24-times the volume of aerated solution.

The largest volume of foam occurred about the time the maximum dissolution rate began. However, the foam volume did not remain constant throughout the period of constant, maximum dissolution. It is thought that the temperature pattern may have affected this behavior; the temperature approached the maximum value attained at about this same time. Because nitrous acid is less stable at higher temperatures, perhaps HNO_2 produced during the early part of the reaction was decomposing and thus increasing the foam volume.

Results of other experiments indicate foaming to be markedly less severe at lower temperatures. In complete dissolution runs at a constant temperature of $\sim 103^\circ\text{C}$ (Section 3.2.8), ratios of the volume of solution + foam to the volume of solution added were typically only 1.05 to 1.10. Thus, the extent of foaming need not be as high as indicated by the data shown in Figure 3.5.

It should be stressed that these results were obtained with relatively massive specimens (~ 1.3 cm thick half-rings cut from fuel elements). With more finely divided material, the weight of uranium dissolved per unit time will initially be much higher, and likewise the degree of foaming.

3.2.3 Effect of Nitric Acid Concentration on Uranium Dissolution Rate

Results of dissolution rate experiments at three HNO_3 concentrations with a single temperature are shown in Figure 3.6. These experiments employed as-cut specimens from a single fuel element. In each instance an initial slower reaction is followed by a more rapid reaction that proceeds at a constant rate for a prolonged period of time. It is assumed that this sustained rate does not become established until other factors (e.g., surface roughness) become

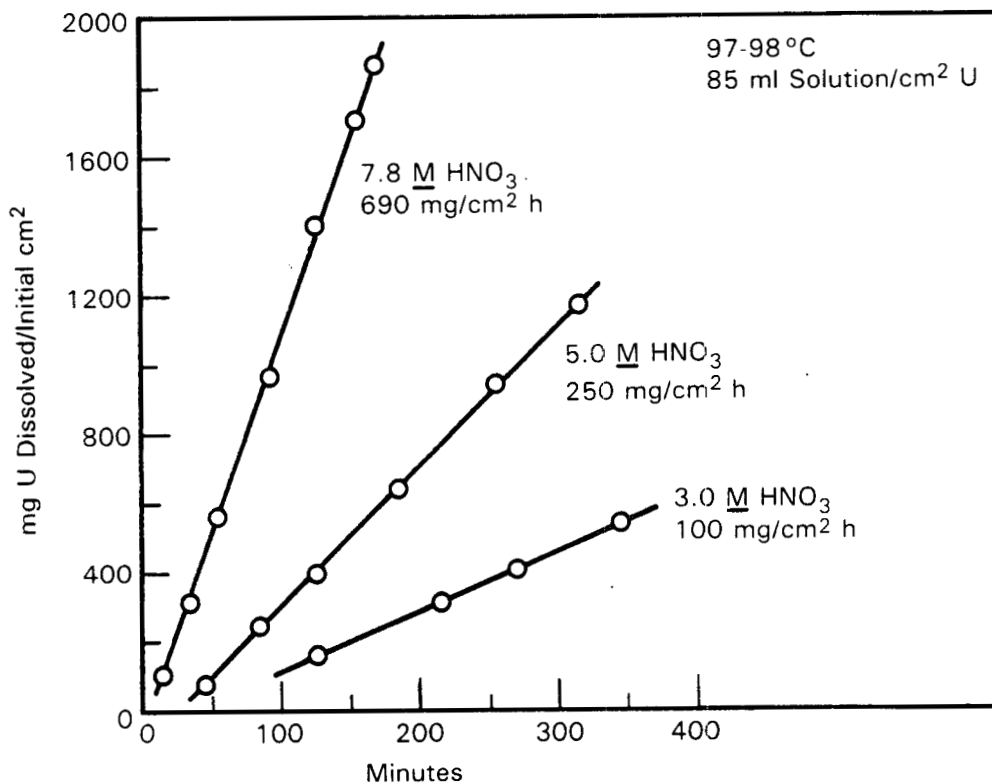


FIGURE 3.6. Uranium Dissolution at Different HNO₃ Concentrations

relatively constant. If surface roughness is the important factor, as appears to be the case, then a "steady-state" roughness appears to become established by the time ~100 mg U/cm² has been dissolved. Because only a small fraction of the uranium in a specimen of any appreciable size is contained in the outer 100 mg/cm², it is the sustained rate that occurs at deeper penetrations that is of primary interest to this work.

Figure 3.7a is a log-log plot of these sustained rates (Figure 3.6) against stoichiometric HNO₃ concentration and Figure 3.7b is a plot of the rates against free nitrate ion activity (which is equal to free hydrogen ion activity in these solutions). The free nitrate ion activity values used here were calculated from the degree of HNO₃ dissociation values and the mean ionic activity coefficient values reported by Davis and deBruin (1964) for 25°C. We assume that comparable relative values exist at ~97°C, which was the temperature of our experiments.

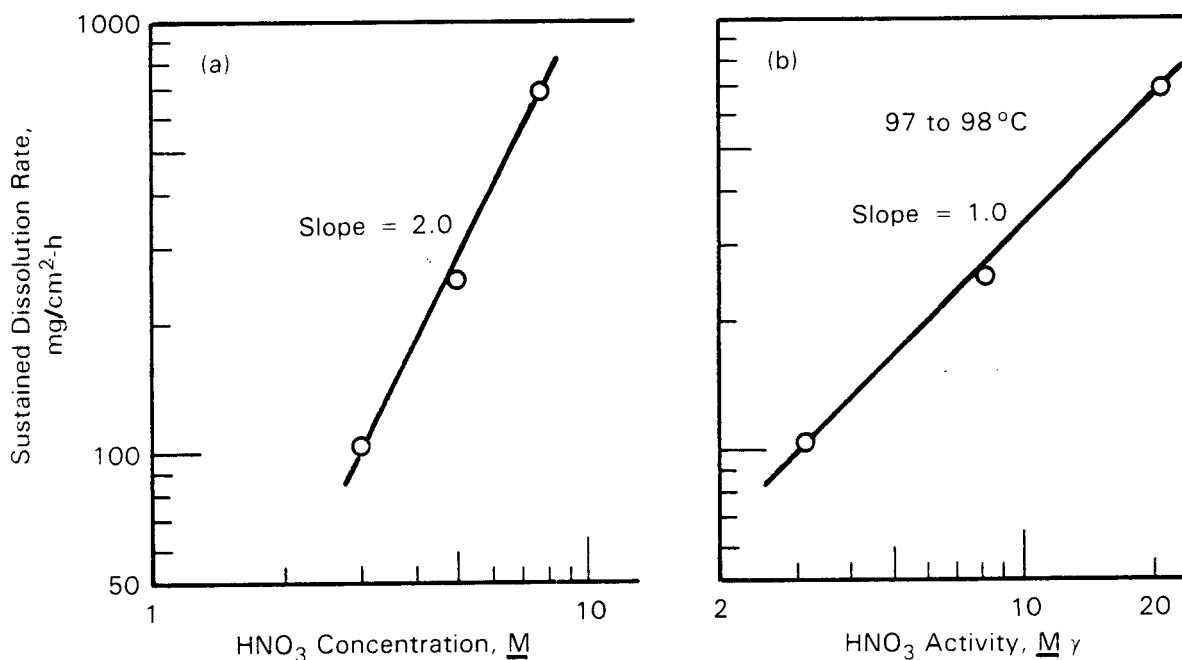


FIGURE 3.7. Dependence of Sustained Dissolution Rate on HNO₃ Concentration and Activity

The correlations shown in Figure 3.7 indicate that uranium dissolution rate is proportional to the first power of free nitrate ion (or hydrogen ion) activity and, because of the dependencies of HNO₃ dissociation and mean ionic activity coefficients on HNO₃ concentration, the rate is proportional to the square of the stoichiometric HNO₃ concentration in this concentration range. The activity correlation has more basic implications, but the concentration correlation is simpler to use.

These data were obtained at relatively constant HNO₃ concentrations and at low uranium concentrations: in the 7.8 M HNO₃ experiment the maximum U concentration was 0.09 M; dissolution of this much U would have reduced the HNO₃ concentration by ~0.45 M, or 6%. At the other acidities, the U concentrations were lower but the percentage reductions in HNO₃ were also ~6%.

3.2.4 Effect of Uranyl Nitrate Concentration on Uranium Dissolution Rate

Experiments were also performed with high uranium, low HNO₃ solutions to measure dissolution rates under conditions near the end of dissolution cycles. These experiments involved weight loss measurements instead of

counting measurements because of the high count rate from the uranium that was already in solution. Separate specimens were used for each exposure; all were cut from the same unirradiated fuel element. Solution compositional adjustments were made between exposures to maintain reasonably comparable conditions throughout. Results of the two experiments of this type are given in Table 3.2.

The data from these two experiments are plotted in Figure 3.8 along with, for comparison, data obtained at a slightly higher temperature (~105°C) with 7.8 M HNO₃ containing little uranium. As before, extrapolation of these lines to lower penetration indicates that the initial reaction rate is lower than the sustained rates shown here.

Figure 3.9 is a log-log plot of these sustained rates against total stoichiometric nitrate concentration. The line through these three data points has a slope of 2.6, as opposed to the slope of 2.0 found for the dependence on stoichiometric HNO₃ concentration (Figure 3.7a). This correlation was also found in complete dissolution experiments to be described in Section 3.2.8. It is thought that this apparent discrepancy between total nitrate concentration dependencies between results in the presence and absence

TABLE 3.2. Dissolution Rate Data in High U Solutions

| Exposure Time, h | Weight Loss, mg U/Initial cm ² | Temperature~104°C | | | | | |
|------------------|---|----------------------|------------------|--------------------|------------------|----------------------------|------------------|
| | | Start of Exposure, M | | End of Exposure, M | | Average During Exposure, M | |
| | | U | HNO ₃ | U | HNO ₃ | U | HNO ₃ |
| 1.0 | 326 | 1.80 | 2.27 | 1.82 | 2.22 | 1.81 | 2.24 |
| 3.0 | 1300 | 1.90 | 2.36 | 1.97 | 2.08 | 1.94 | 2.22 |
| 5.0 | 2060 | 1.91 | 2.25 | 2.06 | 1.77 | <u>1.98</u> | <u>2.01</u> |
| | | | | Average | | 1.91 | 2.16 |
| 1.0 | 158 | 1.83 | 1.28 | 1.83 | 1.26 | 1.83 | 1.27 |
| 3.0 | 690 | 1.82 | 1.38 | 1.86 | 1.24 | 1.84 | 1.31 |
| 5.0 | 1210 | 1.76 | 1.32 | 1.84 | 1.10 | <u>1.80</u> | <u>1.21</u> |
| | | | | Average | | 1.82 | 1.26 |

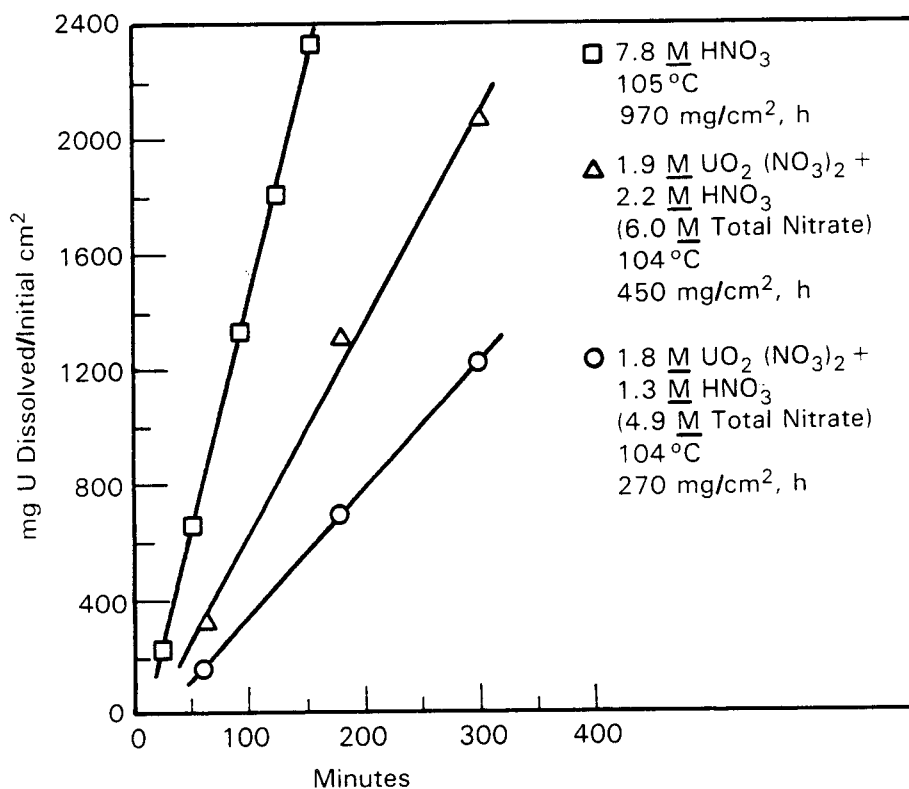


FIGURE 3.8. Dissolution Rate Data in Uranyl Nitrate + HNO₃ Solutions

of high uranium concentrations is due to nitrate complexing of the uranyl ion so that the free nitrate concentration is appreciably lower than the total nitrate concentration. Total nitrate concentration is made up of the concentration of free nitrate ion, the concentration of undissociated HNO₃, and the concentrations of uranyl nitrate complexes. We do not have adequate stability constant and activity coefficient data to calculate the free nitrate activities of these solutions and thus cannot say if the first order dependence of dissolution rate on free nitrate activity observed in HNO₃ solutions (Figure 3.7b) also prevails in uranyl nitrate/nitric acid solutions.

Regardless of this lack, however, the effect of uranyl nitrate concentration on uranium dissolution rate appears to be one of contributing to the total nitrate concentration. As indicated here, and by results to be presented in Section 3.2.8 as well, the dissolution rate in uranyl nitrate/nitric acid mixtures typical of those resulting during dissolution of

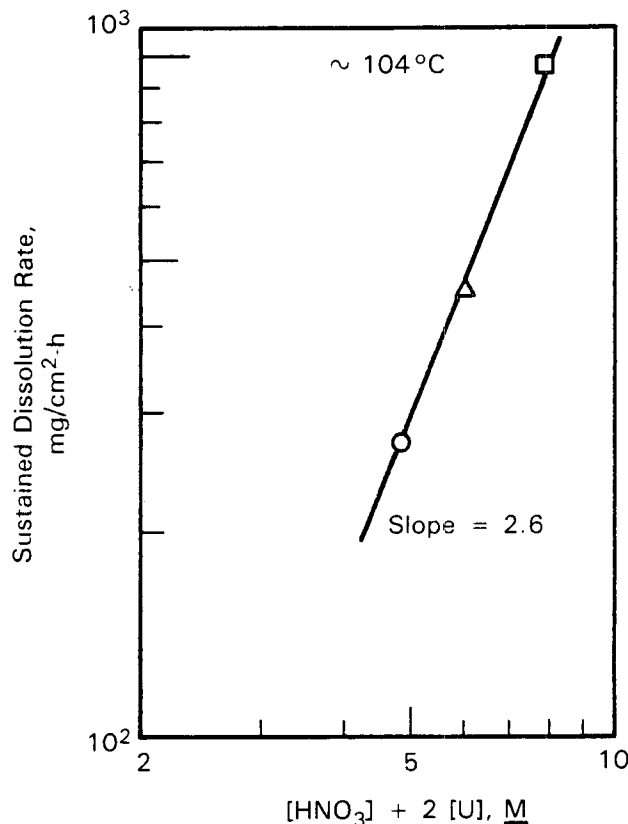


FIGURE 3.9. Dependence of Uranium Dissolution Rate on Nitrate Concentration

uranium under typical plant conditions is proportional to the total nitrate concentration raised to the 2.6 power. This relationship is easy to apply in actual dissolution rate predictions.

3.2.5 Effect of Temperature on Uranium Dissolution Rate

The results of a series of runs in which dissolution rates in 7.8 M HNO₃ were measured at temperatures from 71 to 112°C (the boiling point) are shown in Figure 3.10. An interesting feature of these results is that dissolution is slower in the boiling solution than it is at 105°C. This is shown more clearly in Figure 3.11 where the logarithm of the sustained rates are plotted against the inverse temperature. The slope of the linear portion of the temperature dependence plot (Figure 3.11) yields an activation energy of ~11 kcal for the rate of uranium dissolution in this range of conditions.

Results obtained at other HNO₃ concentrations are also shown in Figure 3.11. These also indicate that dissolution is slower in boiling solution than

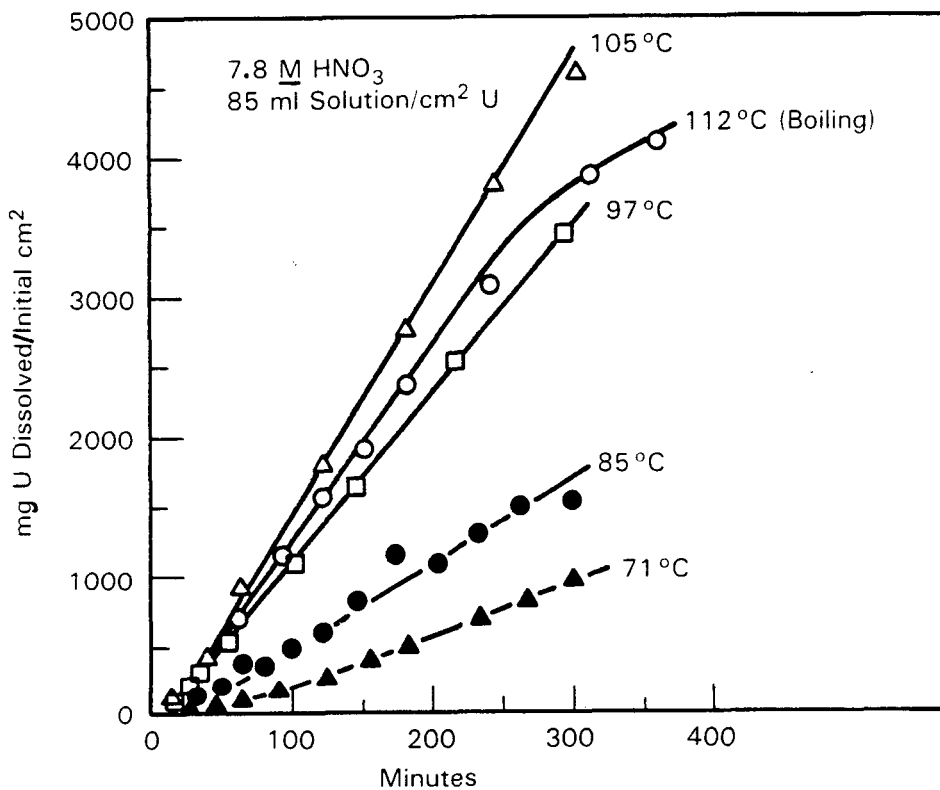


FIGURE 3.10. Uranium Dissolution at Different Temperatures

it is at slightly lower temperatures. Such an effect has been observed earlier for dissolution of UO₂ in HNO₃ (Taylor et al. 1963). Those authors attributed the effect to a lowering of the nitrous acid concentration at the boiling point. This is discussed in more detail in the following section.

3.2.6 Effect of Nitrous Acid Concentration

Because of experimental difficulties, we were unable to obtain quantitative data on the effect of nitrous acid concentration on the rate of uranium dissolution in nitric acid. However, we were able to show that the presence of at least a small amount of nitrous acid is necessary to achieve the maximum dissolution rate. Because nitrous acid is a product of the dissolution reaction, this is usually no problem. Low initial nitrous acid concentrations may have contributed to the "induction period" observed in some of the rate experiments, but it is thought that surface roughening was a more important factor, as will be discussed in the following section.

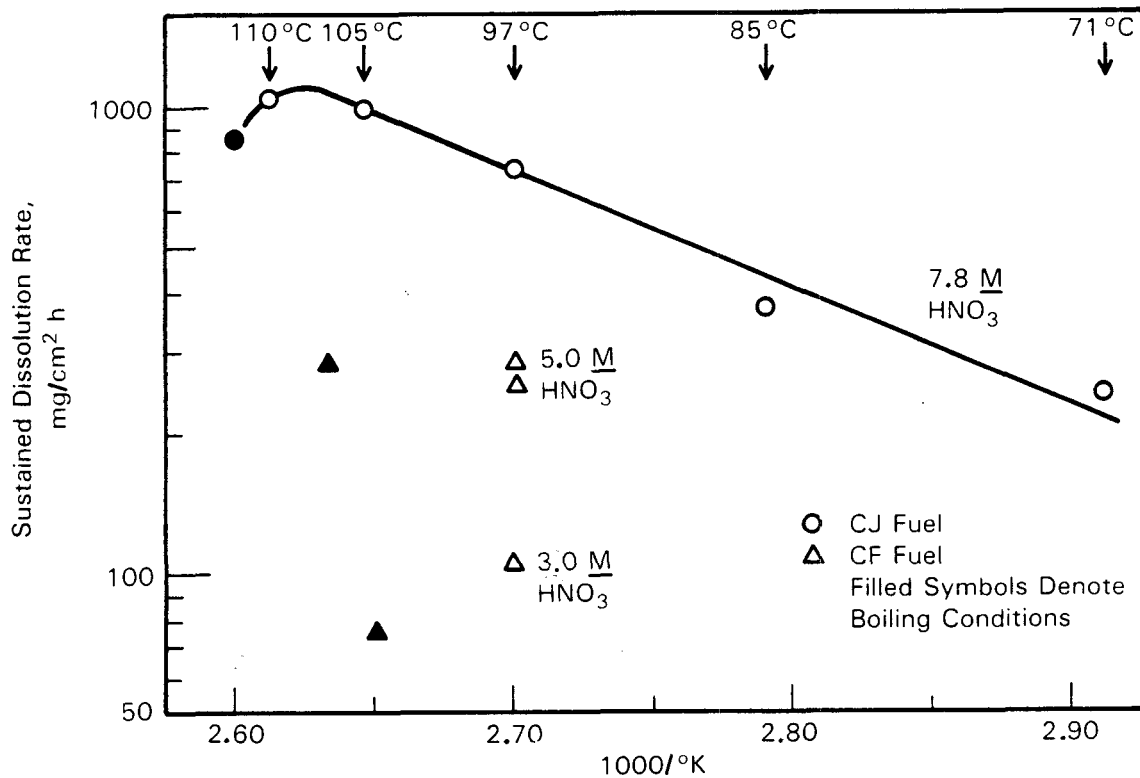


FIGURE 3.11. Effect of Temperature on Uranium Dissolution Rate

Figure 3.12 presents two sets of data illustrating the effect of adding hydrazine (to prevent HNO_2 accumulation) on the rate of uranium dissolution. In (a), a $7.8 \text{ M HNO}_3 + 0.01 \text{ M N}_2\text{H}_5\text{NO}_3$ solution was heated to 98°C , and additional hydrazine was added periodically after the uranium specimen was introduced. For the first 30 minutes, these additions were made at 10 minute intervals and each addition raised the hydrazine concentration by 0.03 M ; a very low uranium dissolution rate was observed during this period. The rate of hydrazine addition was then decreased (and eventually stopped after 87 minutes), and nitrous acid accumulated in solution; this resulted in an increased uranium dissolution rate, which eventually equalled that observed from near the beginning of a similar experiment in which hydrazine was not added.

Figure 3.12(b) illustrates the effect of adding hydrazine to destroy nitrous acid after reaction had proceeded for an appreciable time; hydrazine essentially stopped the dissolution reaction. The HNO_3 concentration in this experiment was initially 3.0 M , but much higher than normal evaporation

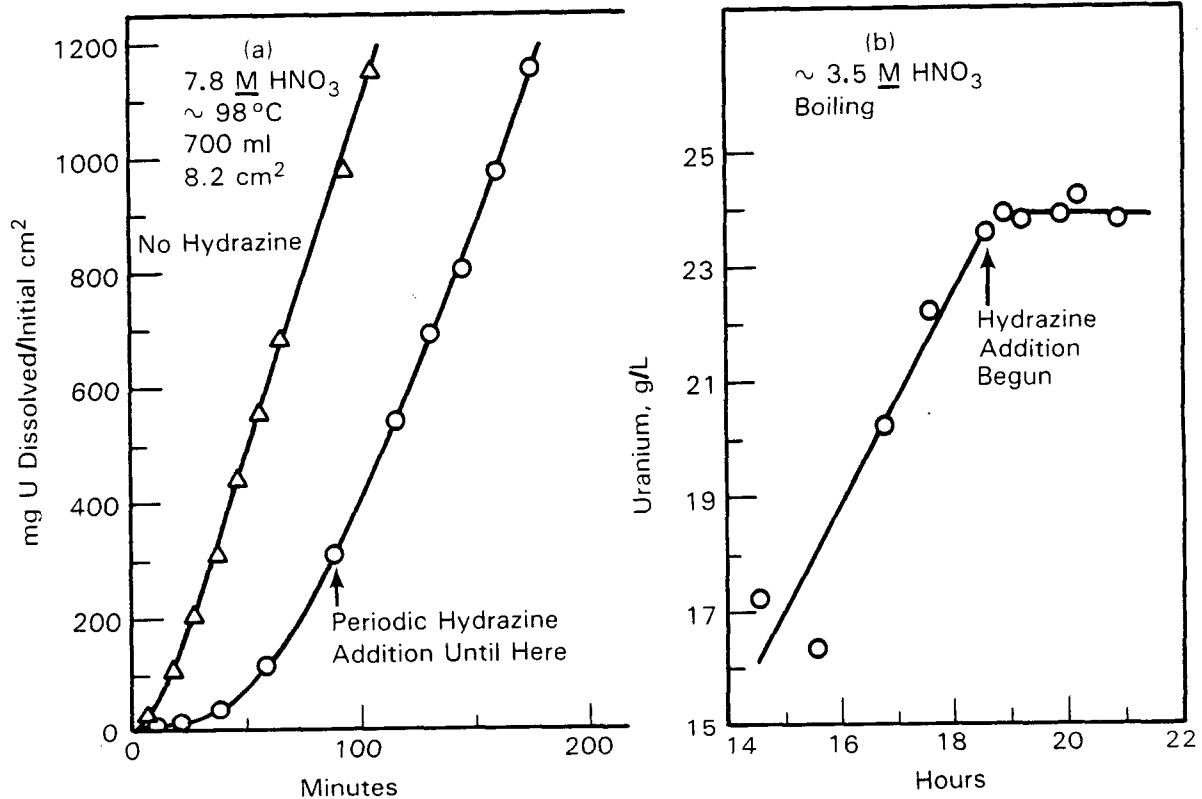


FIGURE 3.12. Effect of Hydrazine Addition (to Destroy Nitrous Acid) on Uranium Dissolution Rate

occurred so that the final acidity was $\sim 3.7 \text{ M}$ (minus that consumed in the reaction). The initial hydrazine addition was sufficient to make the solution 0.025 M in hydrazine. Additions sufficient to increase that concentration by 0.005 M were then made at 15 minute intervals.

In the absence of nitrous acid suppressors such as hydrazine, the nitrous acid concentration in a uranium dissolver at any time will represent a balance between that being formed by the dissolution reaction and that being lost by decomposition and volatilization. Nitrous acid concentrations were measured in many of the dissolution rate experiments; Figure 3.13 illustrates such concentrations (and U concentrations) found in experiments with different acidities at a constant temperature, and Figure 3.14 shows results with different temperatures at a constant acidity.

In the initial portions of these experiments, there was close correlation of nitrous acid concentration with uranium concentration but nitrous acid

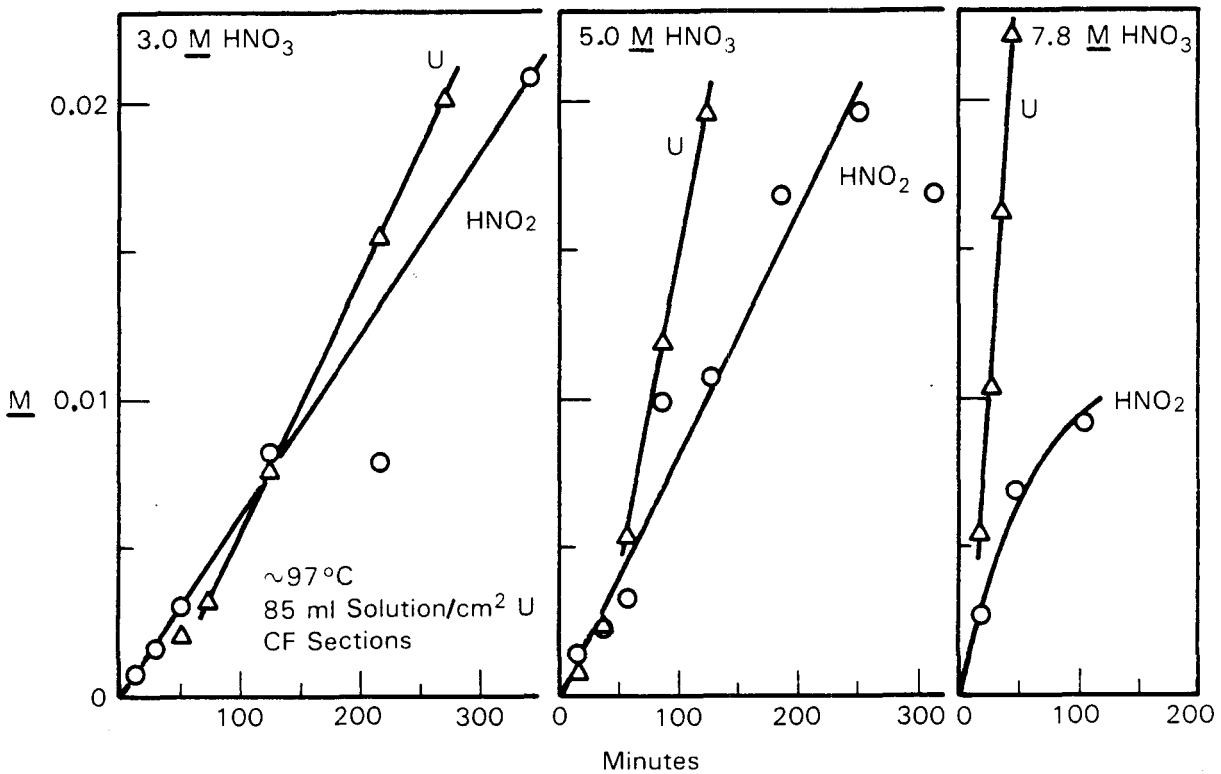


FIGURE 3.13. Nitrous Acid and Uranium Concentrations During Dissolution at Different Acidities

concentration soon did not increase as rapidly as did uranium concentration, indicating that nitrous acid loss became substantial. In Figure 3.13, nitrous acid loss is seen to be more pronounced at 7.8 M HNO₃ than at 5.0 or 3.0 M HNO₃; this is in accord with expectations. Figure 3.14 illustrates that nitrous acid loss is less pronounced at lower temperatures; this is also in accord with expectations.

In the experiments shown in Figure 3.14 a steady-state nitrous acid concentration was eventually established. This concentration was generally lower at higher temperatures, but the available data do not show a regular correlation between steady-state concentration and temperature. Nitrous acid concentrations were not measured in the corresponding experiment at the boiling point, which gave slower U dissolution (Figure 3.10); however, a similar experiment at a 2-fold lower solution volume-to-uranium surface area ratio gave a steady state nitrous acid concentration of $\sim 3 \times 10^{-3}$ M. Since the steady state nitrous acid concentration would be expected to be higher at a lower volume-to-surface area ratio, this result suggests that the steady

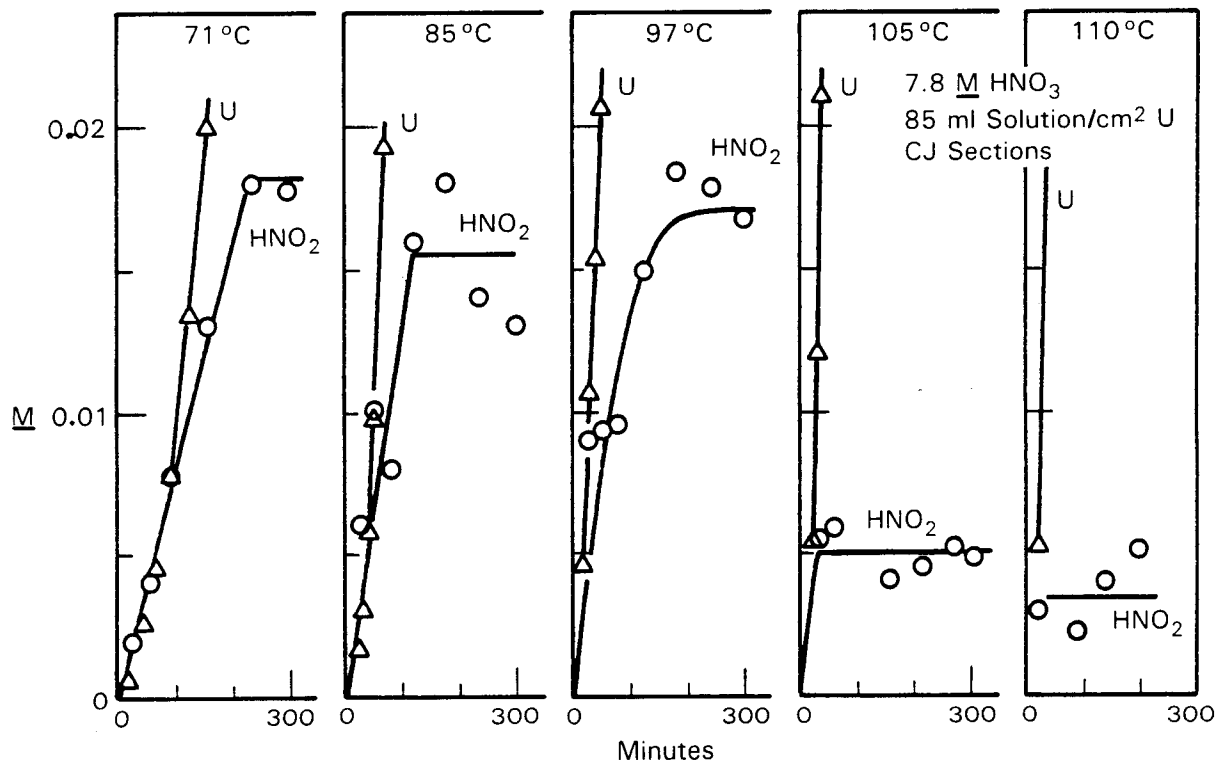


FIGURE 3.14. Nitrous Acid and Uranium Concentrations During Dissolution at Different Temperatures

state nitrous acid concentration at the boiling point with the volume-to-surface area ratio of the experiments in Figure 3.14 was no less than half that at 110°C. This difference may have contributed to the lower dissolution rate observed at the boiling point, as was discussed in Section 3.2.5, but the HNO₂ contribution does not appear to be sufficient to account for the total difference in dissolution rate that was observed.

The facts that: 1) the presence of nitrous acid is necessary to rapid U dissolution (Figure 3.12) but, 2) U dissolution proceeds at a constant rate while nitrous acid concentration increases by a factor of 4 to 5 (Figure 3.13) indicate that U dissolution rate varies with HNO₂ concentration raised to some low power or that the effect of nitrous acid is a catalytic one and there is no concentration effect above a threshold level. Lacher, Salzman, and Park (1961) report a nitrous acid dependence of 0.5 for the initial dissolution rate in 15.6 M HNO₃ at 25°C. Our sustained dissolution rate data do not support this dependence; a 4-fold increase in nitrous acid concentration would

increase the uranium dissolution rate by 100%, and this would certainly have been apparent in our rate data (Figure 3.13). If there is a concentration effect above a threshold level, a 0.1 power dependence, which gives a 15% dissolution rate increase for a 4-fold increase in nitrous acid concentration, appears to be more in accord with our results.

3.2.7 Surface Roughening During Dissolution

Visual comparison of the uranium surfaces before and after partial dissolution showed that, while some surface roughening did occur during dissolution, the depths of penetration over the surface were relatively constant. A few experiments were done in an effort to quantify the extent of roughening.

Figure 3.15 compares uranium dissolution rates in successive exposures of

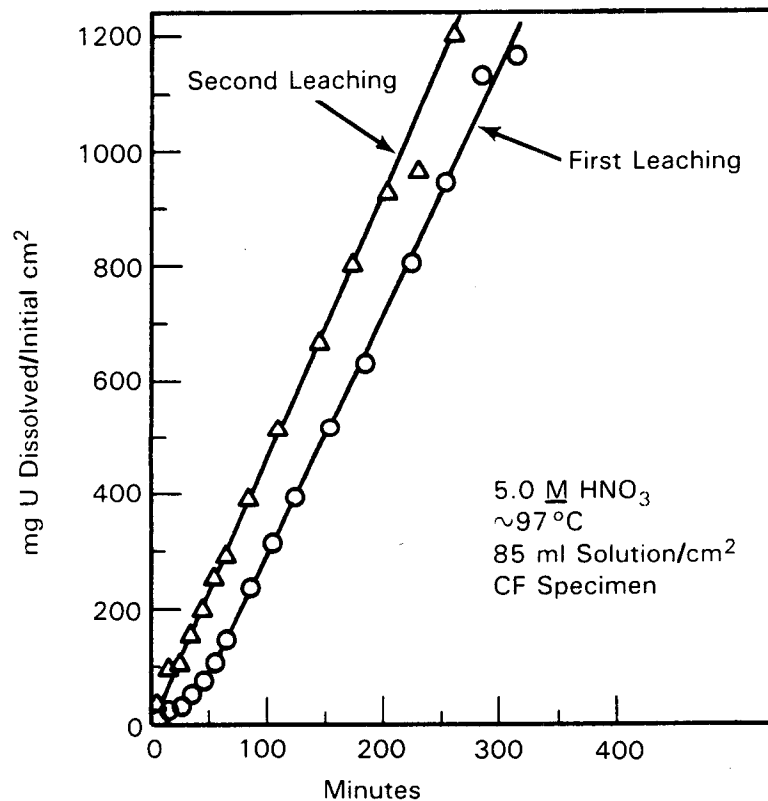


FIGURE 3.15. Uranium Dissolution Rates in Successive Leachings of One Specimen

one specimen to 5 M HNO₃ at ~97°C. In the first exposure, using the as-cut specimen, the dissolution rate was initially slow but then increased to a rate that held constant for a long time period. When the same specimen, after standing overnight in the first solution as it cooled, was placed in a fresh boiling solution there was no induction period and the dissolution rate agreed well with the sustained rate in the first exposure. These results indicate that surface roughening accounts for the apparent induction period, and that the degree of roughening remains constant over a penetration corresponding to dissolution from ~100 to at least ~2500 mg/cm² (~0.005 to ~0.13 cm). The initial dissolution rate in the first exposure was about one-fourth as great as the sustained rate, indicating that the true surface area after ~0.005 cm penetration was about 4-fold greater than the surface area of the as-cut specimen.

A qualitatively similar, but quantitatively different, picture was obtained in experiments employing both as-cut and partially dissolved specimens and boiling 3 M HNO₃. Figure 3.16 shows the data obtained with two as-cut specimens and two partially dissolved specimens. The partially dissolved specimens had both been exposed to 7.8 M HNO₃ long enough that penetrations of ~4000 mg/cm² (~0.2 cm) had occurred.

Comparison of the initial and sustained dissolution rates with the as-cut specimens indicates that partial dissolution in boiling 3 M HNO₃ increased the surface area by a factor of ~2.4, rather than the factor of ~4.0 observed in 5 M HNO₃. With the specimens that had been partially dissolved in 7.8 M HNO₃, the sustained rate in boiling 3 M HNO₃ was ~2.6-fold greater than the initial rate with as-cut specimens. This indicates that the degree of roughness was approximately the same after dissolution of ~4000 mg/cm² (~0.2 cm penetration) in 7.8 M HNO₃ as after dissolution of ~300 mg/cm² (~0.016 cm penetration) in 3 M HNO₃. Results to be presented later (Section 3.2.8) support this indication at even deeper penetrations.

Based on these limited data, it appears that dissolution of uranium to a small penetration produces a roughened surface having an area 3- to 4-fold higher than the initial as-cut area. This factor is relatively independent of additional penetration depth and of acid concentration in the dissolvent.

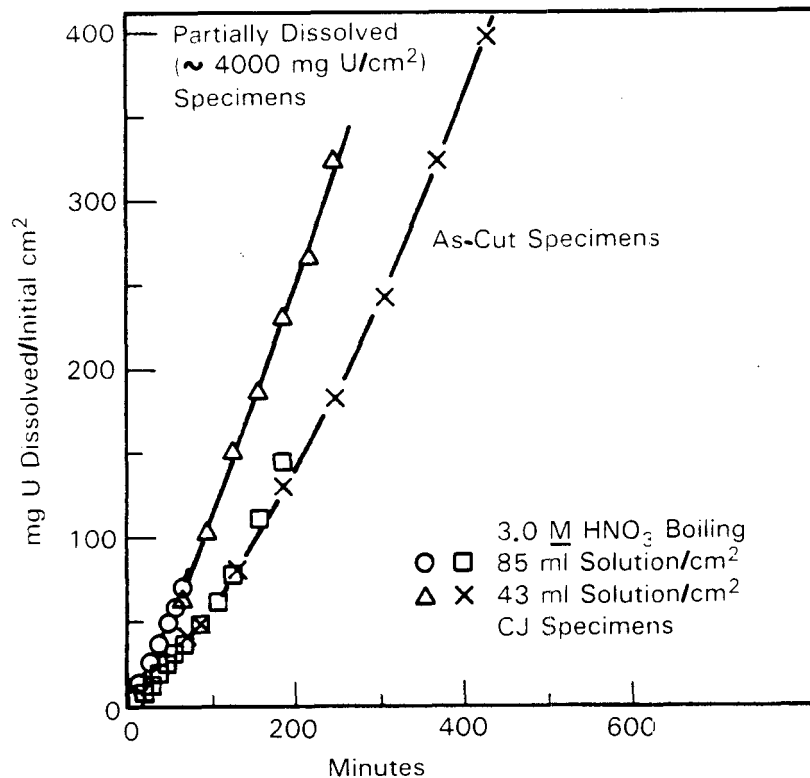


FIGURE 3.16. Dissolution Rates of As-Cut and of Partially Dissolved Uranium Specimens

3.2.8 Complete Dissolution Experiments

To obtain data to allow more certain prediction of dissolution rates through a complete dissolution cycle, a series of complete dissolution runs were performed under carefully controlled conditions and with frequent sampling. Four such runs were performed to examine the effects of HNO_3 -to-U charge ratio and of specimen thickness, at a given temperature (103°C) and terminal U concentration (1.8 M).

This series of four experiments was done in a vessel fitted with a downdraft condenser, which was cooled to below 10°C . The solution was sparged with air (at 0.04 ml/min , ml of solution) and air was swept above the surface of the solution (at $\sim 0.5 \text{ ml/min}$, ml of solution). These conditions increase the reconversion of NO and NO_2 to nitrous and nitric acids and thus reduce the consumption of HNO_3 in the dissolution process. The air sweep was bubbled through room temperature water before it entered the vessel; this water

addition to the system apparently essentially balanced water losses by evaporation, based on the observation that the final solution volume was essentially identical to the initial volume (corrected for the volume removed in samples).

The uranium specimens used in these four experiments were whole rings cut from an as-fabricated inner element; thus only end-grain attack occurred until near completion of dissolution, when holes were dissolved through the residual uranium. This did not occur until the thickness of the residual uranium was ~ 0.10 to 0.15 cm.

Some of the results of the first of these experiments (A), which employed 9.5 M HNO_3 and two fuel element sections (giving an initial uranium surface area of 25 cm^2) are shown in Figure 3.17. Both of these sections were ~ 1.27 cm thick. Holes through the uranium became apparent after ~ 10.5 h, at which

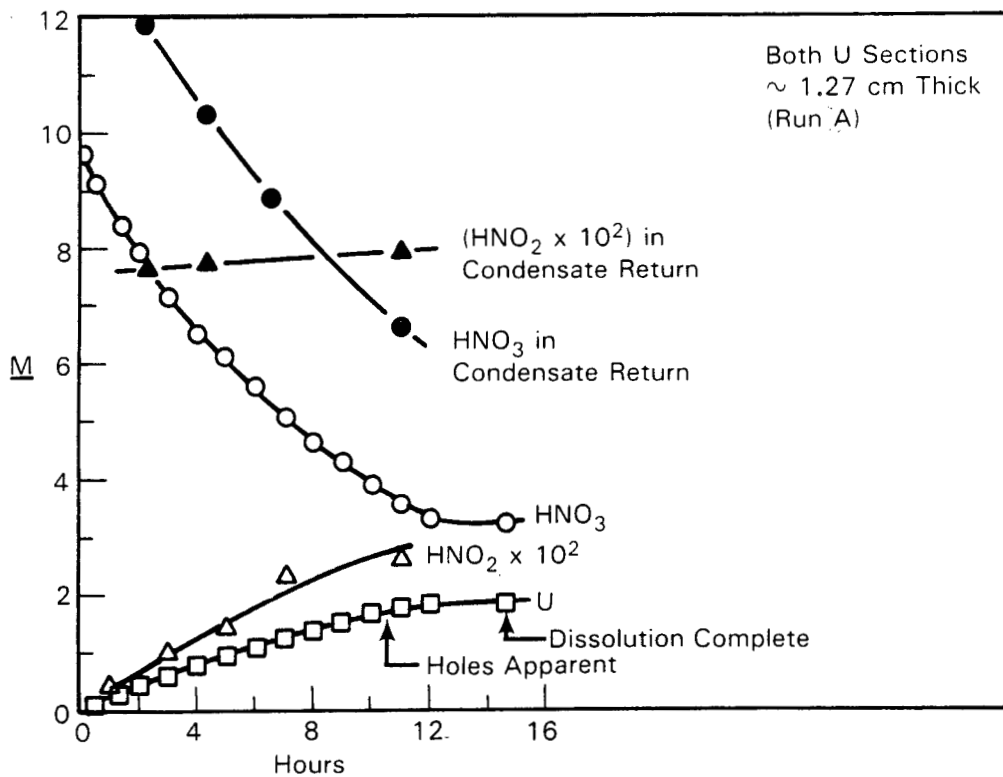


FIGURE 3.17. Complete Dissolution Experiment with Two Uranium Sections and 9.5 M HNO_3

time ~90% of the uranium was dissolved. Another ~4 h was required for dissolution to become complete.

Figure 3.17 shows the concentrations of U, HNO_3 , and HNO_2 in the dissolver solution and of HNO_3 and HNO_2 in the condensate draining from the bottom of the downdraft condenser back into the dissolver. The rate of uranium concentration increase is seen to decrease gradually as dissolution proceeds; however, this decrease is not very pronounced until dissolution is nearly complete. These rate data will be treated quantitatively later in this section.

Dissolver solution HNO_3 concentration decreases regularly as it is consumed by the dissolution reaction; the HNO_3 consumption initially was ~4.0 mole/mole U dissolved but was ~3.5 mole/mole overall. Nitrous acid concentration in the dissolver solution gradually increased throughout the dissolution, eventually reaching 0.026 M. Nitrous acid concentration in the condensate return was ~0.08 M, but the flow rate of this stream was low so this accounted for only a small fraction of the HNO_2 in the system. Nitric acid concentration in the condensate return remained substantially higher than in the dissolver solution; this is not in accord with expectations based on HNO_3 vapor pressure data, and is qualitatively attributed to conversion of oxides of nitrogen to HNO_3 in the condenser.

Some of the results of a similar experiment (C), except that 8.1 M HNO_3 was used in place of 9.5 M HNO_3 , are given in Figure 3.18. The overall picture is the same as at the higher acidity (Figure 3.17), but a longer time was required for (~90%) complete dissolution to be achieved. Whereas ~10.5 h were required for holes through the uranium to be apparent in the 9.5 M HNO_3 case, ~15 h were required in the 8.1 M HNO_3 case. The acidities at the times the holes appeared were ~3.7 M and ~2.9 M respectively in these two cases. Higher acidity is obviously desirable for shorter dissolution time cycles, but this advantage must be balanced against solubility problems in cooled dissolver solutions and solvent extraction disadvantages at higher acidities. The HNO_3 consumption in this run was ~3.2 mole/mole U dissolved, both as determined from the initial slopes and from the initial and final concentrations.

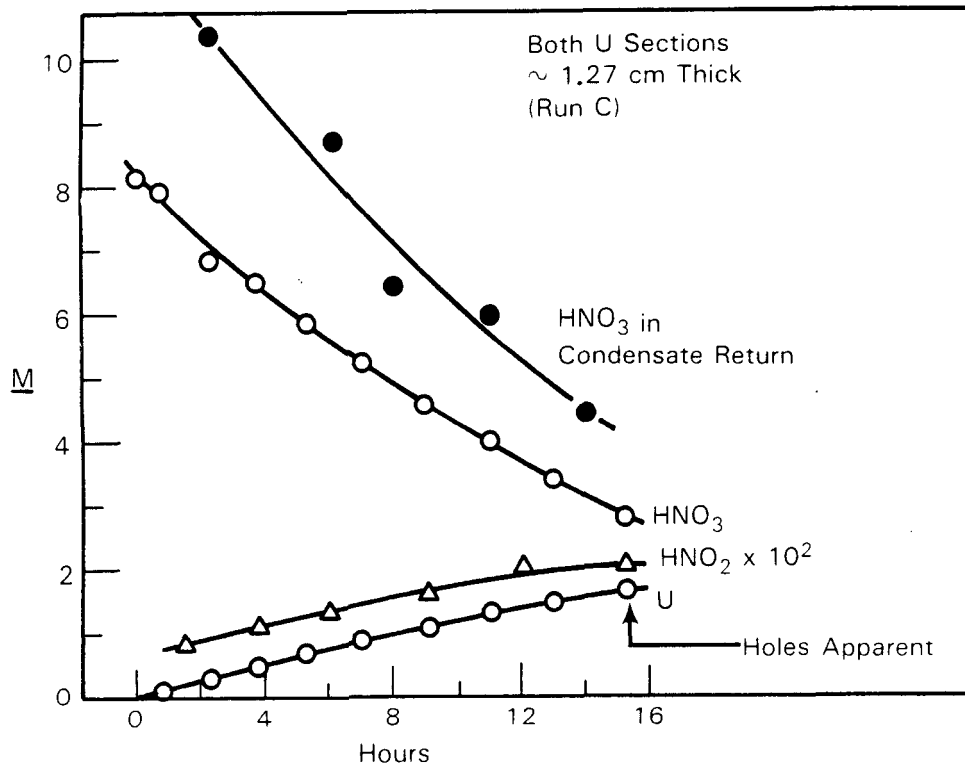


FIGURE 3.18. Complete Dissolution Experiment with Two Uranium Sections and 8.1 M HNO₃

Figure 3.19 contains data from an experiment (B) in which the initial uranium surface area was made much higher by using five uranium rings instead of two, but in which the largest uranium piece was the same size as in the previously described runs. Comparison of these results with those of figure 3.18, where the same acidity and maximum uranium thickness were used, shows that even though the initial dissolution rate was much faster with more rings, the time required to approach complete dissolution was the same. This illustrates the very important point that, even though a higher surface area gives a faster initial dissolution rate, the time required for complete dissolution of a batch of fuel under a given set of concentration conditions and at a given temperature, is not affected by the initial area; it depends instead on the maximum thickness of material to be dissolved. The HNO₃ consumption in this run was ~3.7 mole/mole U dissolved initially and ~3.4 mole/mole overall.

The final experiment (D) of this set also related to the importance of maximum thickness on the time required for complete dissolution; it involved a

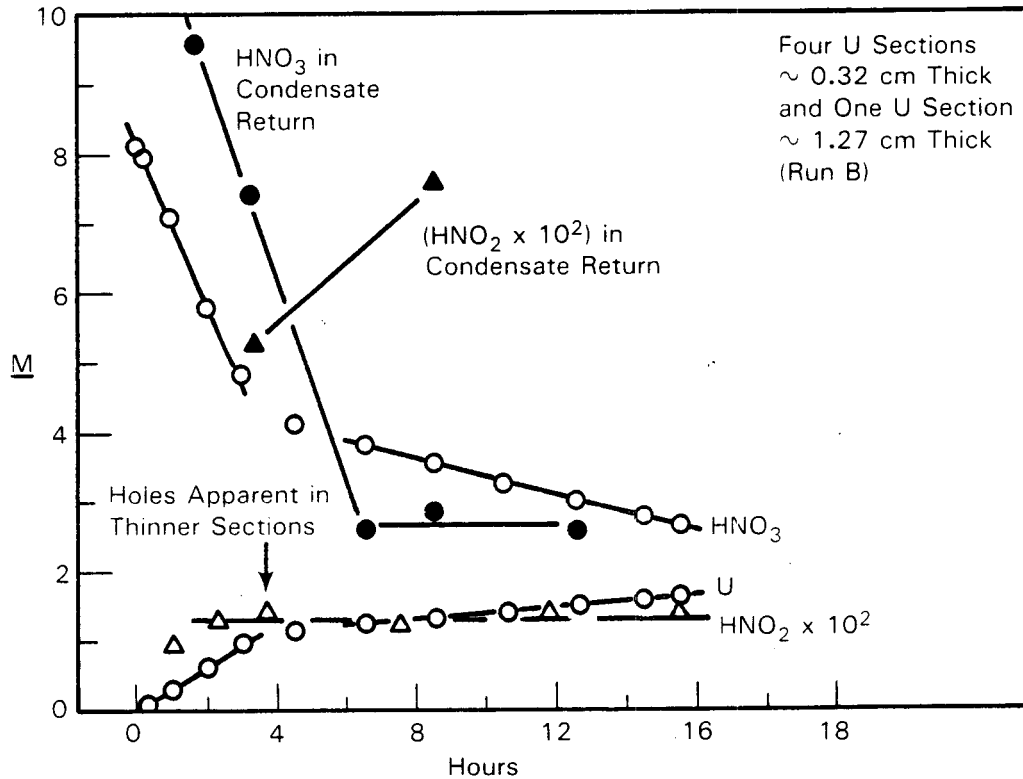


FIGURE 3.19. Complete Dissolution Experiment with Five Uranium Sections and 8.1 M HNO_3

single fuel element ring (giving a uranium surface area of only $\sim 12.5 \text{ cm}^2$) that was twice as long (2.54 cm) as the longest used previously. The results, given in Figure 3.20, show the expected slower reaction rate and an approximate doubling of the time required for near-complete dissolution (compare with Figure 3.17). The HNO_3 consumption in this run was ~ 3.8 mole/mole U dissolved initially and ~ 3.5 mole/mole overall.

Incremental uranium dissolution rates and total nitrate concentrations calculated from the results of these four complete dissolution experiments are shown in Figure 3.21. These results are in excellent agreement with those reported earlier (Figure 3.9) from experiments with total uranium penetrations in the range ~ 0.005 to 0.1 cm. The results shown in Figure 3.21 include many at penetrations near 0.6 cm and some at penetrations near 1.2 cm. This agreement further supports the earlier observation (Section 3.2.7) that the degree of surface roughening is relatively independent of penetration depth, beyond a minimal initial penetration.

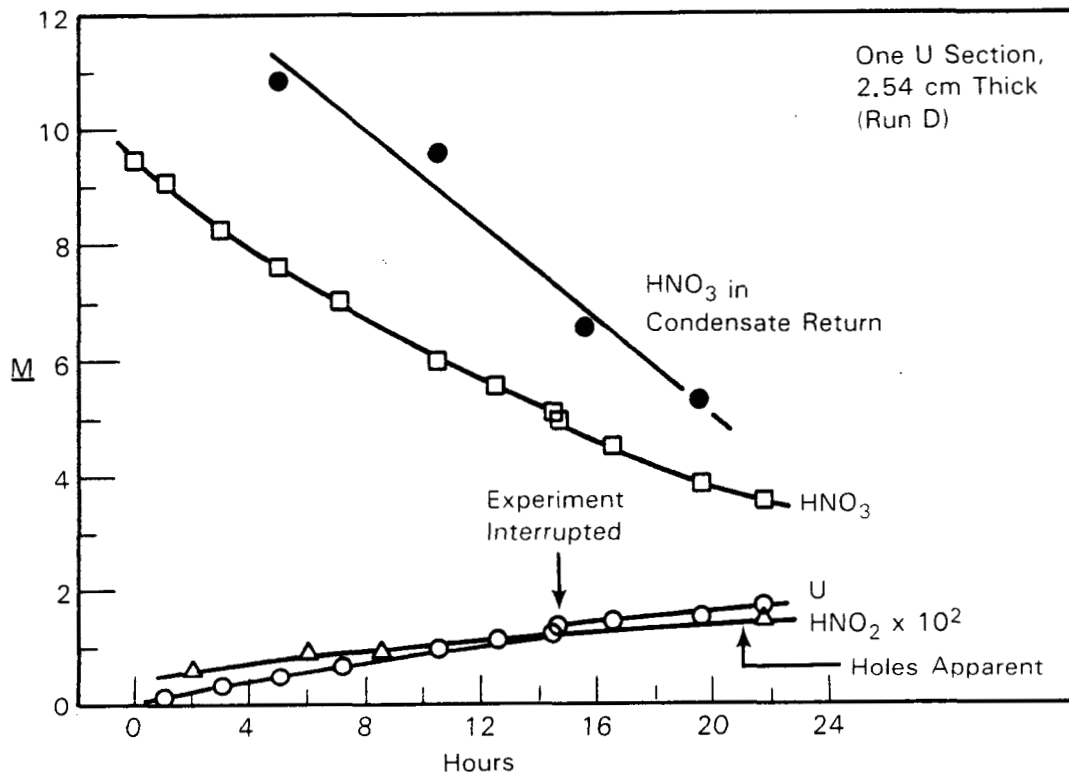


FIGURE 3.20. Complete Dissolution of Thicker Uranium Section and 9.5 M HNO₃

Another complete dissolution experiment was done earlier in the project, primarily to establish conditions and procedures to be used in preparing leached irradiated cladding hulls for analysis of their transuranic element concentration (Section 4.0). The experimental procedure and the results obtained in the subsequent hot cell work were described in Section 3.2.1 (and Figure 3.4); the results obtained in this first laboratory test are presented here in Figure 3.22 for completeness.

This early experiment differed from those discussed earlier in this section in several respects. It employed an updraft condenser and no air sparge or sweep was used. Half-ring sections of uranium (outer, CL sections, as well as inner, CJ sections) were used and HNO₃ was added in increments over the first ~200 minutes. These increments of HNO₃ were sufficient to increase the HNO₃ concentration by ~2 M initially and by ~0.7 M at the end of the additive period. Samples taken for analysis during this period were withdrawn just prior to these additions.

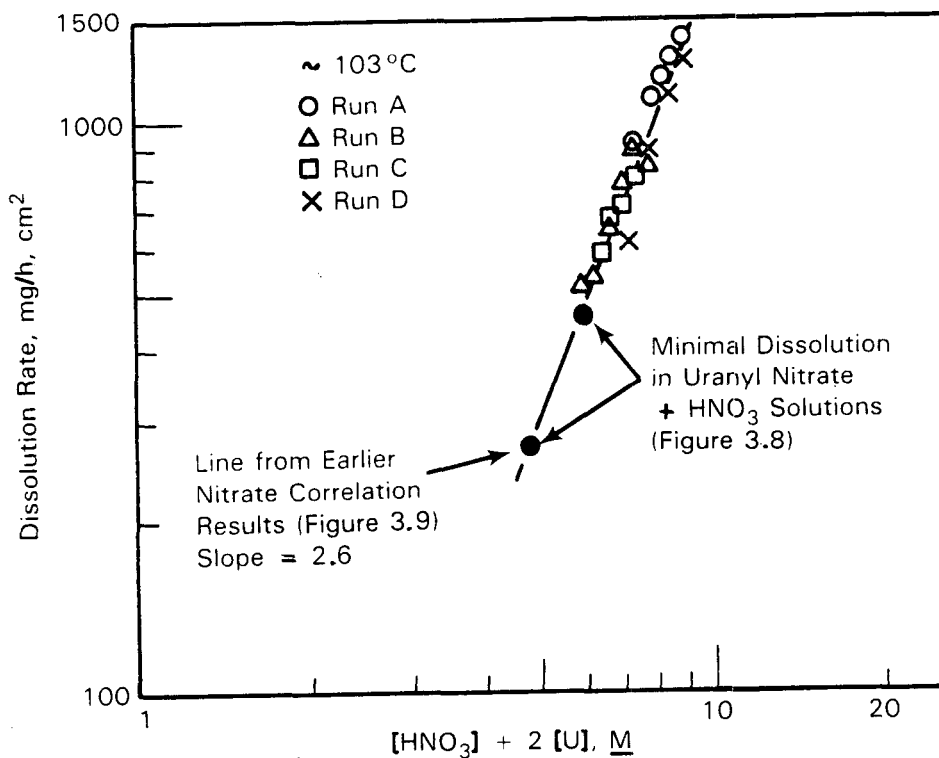


FIGURE 3.21. Total Nitrate Correlation of Incremental Dissolution Rate Data from Complete Dissolution Runs

The weights of U dissolved shown in Figure 3.22 are somewhat in error because of evaporation that occurred; data indicate that the final volume was ~17% lower than expected from the volumes added. However, a reasonably accurate dissolution rate can be calculated from these data for comparison with those obtained in the other experiments. About 250 minutes into the experiment the dissolution rate was ~1900 mgU/cm²-h and the solution composition was ~1.44 M UO₂(NO₃)₂ + 6.3 M HNO₃, giving a total nitrate concentration of ~9.2 M. From the results of the other complete dissolution experiments (Figure 3.21), a rate of ~1450 mg/cm²-h is expected for 9.2 M total nitrate concentration at 103°C. This expected rate is 76% as high as that measured here (Figure 3.22) at ~111°C. The temperature effect observed in 7.8 M total nitrate (Figure 3.11) would account for only a small part of this discrepancy. However, duplication to within 20% or so is considered quite good, considering all the differences in these experiments.

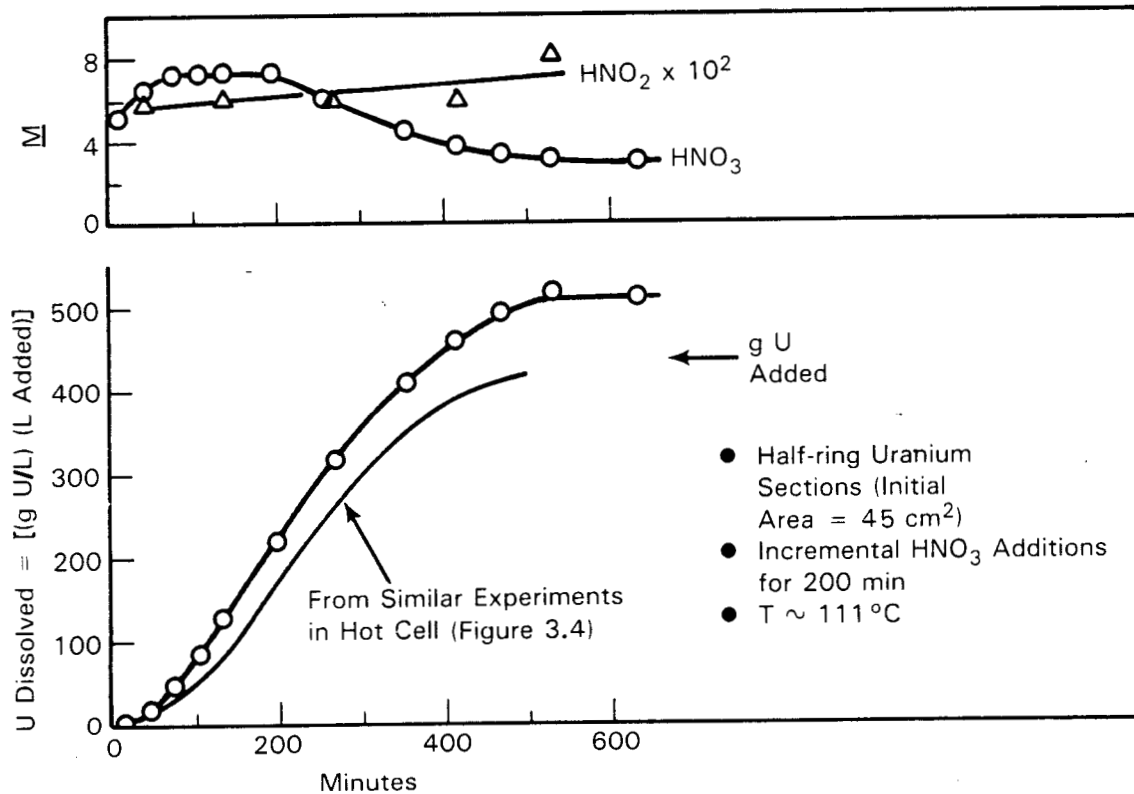


FIGURE 3.22. Early Complete Dissolution Experiment with Updraft Condenser

The final complete dissolution experiment was done primarily to obtain, for pyrophoricity testing, leached cladding hulls from the affected areas of ruptured fuel elements. Some dissolution rate data were also obtained during the initial dissolution period to get a semi-quantitative comparison of the dissolution rate of ruptured fuel.

The uranium dissolved in this experiment was a mixture of relatively small chunks, primarily from a ruptured inner element; of cracked, but nearly intact ~1.27 cm thick half-ring sections cut from a ruptured outer element; and of "sawdust" generated during the sectioning of the inner element. Of the 360 g U dissolved in this experiment, ~4% was in the "sawdust" fraction.

The uranium was immersed in 400 ml of 8 M HNO_3 in a vessel fitted with an updraft condenser and heat was applied to initiate the reaction. Severe foaming was encountered within ~10 minutes, apparently caused by the water soluble oil used as cutter lubricant, as discussed in Section 3.2.1. Because of this foaming, the heat input rate had to be decreased and it is probable

that the solution was not boiling. Solution temperature could not be measured in this experiment because of an equipment malfunction.

Analysis of solution samples, taken 0.5, 1.0, and 1.4 h after initiation of the reaction, showed the extent of U reaction to have been 10, 18 and 27% respectively. Comparison of these results with those shown in Figure 3.18 for intact ~1.27 cm thick rings in 8 M HNO_3 , where ~8% of the U reacted in the first 1.4 h, shows that the initial reaction rate was 3- to 4-fold higher with the segments of ruptured fuel than with intact fuel element sections. This much difference appears to be easily explainable on the basis of a larger surface area in the ruptured fuel case; however, a quantitative comparison is not possible because of the problems encountered in this experiment.

3.3 REFERENCES FOR SECTION 3.0

Bement, A. L. and J. L. Swanson. 1957. The Effects of Carbon Content on the Rate of Dissolution of Dinged Uranium in Nitric Acid. HW-52430, General Electric Company, Richland, Washington.

Davis, W., and H. J. deBruin. 1964. "New Activity Coefficients of 0-100 Percent Aqueous Nitric Acid." J. Inorg. Nucl. Chem. 26:1069-1083.

Dukes, E. K. and R. M. Wallace. 1961. "Determination of Hydrazoic Acid and Ferric Ion by Spectrophotometric Measurement of the Ferric Azide Complex". Analytical Chemistry 33(2):242-244.

Lacher, J. R., J. D. Salzman, and J. D. Park. 1961. "Dissolving Uranium in Nitric Acid". Industrial and Engineering Chemistry 53(4):282-284.

Pajunen, A. L., L. R. Michels, and D. J. Peck. 1984. Continuous Dissolver for Sheared N-Reactor Fuel - Preliminary Equipment Selection. SD-PFM-ES-002, Rockwell Hanford Operations, Richland, Washington.

Ryan, J. L., G. H. Bryan, M. C. Burt, and D. A. Costanzo. 1985. "Preparation of Acid Standards for and Determination of Free Acid in Concentrated Plutonium-Uranium Solutions." Analytical Chemistry 57:1423-1427.

Schulz, W. W. 1972. Shear-Leach Processing of N-Reactor Fuel -- Cladding Fires. ARH-2351, Atlantic Richfield Hanford Company, Richland, Washington.

Taylor, R. F., E. W. Sharratt, L. E. M. deChazal, and D. H. Logsdail. 1963. "Dissolution Rates of Uranium Dioxide Sintered Pellets in Nitric Acid Systems." J. Appl. Chem. 13:32-40.

4.0 TRANSURANIC ELEMENT CONTENT OF LEACHED FUEL HULLS

The transuranic element content of wastes is one of the factors that affects requirements for, and therefore the cost of, waste disposal. Accordingly, experiments were performed to measure the quantities of such elements in HNO_3 leached cladding hulls from irradiated fuel. The amounts found after leach conditions simulating those planned for use during processing of N-Reactor fuel elements in the PFM totalled 420 nCi/g hulls. An additional, more rigorous HNO_3 leach step reduced this amount, but only to 280 nCi/g hulls. These amounts are well above the maximum (100 nCi/g) allowed for disposal as low-level waste, so the hulls will require more expensive disposal as transuranic waste unless a more rigorous hulls decontamination process is developed.

The hulls used in these determinations were obtained from the complete dissolution experiment with irradiated uranium discussed in Section 3.2.1. Following dissolution of the irradiated uranium, the hulls were added to a dissolution of unirradiated uranium to simulate a batch dissolution procedure in which leached hulls are exposed to a second dissolution cycle to assure that reaction is complete. Following this second dissolution cycle half of the hulls were rinsed extensively with dilute HNO_3 and then dissolved for analysis. The other half of the irradiated hulls and half of the unirradiated hulls were leached for 7 h in boiling 8 M HNO_3 before they were rinsed and dissolved for analysis.

The hulls were obtained from two half-sections of an outer element and two half-sections of an inner element; both elements had been irradiated to the level giving a ^{240}Pu content of 6%. Each half portion that was dissolved for analysis consisted of one piece of each type of cladding.

The rinsing procedure involved extreme care to minimize the chance of cross-contamination from other sources within the hot cell. The samples were then added to a quantity of 0.8 M HF sufficient to give 0.15 M Zr and dissolved on standing overnight at room temperature. Nitric acid was then added to dissolve tin (Zircaloy contains 1.5% Sn) and the solutions were sampled for analysis.

The solutions containing the dissolved cladding hulls were analyzed for alpha- and gamma-emitting radionuclides, by decay energy analyses and for uranium by pulsed laser fluorimetry. Results are shown in Table 4.1.

As was pointed out earlier, the content of alpha-emitting transuranic radionuclides was found to be considerably greater than the 100 nCi/g level allowed for disposal as low-level waste. This was true even after the special leach under rigorous conditions, which did reduce the level from 420 to 280 nCi/g. The special leach also markedly reduced the uranium and fission product (^{125}Sb , ^{137}Cs , and ^{144}Ce) contents, but it had little effect on the content of ^{60}Co , which is an activation product formed within the cladding. The ^{125}Sb behavior appears to be anomalous, but was not investigated farther.

The uranium content of the unirradiated hulls that had undergone fuel dissolution plus special leach cycles was within a factor of two of the uranium content of the irradiated hulls that had undergone two fuel dissolution cycles. This fact, together with the roughly parallel behavior of uranium, transuranic elements, and most fission products observed with irradiated hulls, suggests that meaningful scouting studies of hulls decontamination methods (should such be desired) could be done with unirradiated fuel.

TABLE 4.1. Alpha- and Gamma-Emitting Radionuclides in N-Reactor Fuel Cladding Hulls

| Hulls Treatment | Uranium Content, g/g Hulls | Radionuclide Content, nCi/g Hulls | | | | |
|---|-------------------------------|--|---------------------|---------------------|---------------------|---------------------|
| | | Transuranic Alpha ^(a) | ⁶⁰ Co | ¹²⁵ Sb | ¹³⁷ Cs | ¹⁴⁴ Ce |
| Fuel dissolution ^(b) plus second dissolution cycle ^(c) | 1.2x10 ⁻³ | 420 | 6.7x10 ³ | 1.0x10 ⁵ | 2.0x10 ⁴ | 4.0x10 ³ |
| Fuel dissolution ^(b) plus second dissolution cycle ^(c) plus special leach ^(d) | 0.6x10 ⁻³ | 280 | 6.2x10 ³ | 1.8x10 ⁴ | 1.6x10 ⁴ | 2.4x10 ³ |
| Fuel dissolution ^(c) plus special leach ^(d) | 1.7x10 ⁻³ | ----- not present ^(e) ----- | | | | |

- (a) Comprised of 88% ²³⁹Pu + ²⁴⁰Pu and 12% ²³⁸Pu + ²⁴¹Am.
 (b) Eleven hour exposure to boiling solution; initially 5.5 M HNO₃, maximum total nitrate condition ~1 M UO₂(NO₃)₂ + ~7 M HNO₃, final composition ~2.2 M U + 3 M HNO₃.
 (c) 8.5 hour exposure to boiling solution, same composition range as in (b) except that the maximum total nitrate condition was somewhat higher because of more rapid acid addition.
 (d) Seven hour exposure to boiling 8 M HNO₃.
 (e) Unirradiated fuel.

5.0 RESIDUAL UNDISSOLVED SOLIDS

Near the end of the complete dissolution tests discussed in Sections 3.2.1 and 3.2.8, black solids flaked off the cladding at what had been the U/Zr interface and began circulating in the solution. These flakes were very thin but some of them were up to 6 to 8 mm in diameter. They appeared to largely disappear as dissolution was continued, but this may have been due at least as much to their breaking up into many tiny particles as to their dissolution. Provisions for dealing with such material should be included in design of a plant for the shear/leach processing of N-Reactor fuel.

These black solids were collected from two of our early complete dissolution tests to conduct some limited characterization tests. In one instance both inner and outer element sections were dissolved and in the other instance only an outer element section was dissolved. In both cases the quantity of solids collected after near-complete dissolution amounted to $\sim 1 \times 10^{-4}$ g solids/g U dissolved. These quantities were determined by the weight gain of 0.8 μ m filters after water rinsing and air drying.

Portions of the rinsed and dried solids were tested for pyrophoricity by sparking with a Tesla coil. The first portion tested did produce one good flash, demonstrating that pyrophoric material was present, but tests of other portions of the same batch and of several portions of the second batch were negative. It was thus concluded that this black solid should not pose a high pyrophoricity hazard. As a result of later tests, which are discussed in Section 10, it is speculated that the one flash that was observed with these solids may have involved a small piece of undissolved uranium metal and thus had nothing to do with the black solids themselves.

Several particles of the black solid were analyzed by scanning electron microscopy/energy dispersive spectroscopy (SEM/EDS) and were found to contain approximately equal weights of U and Zr; this gives a mole ratio of Zr-to-U of about 2.6. The relatively high U content means that solids from irradiated fuel should be expected to be highly radioactive from the contained plutonium and fission products.

Qualitative observations indicate that the nature and amount of black solids resulting from dissolution of irradiated fuel were approximately the same as from dissolution of unirradiated fuel. However, because of the difficulties involved, no attempt was made to collect and characterize the solids resulting from irradiated fuel dissolutions.

6.0 SHEAR COVER-GAS EVALUATION

The only aspect of the shearing operation of the shear/leach process that was examined in this study involved the atmosphere to be maintained within the shear to minimize or prevent sparks or fires involving uranium or zirconium. This was addressed only through examination of the literature.

The result of this review leads us to believe that several methods exist to assure the safety of the shearing of N-Reactor fuel. The information we reviewed indicates that shearing in air may, in fact, be safe enough. Several approaches exist for further increasing the safety level. Considering processing as well as safety aspects, use of a water deluge appears to be the best choice for further development and testing.

Any conclusions drawn as a result of this review must be qualitative because of the current lack of some information needed to quantify effects. Two such pieces of information are 1) the quantity and size of the small fragments produced during shearing of N-Reactor fuel and, 2) the localized surface temperatures that result from shearing. Even if this information were known for unirradiated fuel, it is likely that different results would be obtained with irradiated fuel.

Another reason for qualitative comparisons is that the magnitude of a reaction that could be tolerated during shearing has not been defined. While the release of small, hot particles (sparks) can be spectacular, it may cause no safety problem. If the quantity of sparks is small and if the sparks cannot contact any readily combustible materials, then the result is probably tolerable; this is especially true if the sparks occur in a location where the offgas will be treated to remove vaporized radionuclides.

Among the highlights of the literature review that are most pertinent to the shearing problem are:

1. Zirconium and uranium can react very rapidly and vigorously with either oxygen, nitrogen or mixtures thereof.
2. The most important parameters leading to higher rates of reaction of zirconium and uranium with oxygen and nitrogen are decreasing solid particle size, increasing moisture content of the gas, and increasing temperature.

3. Any cover gas must be quite dry to be completely effective in preventing sparking during shearing. The safest cover gas is dry argon; no reaction is possible under this condition. Argon can contain up to ~2% O_2 and still be safe. No quantitative data on allowable moisture content were found, but indications are that it should be quite low.
4. Nitrogen cover gas would be safer than air, but not as safe as argon.
5. Air cover gas may be safe enough, even though some sparking will doubtless occur.
6. Cutting and machining of zirconium and uranium have routinely been performed safely "under water" (either submerged or with a good stream of water directed at the affected area).

While blanketing the shear with dry argon may be the safest approach, other approaches may well be safe enough, and may, in fact, be the preferred choice because of cost or operational considerations. The question tends to resolve to "how safe is safe enough." There appear to be differences of opinion throughout industry on this question, as illustrated in the following discussion.

Considerable work has been done on shearing of light water reactor (LWR) fuels, which are UO_2 in Zircaloy and hence pose the same problem as N-Reactor fuel with regard to Zr reactions, but not with regard to U reactions. Some LWR fuel reprocessors (and prospective reprocessors) have sheared (or planned to shear) under an inert gas blanket, while others have decided that shearing in air is adequately safe. For example, at the WAK pilot plant in Germany, the fuel is cut in air (using a water spray to control dust) while at the SAP pilot plant in France, a nitrogen purge is used. In this country, the Allied General Nuclear Services (AGNS) plant was planning to use an air purge in their shear while Exxon Nuclear was planning to use an inert gas purge.

When irradiated N-Reactor fuel was reprocessed at Nuclear Fuels Services (NFS), the shear was purged with argon. However, some former NFS employees feel that there were times when shearing was done in an air atmosphere with no noticeable impact. In shearing tests performed in air at Oak Ridge National

Laboratory with unirradiated N-Reactor fuel, it was reported "Some sparking occurred during shearing, but there appeared to be no real hazard involved in shearing this type of fuel." (Ferguson 1965). Thus, there is some reason to believe that shearing in air may be adequately safe, especially if the sheared fuel is not allowed to accumulate where subsequent sparks might ignite it.

N-Reactor fuel element crushing tests have also been performed (in air); these results are thought to have some pertinence to the shearing case. Smithers (1967) observed only minor sparking with unirradiated material, but more pronounced sparking with irradiated fuel. He also observed a greater degree of uranium crumbling and cracking, and a more extensive separation of cladding, with irradiated fuel.

In the N-Reactor fuel fabrication process, the elements are routinely cut and machined "under water". Some of these operations are performed with the fuel actually submerged under water, while others involve the use of water jets directed at the affected surface. Such processes appear to be very safe, and appear to offer a simple way to improve the safety of a fuel shearing operation. The water approach also blends well with the fuel storage step preceding shearing and the storage (or dissolution) step following shearing, where water is used.

Regardless of the protective atmosphere used in the shear, accumulation of shear fines under water should be minimized. Periodic eruptions have been observed with uranium fines stored under water (Smith 1956a). Such events can be prevented by routing fines to the dissolver, where uranium is dissolved in nitric acid. Zircaloy fines will not dissolve; they should be collected and removed to prevent them from causing problems in subsequent process steps. These collected fines may pose a safety problem, depending on their quantity and size. The magnitude of such a problem would likely be less if shearing is done in an aggressive environment, so that potentially reactive particles can react as they form, than if shearing is done in an inert environment.

6.1 HIGHLIGHTS OF THE LITERATURE SURVEY

The publications examined during this review are listed in the following section. This section presents excerpts of some of the key information of

special relevance to the safety aspects of the shearing operation.

Inconsistencies in numerical values exist between different sources; no effort was made to explain these.

- Zr particles under ~ 0.06 mm diameter are considered to be explosive, and those under ~ 1 mm diameter are considered to be a fire hazard; their pyrophoricity in a gaseous environment increases with the oxidizing power of the gas; their pyrophoricity in a water environment is maximum at 3 to 25% water; alternating wet and dry conditions increases pyrophoricity (Kullen, Levitz and Steindler 1977).
- Zr powder is usually stored under water (Kopelman and Compton 1953). Wet Zr powder is safer to handle than dry powder but, once ignited, wet powder will burn more violently than dry powder; powder containing 5-10% H_2O is the most dangerous (Van Atta 1949). Water content of wet Zr powder recommended to be $>25\%$; water content 5 to 10% burns more violently than dry powder and is apt to explode (Allison 1960).
- Ignition by electric spark of Zr dust clouds can occur in Ar/ O_2 mixtures containing $>4\%$ O_2 and in N_2/O_2 mixtures containing $>3.3\%$ O_2 (Bulmer 1969). Another source (Jacobson, Cooper and Nagy 1964) lists 3% O_2 in Ar/ O_2 Ar mixtures and 3 to 4% O_2 in N_2/O_2 mixtures. Dusts of Zr will ignite in pure N_2 (or CO_2) under some conditions (Santangelo 1956).
- Electric spark ignition of dust clouds of U occurs at lower O_2 concentrations than does ignition of Zr; 2% O_2 is sufficient for U in O_2 /Ar mixtures, while only 1% O_2 is sufficient in O_2/N_2 mixtures (Jacobson, Cooper and Nagy 1964). Pure N_2 reacts with massive U at elevated temperatures, $\sim 330^\circ C$ being required with moist N_2 and $\sim 370^\circ C$ being required with dry N_2 (Wilkinson 1962).
- In tests to compare the U-fire extinguishing properties of Ar and N_2 , Ar was effective but N_2 gave an initial intensification of burning; thus N_2 is not recommended (McLaughlin 1970).
- Corrosion of U in air increases with increasing relative humidity up to $\sim 1\%$ (Wilkinson 1962).

- Vigorous reactions have occurred with U powder stored under water when sufficient powder accumulated; conversely, burning U chips have been extinguished by water (Smith 1956b). U fines stored under water produced geysers at ~1 month intervals (Smith 1956a).
- Recommendation that scrap U be stored under mineral oil or water; U slowly oxidizes in contact with water to form hydrogen (Jacobson, Cooper, and Nagy 1964).

6.2 BIBLIOGRAPHY FOR SECTION 6.0

- Allison W. W. 1960. Zirconium, Zircaloy, and Hafnium Safe Practice Guide for Shipping, Storing, Handling, Processing and Scrap Disposal. WAPD-TM-17, Bettis Atomic Power Laboratory, Pittsburg, Pennsylvania.
- Andersen, H. C. and L. H. Belz. 1953. "Factors Controlling the Combustion of Zirconium Powders." J. Electrochem. Soc. 100(5):240-249.
- Bennellick, E. J. 1966. A Review of the Toxicology and Potential Hazards of Natural, Depleted and Enriched Uranium. AHSB(RP)-R-58, United Kingdom Atomic Energy Authority, Harwell, Didcot, Berkshire.
- Bulmer, G. H. 1969. Recommendations on the Safe Handling of Zirconium Metal and Zirconium Alloys. AHSB(S)R-167, United Kingdom Atomic Energy Authority, Authority Health and Safety Branch, Risley, Warrington, Lancashire, England.
- Committee on Combustible Metals, A. S. Prokopovitsch, Chm. 1982. Standard for the Production, Processing, Handling, and Storage of Zirconium. National Fire Protection Association, Batterymarch Park, Quincy, Massachusetts.
- DeHollander, W. R. 1956. An Evaluation of the Zirconium Hazard. HW-44989, Hanford Atomic Products Operation, Richland, Washington.
- Dravnieks, A. 1950. "The Kinetics of the Zirconium-Nitrogen Reaction at High Temperatures." J. Am. Chem. Soc. 72:3568-3571.
- Exxon Nuclear Company. 1977. Preliminary Safety Analysis Report, Nuclear Fuel Recovery and Recycling Center. XN-FR-32, Rev. 1, Exxon Nuclear Company, Inc., Richland, Washington.
- Ferguson, D. E. 1965. Chemical Technology Division Annual Progress Report for Period Ending May 13, 1965. ORNL-3830, p. 51, Oak Ridge National Laboratory, Oak Ridge, Tennessee.
- Gulbransen, E. A. and K. F. Andrew. 1949. "Kinetics of the Reactions of Zirconium with O₂, N₂ and H₂." Metals Trans. 185:515-525.

- Guldner, W. G. and L. A. Wooten. 1948. "Reactions of Zirconium with Gases at Low Pressure." Trans. Electrochem. Soc. 93(6):223-235.
- Hanford Operations Office. 1954. AEC Uranium Fire Experience. HAN-64841, Atomic Energy Commission, Richland, Washington.
- Hartmann, I. 1948. "Recent Research on the Explosibility of Dust Dispersions." Ind. Eng. Chem. 40(4):752-758.
- Hartmann, I., J. Nagy and H. R. Brown. 1943. Inflammability and Explosibility of Metal Powders. Bureau of Mines Report of Investigations 3722. U.S. Dept. of the Interior, Bureau of Mines, Washington, D. C.
- Hartmann, I., J. Nagy and M. Jacobson. 1951. Explosive Characteristics of Titanium, Zirconium, Thorium, Uranium and Their Hydrides. Bureau of Mines Report of Investigations 4835. U.S. Dept. of the Interior, Bureau of Mines, Washington, D. C.
- Hayes, E. T. and A. H. Roberson. 1949. "Some Effects of Heating Zirconium in Air, Oxygen, and Nitrogen." Trans. Electrochem. Soc. 96(3):142-151.
- Jacobson, M., A. R. Cooper and J. Nagy. 1964. Explosibility of Metal Powders. Bureau of Mines Report of Investigations 6516. U.S. Dept. of the Interior, Bureau of Mines, Washington, D. C.
- Katz, J. J. and E. Rabinowitch. 1951. The Chemistry of Uranium Part I. The Element, Its Binary and Related Compounds. National Nuclear Energy Series Division VIII. Vol. 5. McGraw-Hill Book Co., Inc., New York.
- Kehoe, E. J., F. L. Brannigan and M. Eisenbud. 1950. Fire Protection Precautions for Handling Uranium Turnings, Chips, Borings, Sawdust, and Powder. NY00-1505, Technical Information Division, ORE, Oak Ridge, Tennessee.
- Kopelman, B. and V. B. Compton. 1953. "Spontaneous Combustion of Metal Powders." Metal Prog. 63(2):77-79.
- Kullen, B. J., N. M. Levitz and M. J. Steindler. 1977. Management of Waste Cladding Hulls Part II. An Assessment of Zirconium Pyrophoricity and Recommendations for Handling Waste Hulls. ANL-77-63, Argonne National Laboratory, Argonne, Illinois.
- Levitz, N. M., B. J. Kullen and M. J. Steindler. 1975. Management of Waste Cladding Hulls Part I. Pyrophoricity and Compaction. ANL-8139, Argonne National Laboratory, Argonne, Illinois.
- Lustman, B. and F. Kerze, Jr. eds. 1955. The Metallurgy of Zirconium. National Nuclear Energy Series Division VII, Vol. 4. McGraw-Hill Book Co., Inc., New York.

- Mallett, M. W., J. Belle and B. B. Cleland. 1954. "The Reaction of Nitrogen with, and the Diffusion of Nitrogen in, Beta Zirconium." J. Electrochem. Soc. 101(1):1-5.
- McCoy, H. E. 1960. "Pyrophoricity of Uranium and Zirconium." Nucl. Safety 2(2):17-19.
- McLaughlin, L. M. 1970. Sprinkler Demonstrations at the Oak Ridge Y-12 Plant. Y-DA-3318, Oak Ridge Y-12 Plant, Union Carbide Corporation, Oak Ridge, Tennessee.
- Pearce, R. J. 1968. The Ignition of Uranium Part I, A Literature Survey. RD B N-1134, Berkeley Nuclear Laboratories, Berkeley, England.
- Safety and Fire Protection Branch. 1956. Zirconium Fire and Explosion Hazard Evaluation. TID-5365, U.S. Atomic Energy Commission, Washington, D. C.
- Santangelo, J. C. 1956. "Fire and Explosion Hazards of Metallic Zirconium." Accident and Fire Prevention Information Issue No. 44, U.S. Atomic Energy Commission. National Technical Information Service, Springfield, Virginia.
- Smith, R. B. 1956a. "Pyrophoricity-A Technical Mystery under Vigorous Attack." Nucleonics 14(12):28-33.
- Smith, R. D. 1956b. The Fire Properties of Metallic Uranium. TID-8011, Technical Information Service, Oak Ridge, Tennessee.
- Smithers, R. M. 1967. Press Crushing of Zirconium Clad Fuel Elements as a Mechanical Decladding Technique. ISO-1038, Isochem, Inc., Richland, Washington.
- Staff of the Northwest Electrodevelopment Laboratory, Bureau of Mines, under the direction of Stephen M. Shelton. 1956. Zirconium Its Production and Properties. Bureau of Mines Bulletin 561, U.S. Government Printing Office, Washington, D. C.
- Tetenbaum, M., L. Mishler, and G. Schnizlein. 1962. "Uranium Powder Ignition Studies." Nuc. Sci. Eng. 14:230-238.
- Van Atta, F. A. 1949. "Zirconium Industrial Data Sheet D-Chem. 45." Nat. Safety News. pp.39-42.
- West, G. A. and C. D. Watson. 1967. Safety Studies of the Shear-Leach Processing of Zircaloy-2-Clad Spent Nuclear Fuels. ORNL-4061, Oak Ridge National Laboratory, Oak Ridge, Tennessee.
- Wheeler, V. J. and R. M. Dell. 1964. The Oxidation and Ignition of Uranium Mononitride and Uranium Monocarbide. AERE-R4600, Atomic Energy Research Establishment, Harwell, Berkshire, England.

Wilkinson, W. D. 1962. Uranium Metallurgy Vol. II: Uranium Corrosion and Alloys. Interscience Publishers, New York.

Zima, G. E. 1959. A Review of the Properties of Zircaloy-2. HW-60908, Hanford Atomic Products Operation, Richland, Washington.

Zima, G. E. 1960. Pyrophoricity of Uranium in Reactor Environments. HW-62442, Hanford Atomic Products Operation, Richland, Washington.

7.0 EVALUATION OF POTENTIAL FOR RUNAWAY REACTIONS DURING DISSOLUTION OF SHEARED N-REACTOR FUEL

The procedure used for processing of irradiated Hanford N-Reactor fuel at the Nuclear Fuels Services (NFS) plant involved collecting sheared fuel within perforated stainless steel baskets fitted with a carbon steel liner; placing filled baskets in wells spaced around the circumference of a circular, annular dissolver; and then adding nitric acid to the empty dissolver to begin the dissolution process. Several fires occurred during the processing. Most of these fires, fourteen out of nineteen total, occurred in the dissolvers and, although not observed directly, were indicated by up to 10- to 12-inch diameter holes having been melted through the one-quarter inch thick stainless steel dissolver baskets (Schulz 1972).

The fourteen incidents represent only a small fraction of the number of baskets processed and in no case did a fire in one basket cause a problem in another basket. In all these cases the fires occurred in the upper portions of the baskets. In addition to these fires, which apparently all occurred while processing fuel irradiated to between 1000 and 4000 MWd/tonne, several other dissolver pressurizations occurred (Schulz 1972).

Schulz (1972) proposed that the fires observed at NFS (both those occurring in the dissolver and the others that occurred in the leached cladding hulls) were due to the ignition of nitric acid-sensitized weld beads resulting from the braze alloy (Zr-5 wt% Be) used in the end closures of this fuel. The purpose of the study described in this section is to examine this and other hypotheses and assess their plausibility in explaining the fires and pressurizations that occurred in the NFS dissolvers. The fires that occurred during handling of leached cladding hulls are addressed in subsequent sections.

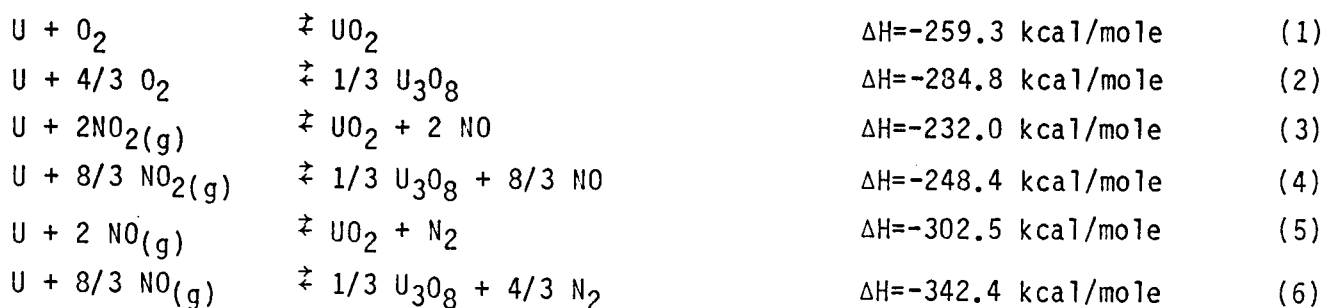
Our study concludes that exothermic reactions of U were the dominant, if not the sole, heat source of the dissolver fires. Fifteen potential exothermic U reactions that can occur in the liquid or vapor space of a U dissolver are listed. Evidence is shown to indicate that at the uranium particle sizes found for some NFS sheared fuel, some of these highly exothermic reactions can be expected to be very fast. Evidence is also

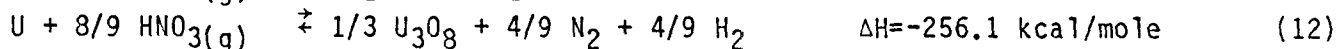
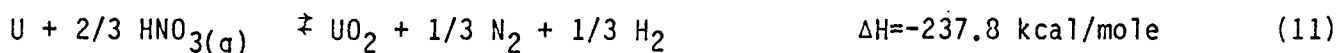
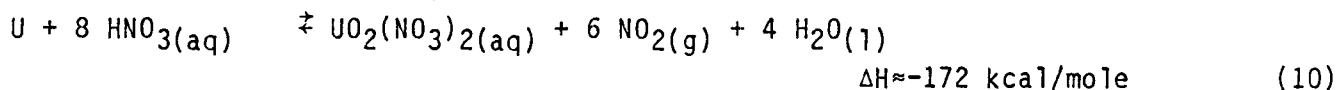
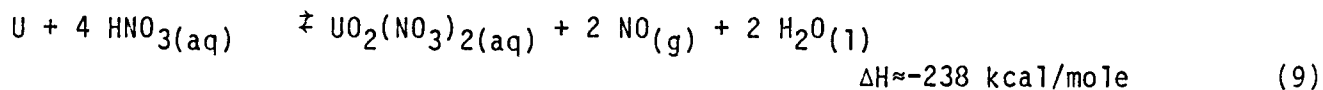
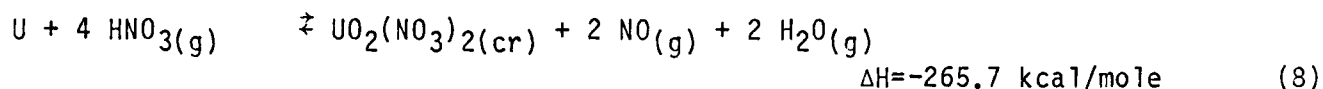
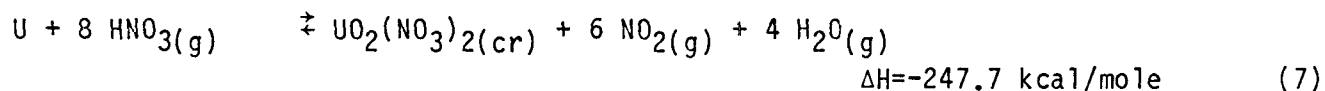
presented to show that these U reactions are much faster than similar reactions with Zr. It is shown that even the relatively slow reaction of water vapor with U metal may have been adequate to produce high temperatures in a reasonably short time under NFS dissolver conditions. Thermodynamic calculations show that burning of all of the braze alloy in the fuel does not come close to producing the energies required to cause the effects observed in the NFS dissolvers, and it is extremely doubtful if even burning all the zirconium present could have produced such consequences. It is our conclusion that uncontrolled (inadequately cooled) exothermic reactions of uranium metal with the oxidants present caused the observed pressure and temperature excursions and the observed damage to the dissolver baskets.

This study also concludes that there is reason to be concerned that shearing of irradiated fuel may produce considerably higher uranium surface area per unit weight and thus more reactive material than that produced in the same manner from unirradiated fuel. It also indicates that it is reasonable to expect that long term water basin storage of failed fuel may further magnify this problem.

7.1 POTENTIAL U METAL REACTIONS AND REACTION ENERGETICS

Uranium and zirconium are highly reactive metals and undergo exothermic reactions with a wide variety of oxidants. In a nitric acid dissolver for uranium, oxidizing agents present and capable of exothermic reaction with U include O_2 , NO_2 , NO , H_2O , HNO_3 , N_2 , and H_2 . The following list of reactions constitute most of the potential reactions that are possible with these oxidants. Values of the heats of reaction per mole at uranium metal at $25^\circ C$, ΔH_{298} , are based on the data from Wagman et al. (1982).





Reactions other than those shown above can be written, but they have comparable energy yields. Some of the above reactions will only occur over a limited temperature range. For example for U that is exposed to liquid nitric acid, reactions (9) and (10) will be major energy producers. Nitric acid vapor can be expected to react with U through reactions (7) and (8) at low temperature ($\sim 200^\circ\text{C}$) and by reactions (12) and (11) at higher temperatures where uranyl nitrate is not stable.

The heats of reaction of U metal with O_2 , HNO_3 (except for reaction 10), NO_2 , and NO , are all more exothermic than 230 kcal/mole U. These are extremely energetic reactions. Even the markedly less energetic reaction of U with water vapor (reaction 13) produces as much heat (144 kcal/mole U) as does the reaction of Mg metal with O_2 . Indeed the adiabatic flame temperature of stoichiometric U burning in steam will be greater than that of Mg burning in air. It is easily shown using appropriate heat capacity data that the adiabatic reaction temperature of the stoichiometric reaction of 100°C steam with U metal will be at least that of the melting point of UO_2 ($\sim 2850^\circ\text{C}$), which is much higher than the melting point of stainless steel.

7.2 U AND Zr METAL REACTION RATES

The preceding section listed fifteen energy producing reactions of U metal that could occur in a nitric acid dissolver. Similar reactions to many of these could also be given for Zr with heats of reaction that are similar to the corresponding ones for uranium. However, the reaction rates at normal temperatures are much lower for Zr than for U. In the cases where oxide is the product or byproduct, this is no doubt at least partly due to the fact that Zr forms a very protective oxide film where U does not. Thus, massive Zr is for practical purposes inert to nitric acid, water, and air whereas U is not; this is the reason for cladding the U with Zr in the first place.

Uranium powder has been found to be much more pyrophoric than zirconium powder and can self-ignite and burn vigorously under water whereas Zr powder of the same particle size is safely stored under water. Spontaneous ignition is also known for massive uranium but is not for zirconium (DeHollander 1956).

Rate of oxidation, rate of heat generation, and in turn rate of temperature rise in an inadequately cooled system will depend upon metal surface area, which is related to particle size. Cooling by convection and conduction is severely decreased when particle size is reduced and the interstices are largely filled by a gas phase either by being above the liquid phase or by rapid gas generation such as might occur through reactions (9) or (10). Thus, whereas massive uranium is dissolved by nitric acid only moderately rapidly, turnings, powder, or sintered metal can react with nitric acid vapor or nitrogen dioxide with explosive violence, and the metal should be added to acid rather than the reverse to minimize vapor phase contact (Warf 1958). Attempts at dissolution of uranium metal sludges and chips have resulted in spontaneous fires and at least one explosion, and uranium powder has been found to explode on mixing with even 5% HNO_3 (Hanford 1954).

N-Reactor fuel weld beads are sensitized by selectively leaching Be from the braze alloy with nitric acid, leaving a Zr matrix having a very high surface area. When dry, the increased surface area both increases the total area (per unit of heat capacity) available for reaction and markedly decreases the heat transfer rates. Poorer heat transfer in this dry material also greatly increases the ease of ignition because the energy of an impact or

other source such as an electrical spark, (and the energy of oxidation resulting from such local heating) is not dissipated as rapidly as in massive metal. This results in high local temperatures and thus continuing oxidation.

In a wet system (such as the ignition of U powder under liquid water cited by Kopelman and Compton (1953)), ignition is achieved because the net reaction rates of high surface area powder throughout the entire powder mass exceed the relatively rapid rate of heat transfer.

An intermediate case exists in which reaction in an immersed system either produces gaseous products (such as reactions (9) and (10)) rapidly or liberates adequate heat to cause rapid boiling. This will first create a gas-filled system with poor heat transfer and low heat capacity, but reaction may still be occurring in an aqueous phase on wetted surfaces. Inadequate heat removal will allow conversion to completely gas-phase reactions as the wet surfaces boil dry.

Spontaneous ignition (or at least runaway reaction to steam explosions, etc.) in either liquid phase or dry phase systems can occur anytime that a reaction or reactions are strongly exothermic, maintain negative free energies of reaction to high temperature, and have a greater rate of heat production than rate of heat transfer away from the reaction zone. In all cases, temperature rise will be exponential because reaction rates increase with temperature. Even reactions that are very slow at the initiation temperature can lead to spontaneous ignition or explosion if heat loss out of the reaction zone is poor. Such poor heat loss can result from very low heat transfer coefficients (such as in dry or drained powders), poor heat transfer out of the overall reaction system (because of external insulation), or increased reaction zone size (which prevents adequate heat removal rates).

Apparently dissolution rates were fast enough in NFS dissolution of N-Reactor fuel to often cause dissolver pressurizations, even during processing of fuel irradiated to <1000 MWd/tonne (Schulz 1972). Liquid from the dissolver was "burped" into the off-gas system at least once (Savannah River 1970). During this study we discussed the NFS processing with J. P. Duckworth, who was in charge of operations at NFS during the period in

question. He described some reactions that were vigorous enough to lift lids of the dissolvers even though the off-gas system was designed for several times the anticipated gas generation rate and the dissolver lid seals were designed to release gas at pressures of 4 to 5 psi. Also cladding hulls were sometimes transported over the top of the dissolver baskets.

Clearly, reaction rates at NFS were sometimes beyond the capacity of the dissolver, and heat production rate was probably beyond the design capacity also. All fires were in the upper portion of the baskets (Schulz 1972) where vapor phase was most likely to hinder heat transfer. Several were in the early stages of dissolution when the dissolver may have been incompletely filled and when a large fraction of U metal fines may have been present. These observations point more strongly to the NFS dissolver pressurizations and fires being due to runaway dissolution and vapor phase oxidation reactions of U metal than they do to ignition of sensitized weld beads.

Further evidence supporting a runaway U metal reaction conclusion is the fact that a spontaneously ignited U metal fire occurred several years ago in the Hanford Redox Plant while processing Al-clad uranium metal fuel; thus no reactions involving Zircaloy cladding or sensitized weld beads could have contributed to this fire. In this incident, a large heel of declad and partially dissolved uranium was allowed to stand with only ~50% of the fuel immersed in water. Pressure excursions were noted after ~1.5 days and cooling was required to maintain temperature control. Subsequent addition of nitric acid resulted almost immediately in a high solution specific gravity, indicating extremely rapid dissolution. A short time later it became evident that both the cooling coils and the dissolver vessel had lost their integrity. This dissolver fire was concluded to have been initiated in the warm moist atmosphere above the water level. Uranium oxides produced by these vapor phase reactions would react very rapidly with HNO_3 , releasing a large amount of heat very rapidly.

Conditions necessary for ignition can be estimated from heats of reaction, rates of reaction, and heat transfer rates. Unfortunately, reaction rates with most of the oxidants in reactions (1) to (15) are not available. The reaction rates at near 100°C , which may initiate an accelerating rise from normal dissolver operating temperature, are of primary importance instead of

those at high temperature because all the strongly exothermic reactions will be rapid at high temperature. The rate of reaction of uranium with dry O_2 is about 5,000-fold slower than the rate with water (Baker et al. 1966a). The reaction rates of U in liquid water and water vapor are about the same (Baker et al. 1966a; Wanklyn and Jones 1962). Reaction rates with NO , NO_2 , and HNO_3 gases are not known, but from qualitative observations (Warf 1958; Hanford 1954) the rates for NO_2 and HNO_3 are expected to be much faster than those for water vapor. Aqueous nitric acid reacts very much more rapidly with U metal than does water.

The possible rate of temperature increase occurring with uranium metal in the vapor phase due to the reaction of water vapor alone at $100^\circ C$ initial temperature can be estimated. This vapor phase situation might arise with baskets of chopped fuel in place either before complete dissolver filling or because rapid gas evolution forces liquid from the basket. Note again that all fires at NFS were in the upper portions of the baskets. The rate of reaction of U with saturated $100^\circ C$ steam is about $4 \text{ mg cm}^{-2} \text{ hr}^{-1}$ (Baker et al. 1966a; Wanklyn and Jones 1962). A 3 kg sample of NFS-sheared N-reactor fuel was found in 1968 to have 64% of the material in the minus 4-mesh size (Schulz 1972). Conservatively assuming that this material had a surface area twice that of uniform 4-mesh spheres, assuming no heat transfer from U metal to its surroundings and using the heat of reaction for reaction (13) and a U heat capacity of $6.61 \text{ cal deg}^{-1} \text{ mole}^{-1}$ (Wagman et al. 1982) gives a temperature rise rate of $2^\circ C \text{ min}^{-1}$. Because the reaction rate increases in this temperature range by a factor of about 1.8 for each ten degree temperature rise (Baker et al. 1966b), the temperature would increase to incandescence in under 15 minutes in an insulated system starting at $100^\circ C$.

The assumption above of no heat transfer out of the system is certainly not completely valid, but the assumption of reaction rate and reaction heat for pure water vapor is extremely conservative for the rates and heats that might be expected in the vapor phase over boiling 11-13 M HNO_3 . These faster reaction rates, higher heats of reaction, possible much larger-surface area than the conservative estimate above, and fission product heating would all increase total heat generation rates thereby offsetting real heat losses.

This calculation shows that there was real potential for runaway reaction and high temperature excursion in vapor space in the NFS dissolvers. Such vapor space existed in the upper portions of the baskets as nitric acid was added to the dissolver with filled baskets in place and may have also formed by rapid gas formation and boiling forcing liquid out of the baskets. The baskets had only 1/8-inch diameter holes and total 5.5% of free space (Schulz 1972), and had, at the start of dissolution, mild steel liners that had to be dissolved through before liquid could enter the baskets. It is likely that when the first nitric acid reached the uranium, the baskets were mostly empty of liquid and the flow area was much less than 5.5%.

Two events demonstrate that, once runaway reaction and temperature excursion occur, the U mass can continue to heat to very high temperatures. One of these is the Redox dissolver incident where holes were burned through the dissolver coils and the dissolver vessel itself after ignition of massive U metal in the vapor space over water (Harmon 1960). The other is experimental work on reaction of steam with Zircaloy-clad massive U metal (Troutner 1960). In this work, a single-pinhole-defected, clad uranium rod 2 to 3 inches long reacted with 310°C steam rupturing the element and leading to an orange-red glow (estimated 700°C) as the uranium reacted.

7.3 NFS DISSOLVER ENERGY BALANCE

The heat required to produce the effects observed in the NFS dissolver baskets (10-to-12-inch diameter holes through one-quarter inch thick walls) was estimated to aid in determining the likely cause of the effects. Two such estimates were made.

The first estimate considered only the heat required to melt a hole of the observed size. The assumptions were made that the hole melted is circular and of 11 inches diameter, that the melting point is 1427°C (that of 304 stainless steel), that the heat of fusion and density of stainless steel are those of iron, and that the heat capacity is that of iron at 100°C and is constant. This latter assumption is conservative, because heat capacity actually increases with temperature. Additional conservatism was introduced by ignoring any possible heats of phase transitions in the steel. Using the properties of iron given by Wicks and Block (1963), melting such a hole would have required 664 kcal.

If only Zr burned in oxygen (either braze alloy or hulls themselves), the amount of Zr required to produce this heat can be calculated from the heat of formation of ZrO_2 of 263 kcal/mole (Wagman et al. 1982). Thus 2.6 moles Zr would have been required if there was perfect heat transfer to the steel, no heating of any uranium, no heating of nitrogen from the air, and no heat capacity for ZrO_2 . Even with such totally unrealistic assumptions, this still amounts to 0.55% of the total Zr expected in the basket.

The second estimate, which is much more realistic, involves consideration of the heat capacities of other materials present and assumes a reasonable distribution of fuel throughout a dissolver basket. If the heat is supplied by burning of Zr in air, enough heat must be released to also heat four moles N_2 per mole O_2 and the U metal intimately associated with the Zr to the melting point of stainless steel. We can postulate no heat concentrating mechanism leading to melting of a hole in a basket; that is, only reactions of the fuel contained in that cross-sectional portion of the basket could be focused on the effected zone. Thus, the fraction of the fuel within a portion of the basket that must react to melt the walls of that portion is the same as the fraction of the total fuel that must react to melt the total basket. Using these reasonable assumptions, we calculated the fraction of Zr that would have had to have burned if only Zr burning in air supplied the heat input. Using the same heat capacity and heat of fusion data and assumptions as before, the heat required to melt an entire NFS basket is found to be 1.89×10^4 kcal. The heat required to bring the associated uranium metal to the stainless steel melting point is 3.91×10^4 kcal, based on the expected basket uranium content determined from the reported packing density and Zr/U ratio of sheared fuel (Ludowise 1983) and reported heat capacities, heats of transition, and heat of fusion (Wicks and Block 1963). The sum of these two heat requirements is 5.80×10^4 kcal.

The heat produced by burning with oxygen all the Zr in the basket is 1.15×10^5 kcal. Thus, burning of 50% of all the Zr in the basket would have been required to raise the temperature of the uranium present to the melting point of stainless steel and to melt the basket assuming absolutely no heat loss from the system before basket melting is accomplished. This does not include the fact that all unburned Zr, all ZrO_2 produced, and four moles of N_2

per mole Zr burned must also be heated to this temperature. Including these indicates that 65% of the Zr must burn without any heat loss whatsoever in order to raise the temperature of all of these materials to the melting point of the stainless steel.

It is extremely unlikely that the observed damage would have occurred in the NFS dissolvers even if all the zirconium present burned. This becomes apparent when one considers that, for the calculated amount of heat to have produced the effects described, one must assume excellent heat transfer through a jumble of chopped fuel to the stainless steel basket, and, on the same time-scale, virtually no heat transfer away from the basket or, if only the Zr in one region reacted, no heat conduction through the 1/4-inch thick stainless steel away from the reaction zone.

With the above analysis demonstrating the improbability that Zr reactions could have burned the holes in the NFS dissolvers, it is completely clear that the energy of burning of the sensitized braze alloy present in the ends of these fuel elements falls very far short of the energy required to produce the effect observed. Based on the quantity of braze alloy per fuel element, according to R. T. Johnson of UNC Nuclear Industries, we calculate that the braze alloy constitutes about 1.3% of the total zirconium present. On this basis, the braze alloy could have supplied no more than 2% of the heat required in the above calculations and its burning could not have created the basket holes.

Because this analysis shows that reactions of Zr could not have caused the dissolver fires observed at NFS, the inescapable conclusion is that runaway oxidation of uranium produced these events. N-Reactor fuel contains 5.5-fold more moles of U than Zr, so there is no shortage of this reactive material.

7.4 POSSIBLE CONTRIBUTIONS OF IRRADIATION LEVEL TO RUNAWAY DISSOLVER REACTIONS

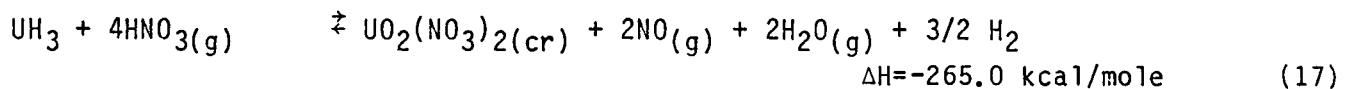
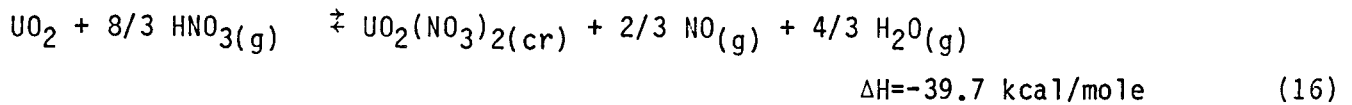
Even though our dissolution rate comparison (Section 3.2.1) showed little difference in the dissolution rates of irradiated and unirradiated N-Reactor fuel, runaway dissolver reactions may be more probable with irradiated fuel.

This is because shearing of irradiated fuel may give smaller particles, and thus a higher uranium surface area, than shearing of as-fabricated fuel. A higher surface area results in more rapid heat generation during dissolution and thus increases the probability of a runaway reaction occurring. This probability may be even greater with ruptured irradiated fuel. Ruptured fuel might give even smaller particles when sheared and, in addition, may contain highly reactive compounds formed by reaction of uranium with water.

It was earlier thought that dissolution rates of irradiated fuel were much faster than those of non-irradiated fuel, and on a production basis at NFS, it appeared that the more highly irradiated fuels dissolved much faster than material of lower irradiation levels. This has been attributed to microcracking on irradiation (Schulz 1972). Current laboratory work (Section 3.2.1) indicates that cut pieces of irradiated fuel do not dissolve faster than unirradiated fuel with the same surface area; therefore, another explanation appears necessary. Because diffusion of aqueous nitric acid into and out of microcracks would be slow, such microcracks probably would contribute little to overall dissolution rates. They might, however, contribute markedly to decreasing the size of segments produced during shearing operation and this in turn would result in more rapid U dissolution (and faster dissolver energy release rates).

Bush (1957) has reported that uranium metal undergoes an extremely pronounced decrease in ductility and undergoes microcracking even at quite low (<200 MWd/ton) irradiation levels. At about 1000 MWd/ton irradiation, elongation under tensile testing was only 0.55% vs 19% for unirradiated metal and microfractographic examination showed that its 25°C fracture properties were typical of a brittle metal. Other work (Smithers 1967) on the press crushing of unirradiated and irradiated N-Reactor fuel in air found that "unirradiated fuel ... is more ductile and difficult to crack open than irradiated material..." and "Irradiated material reacted differently from unirradiated to the extent of lesser deformation before fracture, greater degree of uranium crumbling and cracking, extensive separation of cladding and a more pronounced sparking." It thus appears that it is not only possible but highly probable that shearing of irradiated uranium will lead to increased fracturing, thus producing higher surface area material than will shearing of unirradiated metal.

Processing of failed fuel elements that have had long term exposure to water in the storage basins may add a further complication. It is generally recognized that the reaction of water with uranium metal at relatively low temperatures produces both uranium hydride (UH₃) and uranium oxide (UO₂). The amount of residual UH₃ remaining after reaction is complete varies markedly with uranium batch and may be up to 15% or more of the original uranium (Baker et al. 1966a). The water attack of uranium in failed N-reactor fuel in the storage basins produces a finely divided black residue, which presumably is a mixture of UH₃ and UO₂. The reaction of both of these, particularly UH₃, with nitric acid will release energy:



Heats of reaction above are shown for nitric acid vapor but reactions in the liquid phase and with other oxidants present (NO, NO₂, O₂) are also exothermic.

This finely divided material can be expected to react very rapidly with nitric acid, and, although the heat release from reactions of UO₂ are low compared to reactions of uranium metal or hydride, it has been reported (Hanford 1954) that uranium oxide (presumably containing some UH₃) obtained by reacting uranium metal with water is pyrophoric. Other methods of preparation of UO₂ have also been reported (Hanford 1954) to yield pyrophoric oxide despite the fact that ΔH is only -25.5 kcal/mole for the reaction of UO₂ with O₂. It has also been reported that spontaneous ignition of an irradiated ruptured (Al-clad) uranium metal slug occurred while the slug was being examined in the dry state (Hanford 1954). The rapid reactivity of such finely divided material with nitric acid is demonstrated by the fact that in the Redox dissolver incident involving Al-clad fuel, after reaction of the uranium slugs with moist air, the second dissolver cut reached a high specific gravity almost immediately. Maximum uranium reaction and peak temperature appeared to

be reached at the time of this dissolution cut as evidenced from an observed increase in radioactivity discharged to the sand filter during this period.

Another mechanism possibly leading to smaller particle sizes during shearing is hydrogen embrittlement. Hydrogen appreciably embrittles uranium metal at very low hydrogen concentrations (<1 ppm); a proposed mechanism for this is hydriding of an impurity at the grain boundaries (Mueller et al. 1968). Because storage of ruptured irradiated N-Reactor fuel elements in water basins for long periods of time has allowed prolonged contact with the hydrogen produced by reaction of water and metal, it is conceivable that hydrogen may have diffused along microcracks formed during irradiation and attacked grain boundaries throughout an appreciable depth into the fuel elements, thereby further weakening and possibly partially disintegrating the metal. Such a hypothesis is in qualitative agreement with the observation, reported to us by D. B. Bechtold of UNC Nuclear Industries, that the fuel elements appear to corrode rather slowly in the basins for a prolonged period of time followed by acceleration and disintegration. If such a process occurred, the failed fuel elements might be expected to produce a large amount of reactive fines on shearing or shredding, more so than might occur with unfailed irradiated fuel.

7.5 REFERENCES FOR SECTION 7.0

- Baker, M. McD., L. N. Less, and S. Orman. 1966a. "Uranium + Water Reactions. Part 1. - Kinetics, Products and Mechanism." Trans. Far. Soc. 62:2513.
- Baker, M. McD., L. N. Less, and S. Orman. 1966b. "Uranium + Water Reactions. Part 2. - Effect of Oxygen and Other Gases." Trans. Far. Soc. 62:2525.
- Bush, S. H. 1957. Irradiation Effects in Uranium. HW-51444, General Electric Company, Richland, Washington.
- DeHollander, W. R. 1956. An Evaluation of the Zirconium Hazard. HW-44989, General Electric Company, Richland, Washington.
- Hanford Operations Office. 1954. AEC Uranium Fire Experience. HAN-64841, Atomic Energy Commission, Richland, Washington.

- Kopelman, B., and V. B. Compton. 1953. "Spontaneous Combustion of Metal Powders." Metal Progress. 63(2):77.
- Ludowise, J. D. 1983. Shear/Leach Process for N-Reactor Fuels Processing at the Purex Plant. SD-CP-ES-027, Rockwell Hanford Company, Richland, Washington.
- Mueller, W. M., J. P. Blackledge, and G. G. Libowitz. 1968. "Metal Hydrides." Academic Press, New York, pp 521-27.
- Savannah River Operations Office. 1970. Reprocessing of NPR Fuel at Nuclear Fuels Service, Inc., West Valley Facility. SRO-344-4, Savannah River, Georgia.
- Schulz, W. W. 1972. Shear-Leach Processing of N-Reactor Fuel--Cladding Fires. ARH-2351, Atlantic Richfield Hanford Company, Richland, Washington.
- Smithers, R. M. 1967. Press Crushing of Zr-Clad Fuel Elements as a Mechanical Decladding Technique. ISO-1038, Isochem. Inc., Richland, Washington.
- Troutner, V. H. 1960. Mechanisms and Kinetics of Uranium Corrosion and Uranium Fuel Element Ruptures in Water and Steam. HW-67370, General Electric Company, Richland, Washington.
- Wagman, D. B., W. H. Evans, V. B. Parker, R. H. Schumm, I. Malow, S. M. Bailey, K. L. Churney, R. L. Nuttall. 1982. "The NBS Tables of Chemical Thermodynamic Properties." J. Phys. Chem. Ref. Data. 11: Suppl. No. 2.
- Wanklyn, J. N., and P. J. Jones. 1962. "The Aqueous Corrosion of Reactor Metals." J. Nucl. Mater. 6:291.
- Warf, J. C. 1958. Paper No. 2 in Chemistry of Uranium, J. J. Katz and E. Rabinowitch, eds. Technical Information Service, Oak Ridge, Tennessee, pp 29-37.
- Wicks, C. E., and F. E. Block. 1963. "Thermodynamic Properties of 65 Elements - Their Oxides, Halides, Carbides and Nitrides." USBM Bulletin 605, U. S. Bureau of Mines, U. S. Dept. of Interior, Washington, D. C.

8.0 SENSITIZATION AND PASSIVATION OF WELD BEADS

As a result of his limited laboratory study addressing the cladding fires that occurred during shear/leach processing of N-Reactor fuel at NFS, Schulz (1972) concluded that the most likely explanation of these fires involved combustion of sensitized weld beads on the ends of the fuel rods. These beads contain Be from the Zr-Be braze alloy used in the manufacturing process. On exposure to HNO_3 , as in the leaching portion of the shear/leach process, Be is preferentially dissolved away; this leaves a sensitized Zr matrix that can react violently when shocked electrically or mechanically in air.

In the preceding section, we showed that reactions of the sensitized braze alloy could not have accounted for the damage that occurred during the dissolver fires at NFS. However, the potential role of sensitized braze alloy in the fires that occurred in a few instances during handling of leached hulls remains to be addressed. Also of interest is an explanation for the mechanism of passivation observed by Schulz (and at NFS) when hulls were dipped into water or NaOH solution following sensitization by HNO_3 ; following such a treatment, pyrophoric activity observed when the Zr matrix was shocked was significantly reduced.

We initially planned to investigate the mechanisms of sensitization and passivation by both chemical studies and by surface science techniques. However, the surface science studies could not be pursued because of the extremely localized nature of the sensitization process.

8.1 WELD BEAD CHEMICAL STUDIES

In our chemical studies, we found HNO_3 -sensitization of N-Reactor weld beads to be much less reproducible or severe than indicated by Schulz (1972). In tests using procedures identical to those described by Schulz we found some welded ends that were not sensitized at all, although in most cases some sensitization did occur. In all cases where sensitization was observed, it was localized in discrete zones; sparking with a Tesla coil resulted in discrete flashes as the Tesla discharge was moved over the surface, rather than in a simultaneous shower of flashes as shown in the Schulz report. Only a small fraction of the flashes we observed were vigorous enough to produce an

audible sound. We did observe several instances of very vigorous reaction, but they were very uncommon and occurred only in small areas.

The reason for the different degree of sensitization in N-Reactor fuel beads observed by us and by Schulz (1972) is not known. Personnel at UNC Nuclear Industries, where the fuel is fabricated, know of no fabrication process or braze alloy difference that could account for it. We note that the current fuel has end caps with flat inner surfaces, rather than the chevron-shaped inner surface in the specimen shown in the Schulz report; however, UNC personnel do not feel that this should result in different weld bead properties. The chevron-shaped end cap shown in the Schulz report was used on only a limited basis, and its use had been discontinued by about 1969.

If Schulz (1972) was correct in his conclusion that sensitized weld beads caused the fires that occurred during hulls handling at NFS, and if the samples he studied were representative of the material processed at NFS, then we can conclude that fires during hulls handling would be less probable now than they were at NFS - because of the lower degree of sensitization we observed with current fuel. However, it would be desirable to lower the probability still more by a simple passivation treatment such as dipping in water or NaOH solution, as was done at NFS to prevent further fires. Among the objectives of this project were to determine the mechanism by which such passivation occurred and to determine conditions necessary for passivation.

Before proceeding to a discussion of our work on the sensitization and passivation of weld beads, we will comment that there is good reason to question the hypothesis that weld bead reactions were responsible for the fires observed during handling of hulls at NFS. Neither Schulz nor we observed any effect on sensitized weld beads that approached the description of the NFS fires ("glow like charcoal"). In another portion of this work, we did observe such an effect with a thin piece of undissolved uranium. This observation, which is discussed in detail elsewhere in this report (Section 10), leads us to believe that incompletely leached uranium could have been responsible for the hulls fires observed at NFS.

Our initial study plan included the use of surface science techniques to study the passivation mechanism. However, this approach had to be abandoned

when the extremely localized nature of the sensitization process became apparent. Because of this localization, we could not be sure to section a zone that was capable of being sensitized nor could we tell whether differences in measured surface properties resulted from differences in sensitization and passivation treatments or merely from different weldment compositions. We thus were left with only chemical tests to examine the mechanisms of sensitization and passivation.

The localized nature of the sensitization process also increased the difficulty of evaluating sensitization and passivation by chemical tests. However, we found that "passivated" surfaces could be "resensitized" by merely dipping back into the leach solution; this means that we could compare passivation treatments without the uncertainty of non-reproducible sensitization among specimens.

Results of tests to define the effectiveness of different rinse solutions in passivating sensitized N-Reactor fuel element weld beads are shown in Table 8.1. Three different sets of results are tabulated: 1) the number of flashes that resulted from Tesla coil-sparking of the weld beads of a sample that had been sensitized in $\text{HNO}_3 + \text{U}$ solution and then rinsed, 2) the number of flashes resulting from sparking the same sample after it was reimmersed in the leach solution, and 3) the percentage of the total flashes observed that occurred when the as-rinsed surface was sparked. The total number of flashes recorded with these specimens is seen to vary greatly from one specimen to another, illustrating the lack of sensitization reproducibility mentioned earlier. However, the percentage values measured with the individual specimens do show some important results.

Rinsing with water is seen to be effective in reducing the pyrophoric nature of the sensitized weld beads to essentially zero. Since reimmersion of the same specimens in the leach solution reestablished the pyrophoric nature, it appears that this "passivation" by water rinsing simply involves removal of nitric acid and/or uranyl nitrate from the reaction area rather than a true passivation of a reactive Zr surface.

TABLE 8.1. Comparison of Rinse Solutions in Reducing Pyrophoricity of Sensitized Weld Beads

| Type of Element | Rinse Solution Composition | Flash/cm ^(a,b) | | | | Sensitivity Remaining After Rinse, % ^(e) | |
|-----------------|---------------------------------|----------------------------|------------|--|------------|---|------------|
| | | After Rinse ^(c) | | After Reimmersion in Leach Solution ^(d) | | Inner Weld | Outer Weld |
| | | Inner Weld | Outer Weld | Inner Weld | Outer Weld | | |
| Inner | H ₂ O | 0.0 | 0.0 | 0.0 | 0.0 | -- | -- |
| Outer | H ₂ O | 0.0 | 0.4 | 5.3 | 2.8 | 0 | 13 |
| Outer | H ₂ O | 0.0 | 0.0 | 5.7 | 2.2 | 0 | 0 |
| Inner | 0.5 <u>M</u> NaHCO ₃ | 0.0 | 0.0 | 0.0 | 2.2 | -- | 0 |
| Inner | 5 <u>M</u> NaOH | 0.0 | 0.0 | 0.0 | 0.4 | -- | 0 |
| Inner | 1 <u>M</u> HNO ₃ | 0.0 | 0.0 | 1.0 | 1.4 | 0 | 0 |
| Inner | 1 <u>M</u> HNO ₃ | 0.0 | 0.0 | 0.0 | 1.2 | -- | 0 |
| Inner | 5 <u>M</u> HNO ₃ | 8.5 | 0.6 | 11.5 | 4.6 | 43 | 12 |
| Inner | 9 <u>M</u> HNO ₃ | 0.5 | 2.4 | 9.5 | 2.2 | 5 | 52 |

(a) Sparked with Tesla coil several times beginning 5 min after removal from solution. Most flashes occurred during first sparking.

(b) Measured on quarter-sections of outer elements and half-sections of inner elements. Approximate circumferences of 20 cm for outer surface of outer element, 12 cm for inner surface of outer element, 10 cm for outer surface of inner element, and 4 cm for inner surface of inner element were used in these calculations.

(c) Immersion for 5 min at room temperature.

(d) Uranium leached out of end caps during overnight treatment with boiling solution. Initial solution composition was 9 M HNO₃ and final composition was ~1 M U + 3 to 4 M HNO₃.

(e) Defined as (flashes after rinse) 100/[(flashes after rinse) + (flashes after reimmersion)].

Rinsing with 0.5 M NaHCO_3 or 5 M NaOH solution was also effective in apparently eliminating the pyrophoric nature. This is hardly surprising in light of the effectiveness of water alone.

Rinsing the sensitized weld beads with 1 M HNO_3 also appeared to be effective in reducing the pyrophoric nature to essentially zero; however, the relative lack of pyrophoricity observed in the specimens tested makes this conclusion somewhat tentative. A significant degree of pyrophoricity persisted after rinsing with 5 M HNO_3 or 9 M HNO_3 . At these higher HNO_3 concentrations, there did appear to be a substantial reduction in pyrophoricity of some welds but not of others. It is thought that the presence of uranyl nitrate might contribute to increased pyrophoricity of some sensitized welds because the higher viscosity of uranyl nitrate solutions might not allow as much drainage of solution away from the Zr.

Table 8.2 summarizes the results obtained with unrinsed sensitized weld beads from a number of end caps. The great variability of pyrophoricity from end cap to end cap and from weld to weld is apparent. One important point here is that pyrophoricity was indeed observed on weld beads that were autoclaved before they were exposed to HNO_3 . It had been wondered if perhaps the protective ZrO_2 film produced during autoclaving might prevent leaching of Be from the weld zone, but this is evidently not the case. This conclusion is also supported by tests with irradiated N-Reactor fuel, which should have an even more protective ZrO_2 film than the specimens shown in Table 8.2.

The preceding results were all obtained with unirradiated N-Reactor fuel. Results of a few tests with irradiated fuel are given in Table 8.3. As with unirradiated fuel (Tables 8.1 and 8.2), pyrophoricity was observed with both unrinsed specimens and with water rinsed specimens that were reimmersed in the dissolver solution. Thus, the irradiation process appears to have little, if any, effect on weld bead sensitization and passivation.

8.2 WELD BEAD METALLOGRAPHY STUDY

Low magnification (10X) optical micrographs were taken of three as-fabricated end cap sections to provide a reference for comparison of weld bead

TABLE 8.2. Comparison of Pyrophoric Nature of Various Unrinsed Weld Bead Samples

| <u>Type of Element</u> | <u>Sample Number</u> | <u>Flash/cm^(a,b)</u> | |
|------------------------|----------------------|---------------------------------|-------------------|
| | | <u>Inner Weld</u> | <u>Outer Weld</u> |
| Inner | G-2 | 11.5 | 3.6 |
| Inner | J | 3.0 | 8.6 |
| Inner | XX | 1.0 | 0.4 |
| Outer | L | 0.0 | 0.0 |
| Outer | L | 0.0 | 8.8 |
| Outer | M | 6.7 | 1.8 |
| Outer | M | 7.0 | 0.8 |
| Outer ^(c) | N-2 | 0.0 | 0.0 |
| Outer ^(c) | N-2 | 0.0 | 1.0 |
| Outer ^(c) | N-1 | 0.8 | 2.4 |
| Outer ^(c) | N-1 | 0.8 | 2.0 |

-
- (a) Uranium leached out of end cap sections during overnight treatment with boiling solution (initially 9 M HNO₃, finally ~1 M U in 3 to 4 M HNO₃), then sparked with Tesla coil several times beginning 5 min after removal from solution.
- (b) Measured on quarter-sections of outer elements and half-sections of inner elements (see Table 8.1 for dimensions).
- (c) From an autoclaved element.

volume and composition with those of sensitized and of sensitized and then passivated weld beads; Figure 8.1 shows these micrographs. Section CA contains all of the reaction zones present. Sections CG and CI both have some reaction layer missing due to the cut location. To obtain better structural detail of the zones and some elemental information, the sections were examined with a Japan Electron Optics Laboratory JSM-U3 scanning electron microscope (SEM) with a Si(Li) energy-dispersive spectroscopy (EDS) system. The EDS data were analyzed using a Tracor Northern NS-880 analyzer.

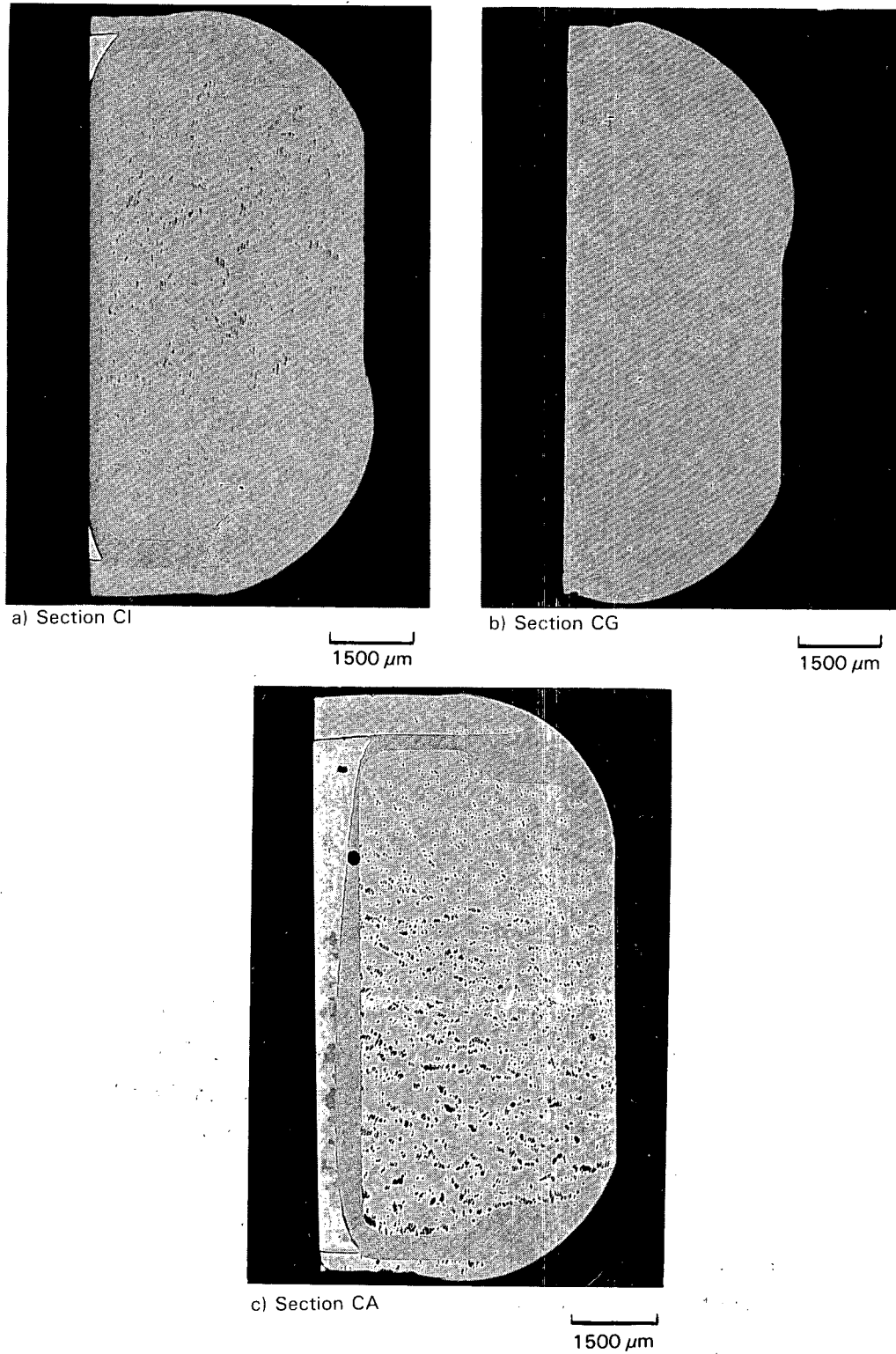


FIGURE 8.1. Optical Micrographs of End Cap Weld Sections

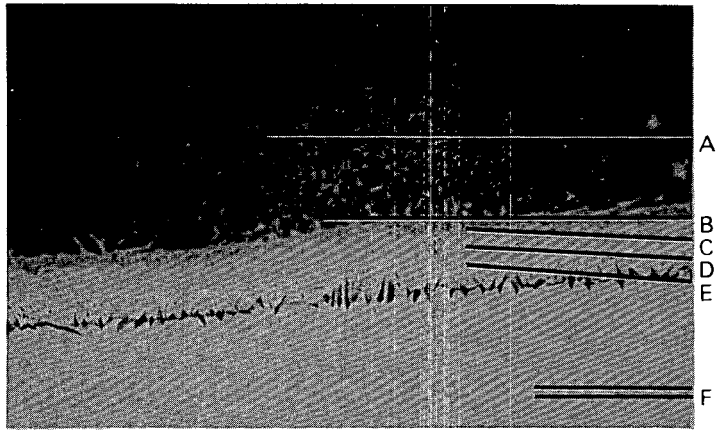
TABLE 8.3. Pyrophoricity of Irradiated Weld Beads after Nitric Acid Leaching

| ^{240}Pu in Fuel, % | Flash/cm (a,b) | | | | | |
|---------------------------------|----------------|---------------|-----------------------|---------------|---------------|---------------|
| | Unrinsed | | Rinsed ^(c) | | Reimmersed | |
| | Inner Weld | Outer Weld | Inner Weld | Outer Weld | Inner Weld | Outer Weld |
| 6 | 0.5 | 0.4 | -- | -- | -- | -- |
| 6 | -- | -- | 0.0 | 0.0 | 0.5 | 0.8 |
| 12 | 1.0 | 0.6 | -- | -- | -- | -- |
| 12 | -- | -- | 0.0 | 0.2 | 1.0 | 1.6 |

- (a) Measured after specimens treated overnight in boiling solution (initially 9 M HNO_3 , finally ~1 M U in 3 to 4 M HNO_3). Specimens were sparked with Tesla coil several times, beginning 5 min after removal from solution.
- (b) Measured on half-sections of inner elements. (See Table 8.1 for dimensions).
- (c) Soaked in water for 5 min.

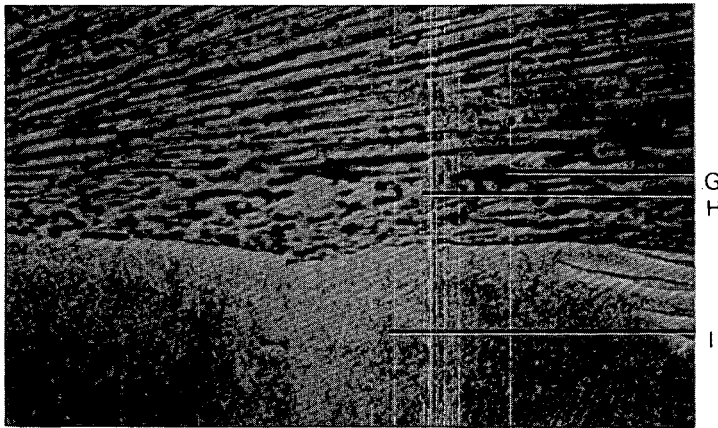
Each reaction layer was examined. Figure 8.2 contains SEM images of the various types of layers found. A diffusion zone of a uranium/zirconium mixture was found between the braze material and the uranium fuel. An elemental x-ray spectrum from each visible phase was acquired for comparison. The uranium/zirconium diffusion zone was similar in appearance to the layer found between the cladding wall and uranium fuel to be discussed in Section 9, but there is a possibility that some beryllium is also in the layer. All other phases contain various levels of zirconium and tin, which are the major components of Zircaloy. Because beryllium is not detectable with the EDS system, the amount of zirconium and tin was used as the basis of comparison. The amount unaccounted for by zirconium, tin, or uranium was attributed to a light element such as beryllium. Table 8.4 lists the measured amounts of the elements at each point marked in Figure 8.2.

As indicated by the structures in Figure 8.2, if the dark (lower Zr) phase were selectively dissolved, a large surface area would be exposed in an



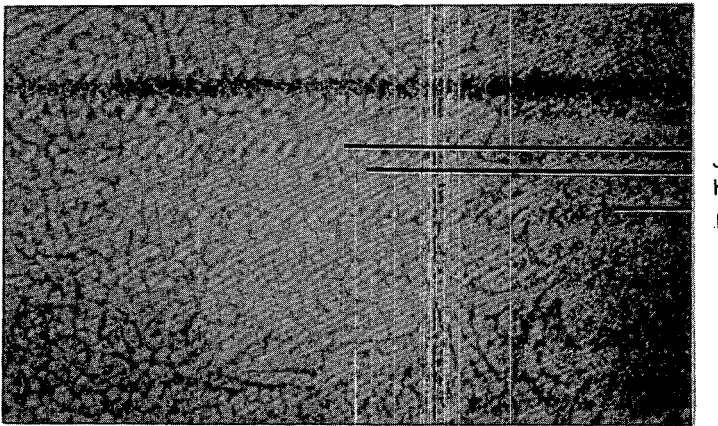
Braze-Uranium Interface

15 μm



Braze-Zircaloy Region

15 μm



Weld Region

15 μm

FIGURE 8.2. SEM Micrographs of Reaction Layers and EDS Analysis Locations

interwoven pattern. This foam-like structure could exhibit pyrophoric behavior; however, this material represents only a small portion of the total mass of Zircaloy present in fuel cladding, as was discussed in Section 7.0.

As discussed in Section 8.1, the tests to sensitize the weld/braze areas had inconsistent results, which made it impossible to produce specimens with known surface conditions. Because of this lack of a repeatable sensitization of the weld beads, no further metallographic studies of the weld bead properties were conducted.

TABLE 8.4. Elemental Concentration from SEM/EDS Analysis

| Location (a) | Element, wt% | | | |
|--------------|--------------|-----|------|---------------------------|
| | Zr | Sn | U | Be or Other Light Element |
| A | 87.1 | 0.0 | 0.0 | 12.9 |
| B | 93.5 | 2.2 | 2.3 | 2.0 |
| C | 65.5 | 0.0 | 29.3 | 5.2 |
| D | 50.5 | 0.8 | 43.5 | 5.2 |
| E | 28.4 | 0.0 | 66.6 | 5.0 |
| F | 0.0 | 0.0 | 99.7 | 0.3 |
| G | 87.1 | 0.0 | 0.0 | 12.9 |
| H | 98.5 | 1.5 | 0.0 | 0.0 |
| I | 98.5 | 1.5 | 0.0 | 0.0 |
| J | 97.9 | 2.1 | 0.0 | 0.0 |
| K | 96.6 | 1.4 | 0.0 | 2.0 |
| L | 98.2 | 1.8 | 0.0 | 0.0 |

(a) Refer to Figure 8.2 for location identification.

8.3 REFERENCES FOR SECTION 8.0

Schulz, W. W. 1972. Shear-Leach Processing of N-Reactor Fuel -- Cladding Fires. ARH-2351. Atlantic Richfield Hanford Company, Richland, WA.

9.0 STUDIES OF U/Zr INTERMETALLIC ZONE

The first explanation advanced to account for the fires observed at NFS involved ignition of a U-Zr alloy present in the intermetallic region produced during N-Reactor fuel manufacture (Schulz 1972). However, the results of the initial investigations did not support this hypothesis. One objective of this current study was to gain additional information in this area; specifically to attempt to estimate, from published data, the amount of UZr_3 that may be present in irradiated fuel and to check this estimate by metallurgical examinations of both as-fabricated and irradiated fuel. In addition, we tested for pyrophoric activity in the intermetallic zone of leached cladding hulls produced in other parts of this project. The results of these studies support those of the earlier studies; it is highly unlikely that pyrophoric activity in this zone could have been a causative factor in the cladding fires observed at NFS.

9.1 METALLURGICAL STUDIES OF U/Zr INTERMETALLIC ZONE

One possible cause for the fires observed at NFS during the shear/leach processing of N-Reactor fuel was thought to be the formation of the epsilon phase (UZr_3) at the fuel-cladding interface. This phase, which is an unstable intermetallic compound, is formed through the interdiffusion of uranium and zirconium. As is shown in Figure 9.1, the epsilon phase is formed between room temperature and $600^{\circ}C$, and may exist over nearly the entire composition range from uranium to zirconium.

The explosion hazard of the epsilon phase has been reported (Schulz et al. 1954b) to arise from its isolation during nitric acid dissolution. The UZr_3 layer between the fuel and the cladding is not dissolved in nitric acid, so it is exposed by the fuel dissolution and remains on the cladding. The surface area of this epsilon phase is high, which contributes to its pyrophoricity. When ignited, the epsilon phase oxidizes rapidly. The epsilon phase passivates upon longer exposure to nitric acid.

We were unable to find sufficient data to estimate the amount of UZr_3 that may be present in irradiated N-Reactor fuel. A number of reports were located that discuss the pyrophoricity of UZr_3 (Hurford 1953, Roth 1952,

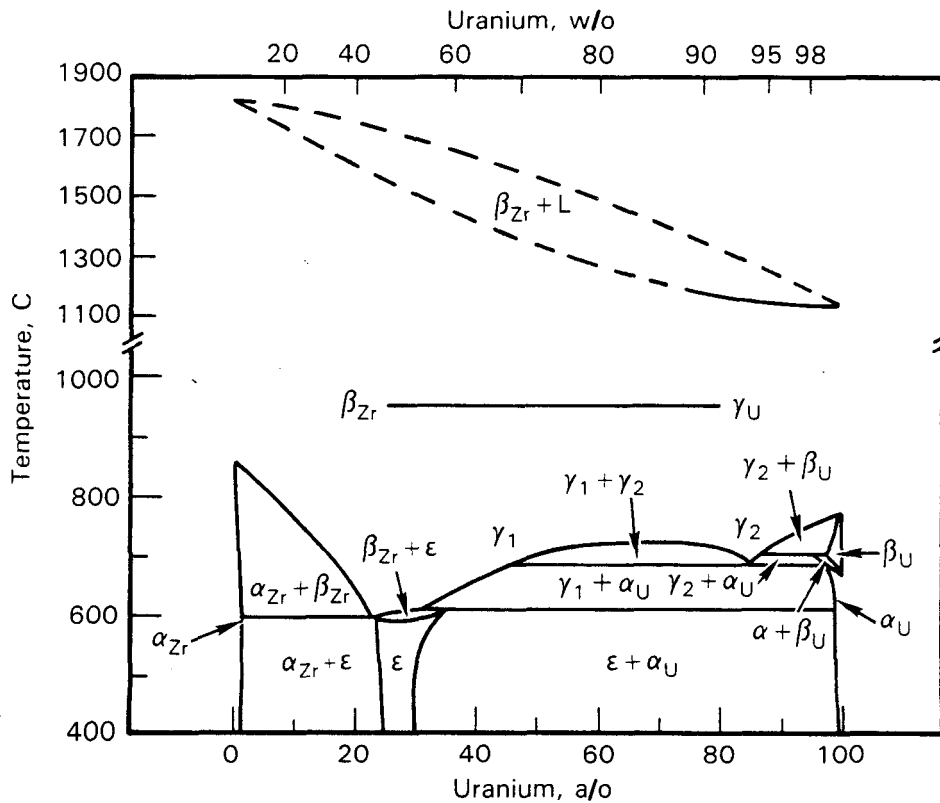


FIGURE 9.1. Zirconium-Uranium Constitutional Diagram

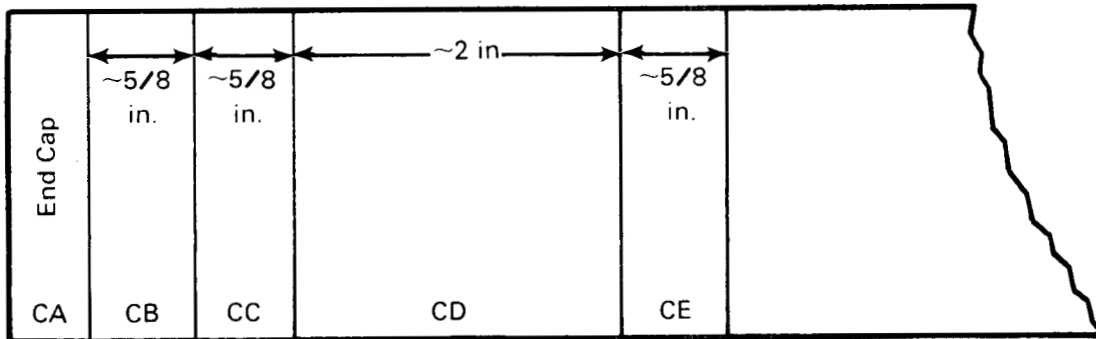
Larsen et al. 1954, Schulz et al. 1954a, 1954b, Schulz 1972). However, no reports were located that discuss the kinetics of UZr_3 formation, and it is not possible to calculate the amount of UZr_3 present in irradiated fuel without this information.

Zircaloy-clad metallic uranium fuel sections were metallographically examined to characterize the interface region between the cladding and the fuel. The objectives of this study were to:

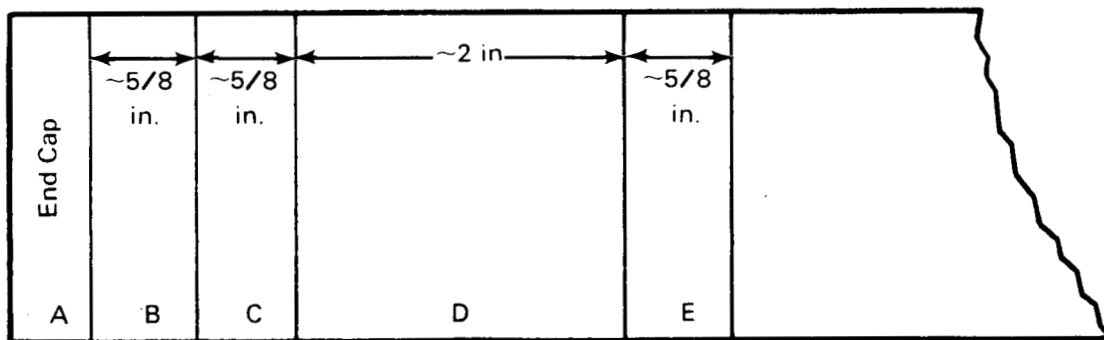
- Measure the size of this intermetallic phase in as-fabricated and irradiated (spent) fuel sections.
- Estimate the percentage of a total fuel segment composed of this intermetallic phase.
- Measure the composition of any diffusion zone between the cladding and fuel.

Three 5/8-in. sections were cut from an as-fabricated fuel rod and three from a spent fuel rod for these metallographic studies. Figure 9.2 shows the locations on the fuel rods from which the sections were cut. The as-fabricated fuel sections were cut at the UNC Nuclear Industries fuel fabrication facility. The sections were then mounted and polished at the Pacific Northwest Laboratory uranium metallography facility. The spent fuel sections were cut, mounted, and polished at the postirradiation testing facility of the Hanford Engineering Development Laboratory.

The methods used to perform this study were optical microscopy and electron beam x-ray analysis. Polished cross-sections were first examined with optical microscopy. The composition of the diffusion zone in the as-



a) As-Fabricated Fuel Rod



b) Spent Fuel Rod

FIGURE 9.2. Specimen Locations from As-Fabricated and Spent Fuel Rods

fabricated fuel was measured with a scanning electron microscope (SEM) with energy-dispersive spectroscopy (EDS). The composition of the diffusion zone in the spent fuel was measured with a shielded electron microprobe (SEMP).

The polished sections were examined by optical microscopy techniques to locate the diffusion layer. Figure 9.3 shows a representative micrograph of each fuel condition. The diffusion zone (as measured by stepped compositional analysis) is not totally visible in these micrographs.

This diffusion zone was then characterized for elemental distribution. The as-fabricated sections were examined with a Japan Electron Optics Laboratory JSM-U3 SEM with a Si(Li) EDS system. The x-ray energy data were acquired and analyzed using a Tracor Northern NS-880 analyzer, and the spent fuel sections were examined using a Perkin-Elmer MAC-450 SEM. The diffusion zones were characterized using 1-to 2- μm steps through the zone. Figure 9.4 shows two representative SEM images of the diffusion zone in the as-fabricated fuel. Because SEM examination of the spent fuel was not done, comparable images are not available. Table 9.1 lists the diffusion zone thickness measurements based on data from optical micrographs, SEM images (when available), and elemental profiles.

Examples of the elemental profiles are shown in Figure 9.5. The uranium and Zircaloy values are shown for each step. The composition of the UZr_3

TABLE 9.1 Diffusion Zone Thickness Measurements

| <u>As Fabricated</u> | <u>Zone Thickness, μm</u> | |
|----------------------|---|-------------------|
| | <u>Area 1</u> | <u>Area 2</u> |
| CB | 17 | 19 |
| CC | 14 | 13 |
| CE | 15 | 16 |
| <u>Spent Fuel</u> | | |
| B | 7 | 15 |
| C | 12 | 32 ^(a) |
| E | 16 | 20 |

(a) Zone was thicker in this area than on the balance of the section.

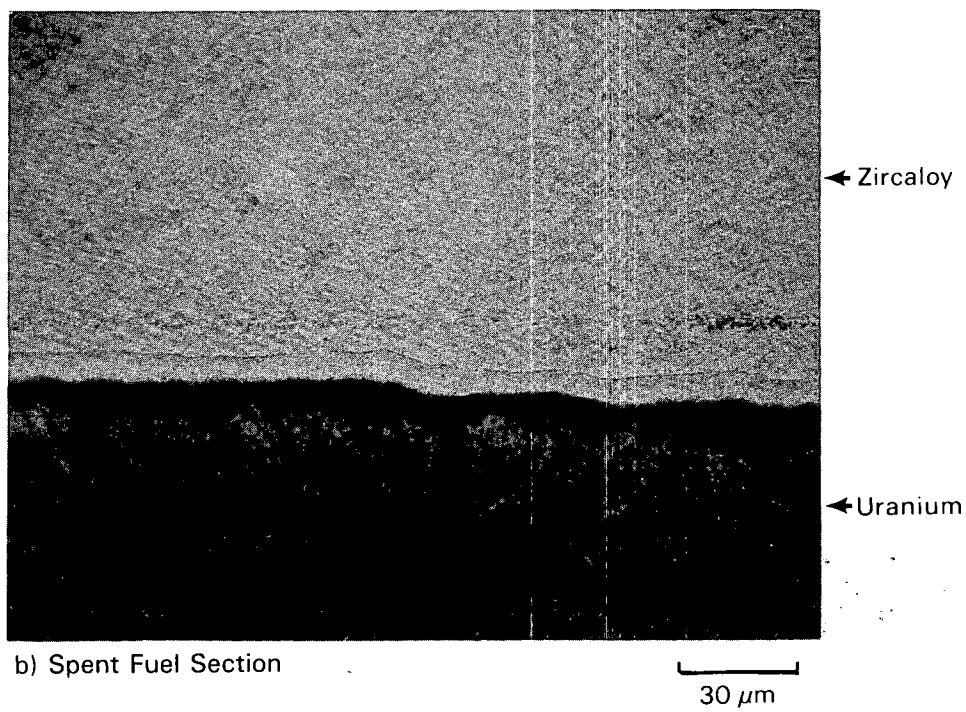
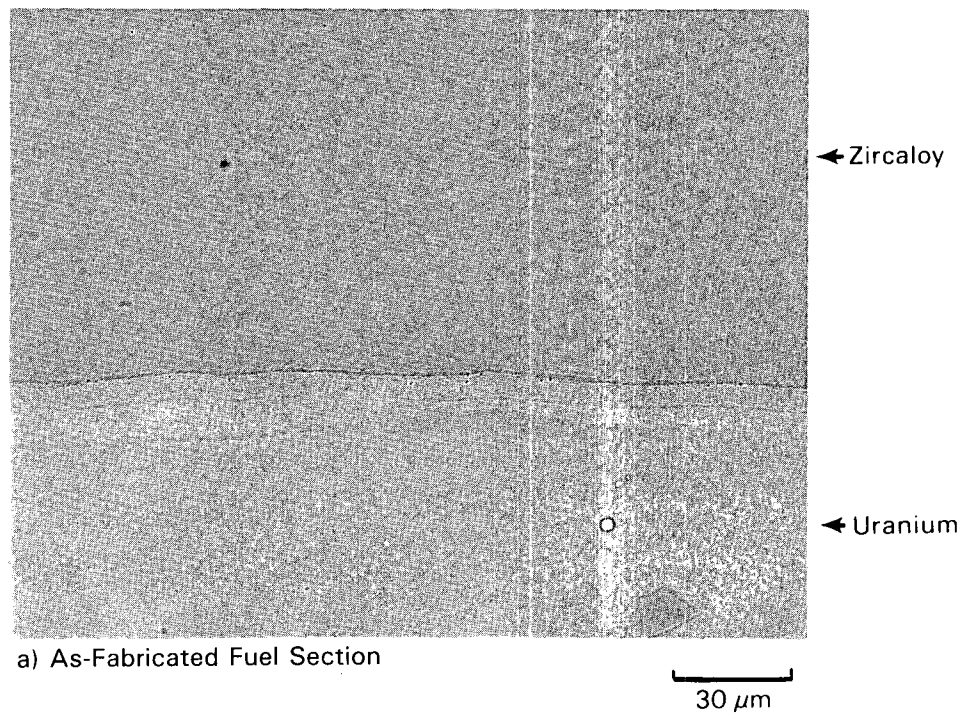


FIGURE 9.3 Representative Optical Micrographs of Fuel Sections

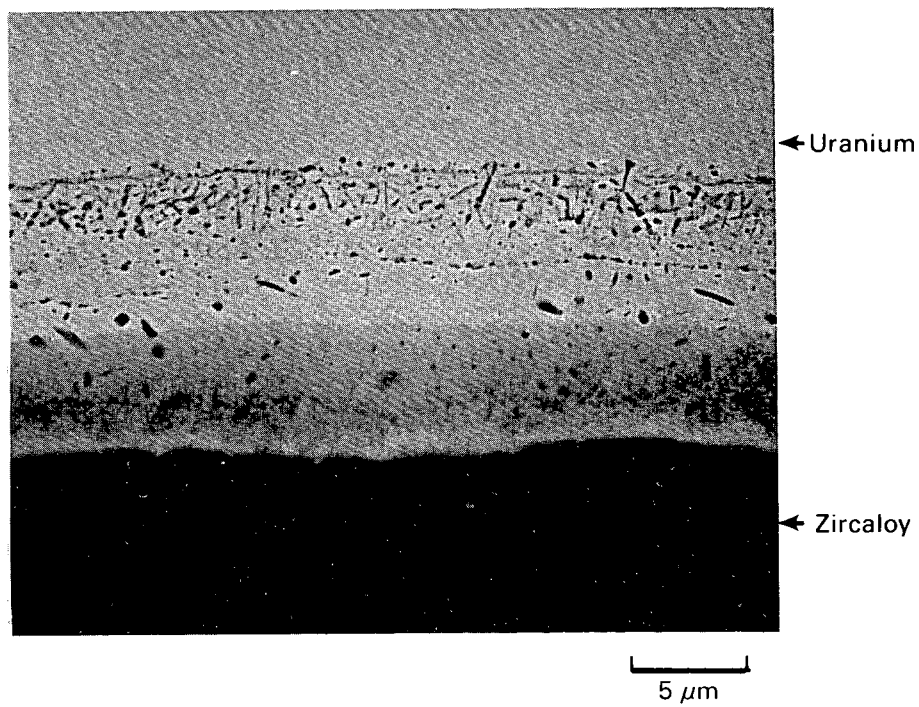
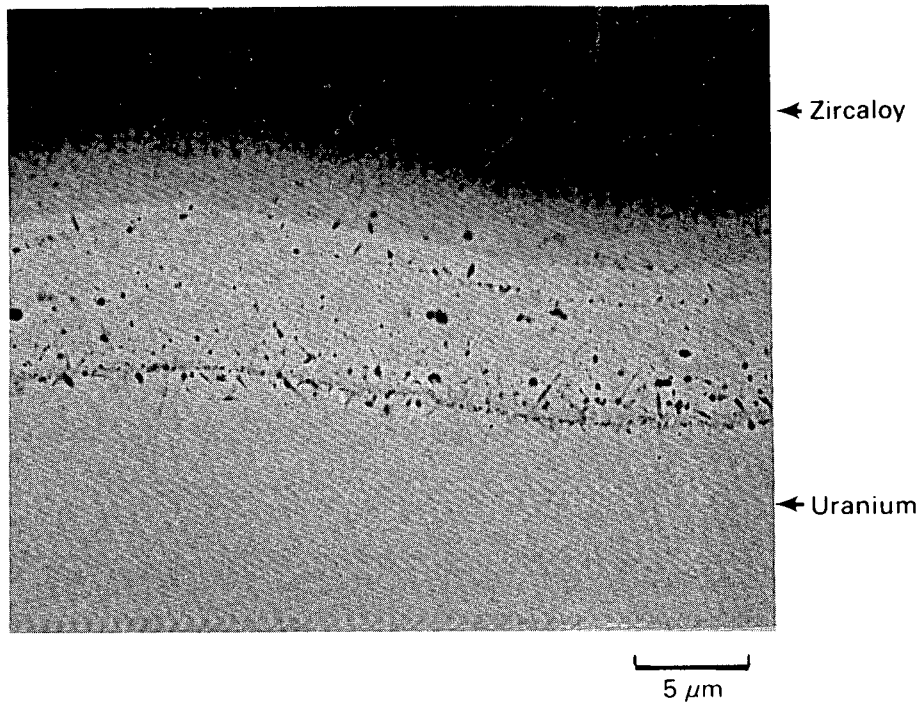


FIGURE 9.4. Representative SEM Micrographs of the As-Fabricated Fuel Section

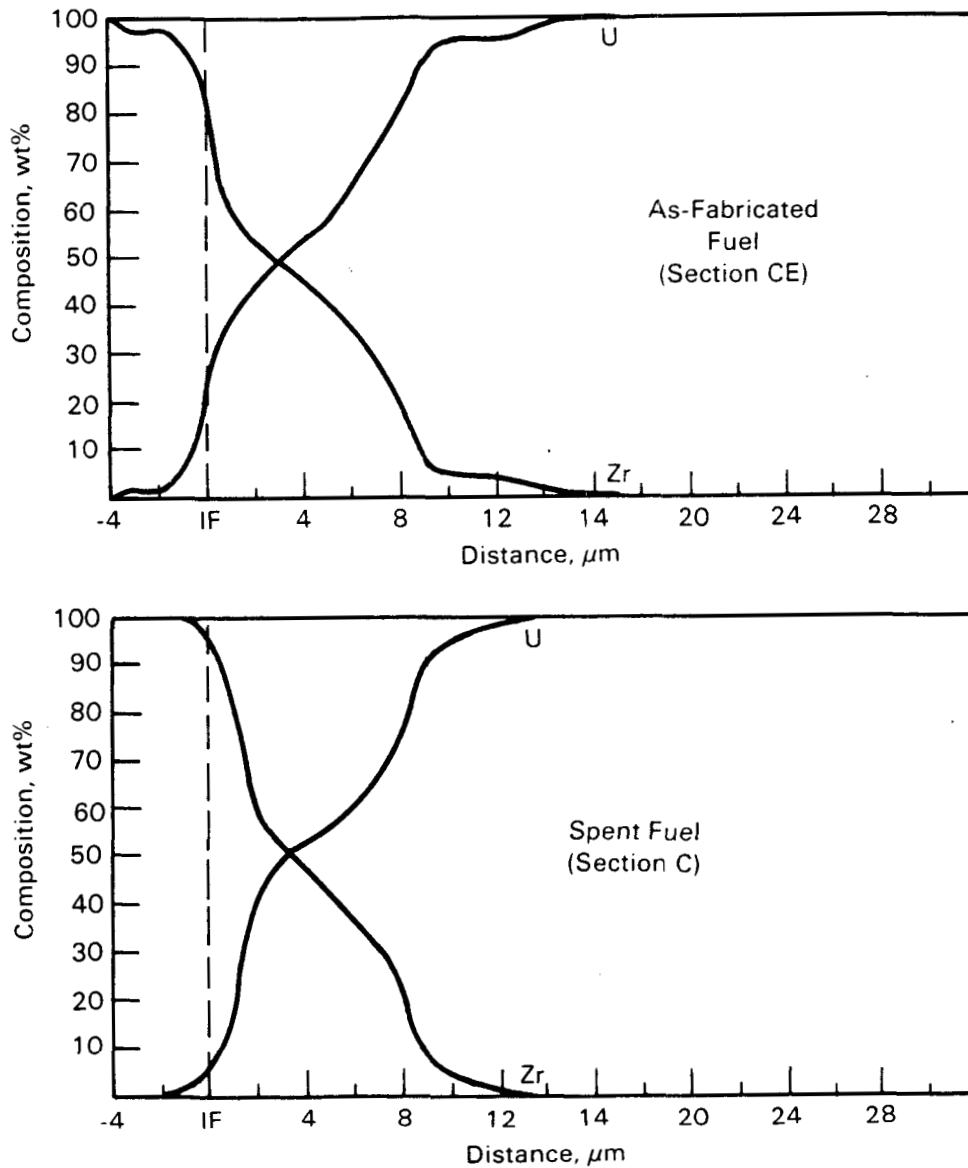


FIGURE 9.5. Uranium/Zircaloy Composition Profile Through Diffusion Zone

intermetallic phase is 47 wt% U and 53 wt% Zr, the amount of material found in this composition range is seen to be a small fraction of the total diffusion zone. Although a U-Zr mixture of this elemental ratio was measured, there was no structural indication of a distinct phase.

For calculating the ratio of the volume of UZr_3 to the volume of fuel, the total diffusion zone was used, rather than the limited elemental range representing the UZr_3 composition; this gives values that are extremely

conservative. Table 9.2 lists the ratio of the total diffusion zone volume to the volume of uranium fuel. Averages of the thickness values were used for the diffusion zone. Uranium volumes were calculated from the nominal fuel outer and inner diameters.

The following conclusions are based on the results of these measurements of the two fuel rods that were studied:

- There is an inconsequential change in the diffusion zone thickness during the irradiation period. Even doubling the zone size would produce an insignificant diffusion layer.
- The diffusion zone size (between 15 μm and 30 μm) represents such a small portion of the uranium present (maximum of 0.3%) it is not possible for this layer to contribute a meaningful mass of pyrophoric material.

Although there is a U-Zr diffusion zone present, it would be too small a quantity to constitute an appreciable source of pyrophoric material on hulls.

9.2 PYROPHOROCITY OF U/Zr INTERMETALLIC ZONE

When the uranium is dissolved in HNO_3 , the possibility exists that potentially pyrophoric U/Zr alloys in the intermetallic zone will remain undissolved and thus provide the potential for undesirable violent reactions. We examined this possibility with both irradiated and unirradiated

TABLE 9.2. Ratio of Diffusion Zone to Total Uranium

| <u>As-Fabricated Fuel</u> | <u>Ratio</u> |
|---------------------------|--------------|
| CB | 0.21% |
| CC | 0.16% |
| CE | 0.18% |
| <u>Spent Fuel</u> | |
| B | 0.13% |
| C | 0.26% |
| E | 0.21% |

N-Reactor fuel. Irradiated fuel sections were taken from both intact elements and from the affected areas of ruptured elements. Ruptured elements were examined because some of the hypotheses for the NFS cladding fires involved such material. Pyrophoric activity was found in some of the leached intermetallic zones, but in no case was it very extensive or vigorous.

Results of these tests are summarized in Table 9.3. The observed events were few in number and varied from section to section in fuel of the same background. These data appear to indicate that pyrophoric activity of the intermetallic zone is reduced by water rinsing, is increased by irradiation, and is greater in zones where fuel element rupture had occurred. However, it should be stressed that the pyrophoric activity of these zones was never found to be very extensive. It is thought to be highly unlikely that pyrophoric activity in this zone could have been a causative factor in the cladding fires observed at NFS.

TABLE 9.3. Results on the Pyrophoric Nature of the U/Zr Intermetallic Zone of Leached Hulls

| <u>Cladding Section^(a)</u> | <u>H₂O Rinsed(?)</u> | <u>Flashes Observed^(b)</u> |
|---------------------------------------|---------------------------------|---------------------------------------|
| <u>With Unirradiated Fuel</u> | | |
| Inner of inner element | No | 0 |
| Outer of inner element | No | 0 |
| Inner of outer element | No | 0 |
| Outer of outer element | No | 0 |
| Outer of outer element | No | 1 |
| Inner of inner element (2 ea) | Yes | 0 |
| Outer of inner element (2 ea) | Yes | 0 |
| Inner of outer element (2 ea) | Yes | 0 |
| Outer of outer element (2 ea) | Yes | 0 |
| <u>With Irradiated Fuel</u> | | |
| Inner of inner element ^(c) | Yes | 0 |
| Outer of inner element ^(c) | Yes | 0 |
| Inner of outer element ^(c) | Yes | 0 |
| Outer of outer element ^(c) | Yes | 0 |
| Inner of inner element ^(d) | No | 0 |
| Outer of inner element ^(d) | No | 1 |
| Inner of outer element ^(d) | No | 1 |
| Outer of outer element ^(d) | No | 2 |
| <u>With Ruptured Irradiated Fuel</u> | | |
| Inner of inner element ^(e) | No | 2 |
| Outer of inner element | No | 12 ^(f) |
| Inner of outer element | No | 3 |
| Outer of outer element | No | 0 |
| Outer of inner element | Yes | 1 + 1 ^(g) |
| Inner of outer element | Yes | 0 + 0 ^(g) |
| Outer of outer element | Yes | 2 + 1 ^(g) |

(a) Half-circular section, ~1.3 cm wide.

(b) When the surface was sparked with a Tesla coil.

(c) From the experiments to measure the transuranic (TRU) content of cladding hulls, after the second dissolution cycle.

(d) From the experiments to measure the TRU content of cladding hulls, after the 8 M HNO₃ final leach.

(e) This section was a full circular section.

(f) One of these flashes resulted in a transitory glow on a cut edge of the cladding.

(g) After dipping back into the dissolver solution.

9.3 REFERENCES FOR SECTION 9.0

- Hurford, W. J. 1953. Explosions Involving Pickling of Zirconium and Uranium Alloys. WAPD-84, Bettis Atomic Power Laboratory, Pittsburgh, Pennsylvania.
- Larsen, R. P., R. S. Shor, H. M. Feder, and D. S. Flickkama. 1954. A Study of the Explosive Properties of Uranium-Zirconium Alloys. ANL-5135, Argonne National Laboratory, Argonne, Illinois.
- Roth, H. P. 1952. Explosions Occurring During Chemical Etching or Pickling of Uranium Zirconium Alloys. MIT 1105, Massachusetts Institute of Technology, Cambridge, Massachusetts.
- Schulz, W. W. 1972. Shear-Leach Processing of N-Reactor Fuel-Cladding Fires. ARH-2351, Atlantic Richfield Hanford Company, Richland, Washington.
- Schulz, W. W., Scott, F. A., and Voiland, E. E. 1954a. Explosion Hazards in the Nitric Acid Dissolution of Uranium-Zirconium Alloy Fuel Elements. HW-32365, Hanford Atomic Products Operation, Richland, Washington.
- Schulz, W. W., Scott, F. A., and Voiland, E. E. 1954b. The Identification and Characterization of Explosive Residues Produced by Dissolution of Uranium-Zirconium Alloys. HW-32410, Hanford Atomics Product Operation, Richland, Washington.

10.0 PYROPHORICITY OF METALLIC URANIUM

The pyrophoric nature of finely divided uranium metal is well known. During our examination of the pyrophoric nature of the U/Zr intermetallic zone, we found metallic uranium to be more pyrophoric than we had anticipated. The resultant "fire" exhibited the characteristic attributed to the fires observed at NFS during handling of the hulls (it "glowed like burning charcoal"). It is suggested that the few hulls-handling fires observed at NFS may have resulted from ignition of uranium on incompletely leached hulls because neither Schulz (1972) nor we observed such characteristics in attempting to ignite sensitized weld beads or intermetallic zones on Zircaloy hulls.

The uranium fire we observed occurred on a thin, finlike piece of unirradiated metal that remained when a dissolution was terminated before reaction was complete. The "fin" was still attached to cladding on one side (the inner cladding of an outer element) but not on the other. The fin was located at the center of the 1.3-cm wide half-circle of cladding and was ~3 cm in length, traversing about half of the circumference of the half circle of cladding. It was quite thin and somewhat porous; the metal had dissolved through in spots. It appeared to be nearly as tall as the original distance between the inner and outer cladding (~0.7 cm).

The cladding and the attached fin were removed from the leach solution to test the exposed intermetallic zone for pyrophoricity before all of the "black solids" (discussed in Section 5.0) had flaked off. The test for pyrophoricity involved the usual sparking with a Tesla coil; it was done without rinsing the specimen.

One flash was observed while sparking the surface on the half of the cladding where uranium dissolution had been complete. As sparking was continued in this area, a spark ignited the uranium at the top of the fin at one end. The resultant red-orange glow gradually worked its way completely along the fin and then extinguished itself. The entire fin did not glow at one time; a glowing zone gradually moved along, leaving a black crusty surface behind. At one point the glowing zone seemed to hesitate, but it then picked up speed again. The time required for the glow to traverse the fin was not

measured, but it is estimated that it amounted to 0.5 to 1 minute. At no time did the Zircaloy hull glow, although later examination showed a heat discoloration pattern on the surface opposite the uranium.

All of the uranium in the fin was not burned; a metallic uranium substrate remained when the black crust was removed by reaction with warm HNO_3 . The residual uranium metal was much more porous than it had been before the fire.

Concerted attempts to ignite this more porous fin by Tesla coil sparking were not successful. Another fin of similar size as the one that did ignite also resisted attempts to ignite it. Apparently ignition of a piece of uranium requires conditions to be within a narrow range. If the piece is too flimsy or porous, the heat dissipation rate is great enough that burning will not occur. On the other hand, if the piece is too thick or solid, there is no site "active" enough to be ignited by a spark.

More evidence that the fires observed at NFS during hulls handling may have been uranium fires was obtained in another experiment in which uranium leaching was more complete. In this case, the residual uranium was in the form of two small "spikes" attached to the cladding. When the cladding was sparked with a Tesla coil, these spikes were the only places where pyrophoric activity was observed. This activity was evidenced only by flashes as reaction occurred; no lasting glow was seen, presumably because of the small size of the U spikes.

Another fire that likely involved ignition of uranium also was observed during the work, although zirconium might also have been involved. When a pile of "sawdust" generated during sectioning of ruptured irradiated fuel was sparked with a Tesla coil, ignition did occur as evidenced by a red-orange glow and the appearance of a flame. This fire was readily extinguished by covering the vessel to prevent access of oxygen. This fire occurred at the top of a pile containing 16 g of fines. Previous tests with a thin layer of fines had given some flashes but no evidence of ignition. This provides another example of the need for precise conditions for ignition to occur.

11.0 URANIUM AND ZIRCONIUM HYDRIDE STUDIES

A hypotheses involving reactions of uranium and zirconium hydrides was among those advanced earlier to explain the fires observed at NFS during processing of irradiated N-Reactor fuel (Schulz 1972). Earlier experimental results did not support this hypothesis, but those studies were very limited in scope and additional data in this area were desired. We examined a ruptured fuel element to obtain data on the extent and nature of hydride formation. The results of this examination also do not support the hypothesis that reactions involving hydrides contributed directly to the fires observed at NFS. Zirconium hydrides were present in the cladding at low levels, and in a dispersed manner, so that they did not cause a pyrophoricity problem. No evidence of the presence of uranium hydride was seen in this ruptured element.

However, as was discussed in Section 7.0, hydrogen embrittlement of uranium could lead to smaller uranium pieces being produced during shearing, thus increasing the probability of runaway uranium reactions occurring during dissolution. The presence of finely divided uranium oxide resulting from water oxidation of uranium metal or of uranium hydride could also contribute to runaway reactions during dissolution.

11.1 HYDRIDING OF URANIUM AND ZIRCONIUM

Both uranium and zirconium form oxides and hydrides through the reaction with water. Hydrogen is often absorbed into the metal as a result of the oxidation reaction. For example, hydrogen is produced by the reaction $Zr + 2 H_2O = ZrO_2 + 2H_2$ and part of the hydrogen is absorbed by the zirconium. It has been estimated that 10-20 percent of the hydrogen produced by the oxidation reaction in water is absorbed by Zircaloy-2 (Wheeler 1956) in the absence of radiation. The absorption efficiency increases with oxide thickness, particularly when corrosion accelerates as a result of thick oxide layers. More recent measurements obtained under irradiated conditions indicate that the absorption efficiency may be between 20-35 percent in the initial portion of the post-transition region and 65-85 percent in the latter portion of the post-transition region (Hillner 1980).

The addition of hydrogen to the system, for example, as a product of the uranium oxidation reaction, could be expected to increase the absorption of corrosion-product hydrogen, by slowing its diffusion away from the metal surface (Thomas and Forscher 1956). As long as the impervious zirconium oxide layer is stable, the maximum amount of hydrogen absorbed by zirconium would be equal to the amount generated from the oxidation of zirconium. This oxide layer is stable to about 600°C, so no significant absorption of hydrogen is expected to occur as a result of the oxidation of uranium fuel.

Many studies have been done on the hydriding of Zircaloy and zirconium, and it is apparent that hydrogen may be redistributed by temperature or stress gradients. It is unlikely, though, that the extent of redistribution is such that a distinct hydride layer of significant thickness will form on Zircaloy cladding under the conditions encountered in reactor or in storage. Thus, it is unlikely that zirconium hydrides are responsible for fires encountered in hull bins or in dissolvers.

In contrast to the behavior observed with zirconium, the hydriding of uranium is not inhibited by the presence of a protective oxide film, and proceeds much more rapidly. Upon exposure to water, uranium hydrides form and are destroyed by the following reactions:

1. $U + 2 H_2O = UO_2 + 2 H_2$
2. $2 U + 3 H_2 = 2 UH_3$
3. $4 H_2O + 2 UH_3 = 2 UO_2 + 7 H_2$

When hydrogen is formed upon exposure of uranium to water, it reacts readily with uranium to form uranium hydride. This hydride collects in the ruptured fuel element and causes swelling and possibly rupturing of the cladding. If the cladding ruptures and the hydride is exposed to water, reaction 3 above causes liberation of hydrogen, but poses no other safety hazard. However, the finely divided UO_2 (and the unreacted UH_3) would be expected to react very rapidly with HNO_3 during the leaching operation and, if present in sufficient quantity, could contribute to initiating runaway uranium reactions as discussed in Section 7.

11.2 METALLOGRAPHIC STUDY OF HYDRIDES IN RUPTURED FUEL

A metallographic study was conducted to determine the relative amounts of uranium and zirconium hydrides (and of uranium-zirconium intermetallics) in a ruptured fuel element. This examination was done on the ruptured inner fuel element shown in Figure 11.1. The end cap of this element was missing, and several cracks in the cladding were observed. The uranium fuel was not present in several inches near the end cap, where it had been oxidized by exposure to water.

Severe swelling of the cladding was apparent, and the cladding was cracked in several places due to internal pressurization from uranium oxidation.

Micrographs of the inner fuel element cladding at a location adjacent to the failed cladding are shown in Figure 11.2. In Figure 11.2a, cracks in the cladding are shown at the Zircaloy-fuel interface. Figure 11.2 (b, c, and d) show a cross-section of the cladding. The hydrogen content of this cladding is estimated, by comparison with micrographs of specimens having known hydrogen contents (Hartcorn and Westerman 1963), to be approximately 400 ppm

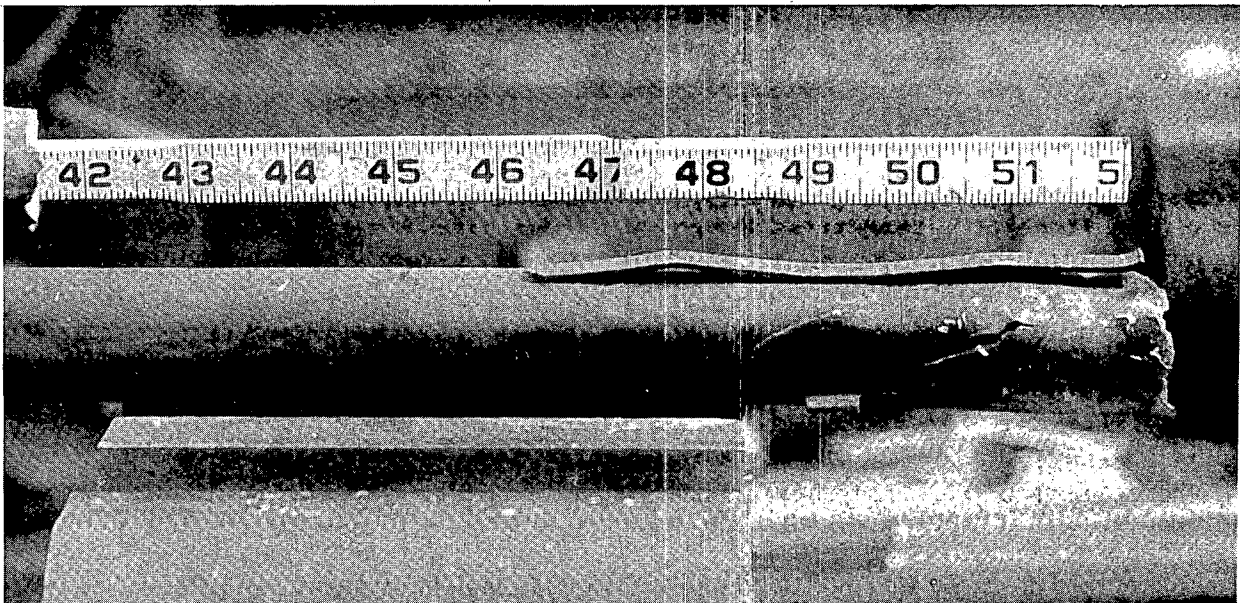
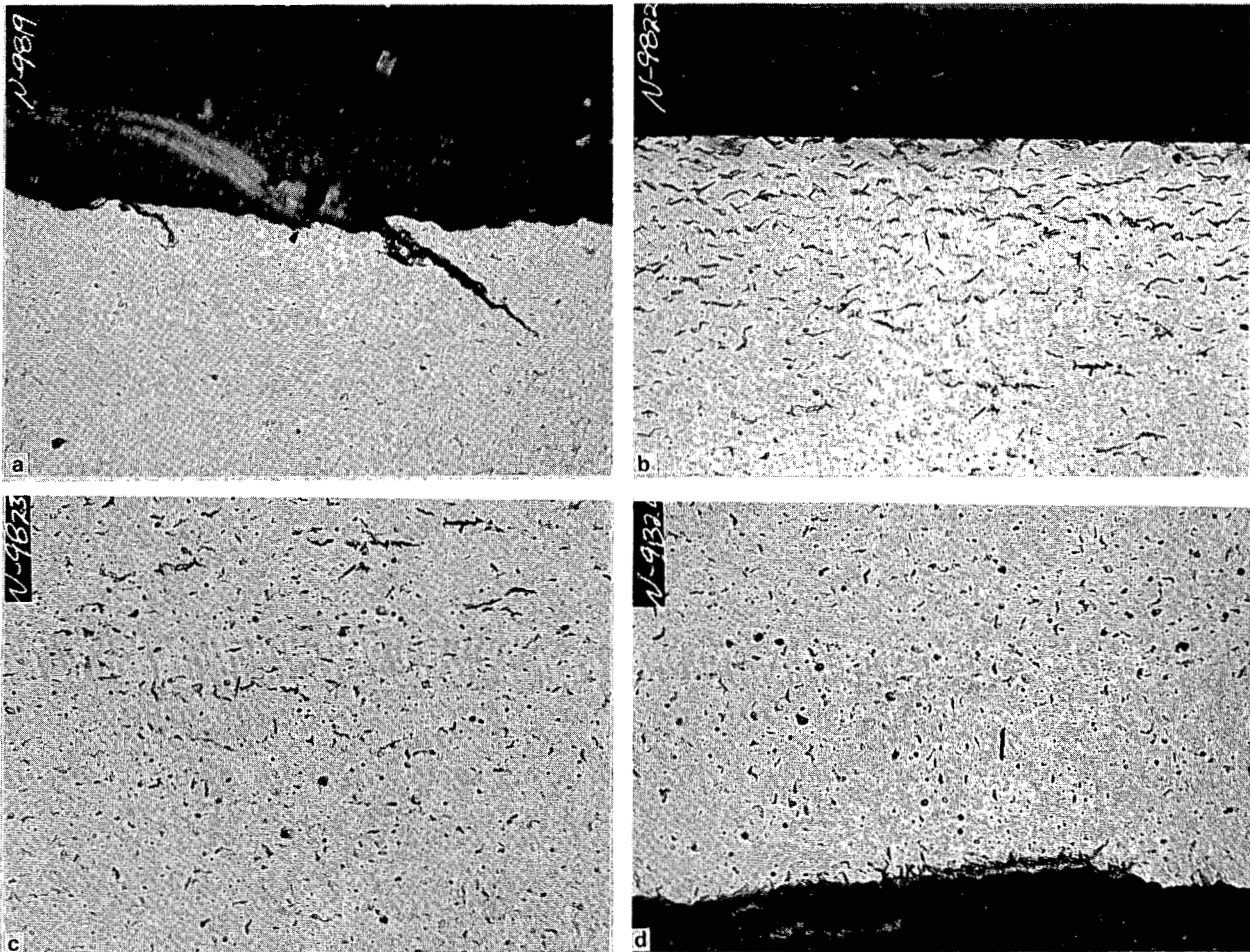


FIGURE 11.1. Side View of Ruptured Inner Element



~150x

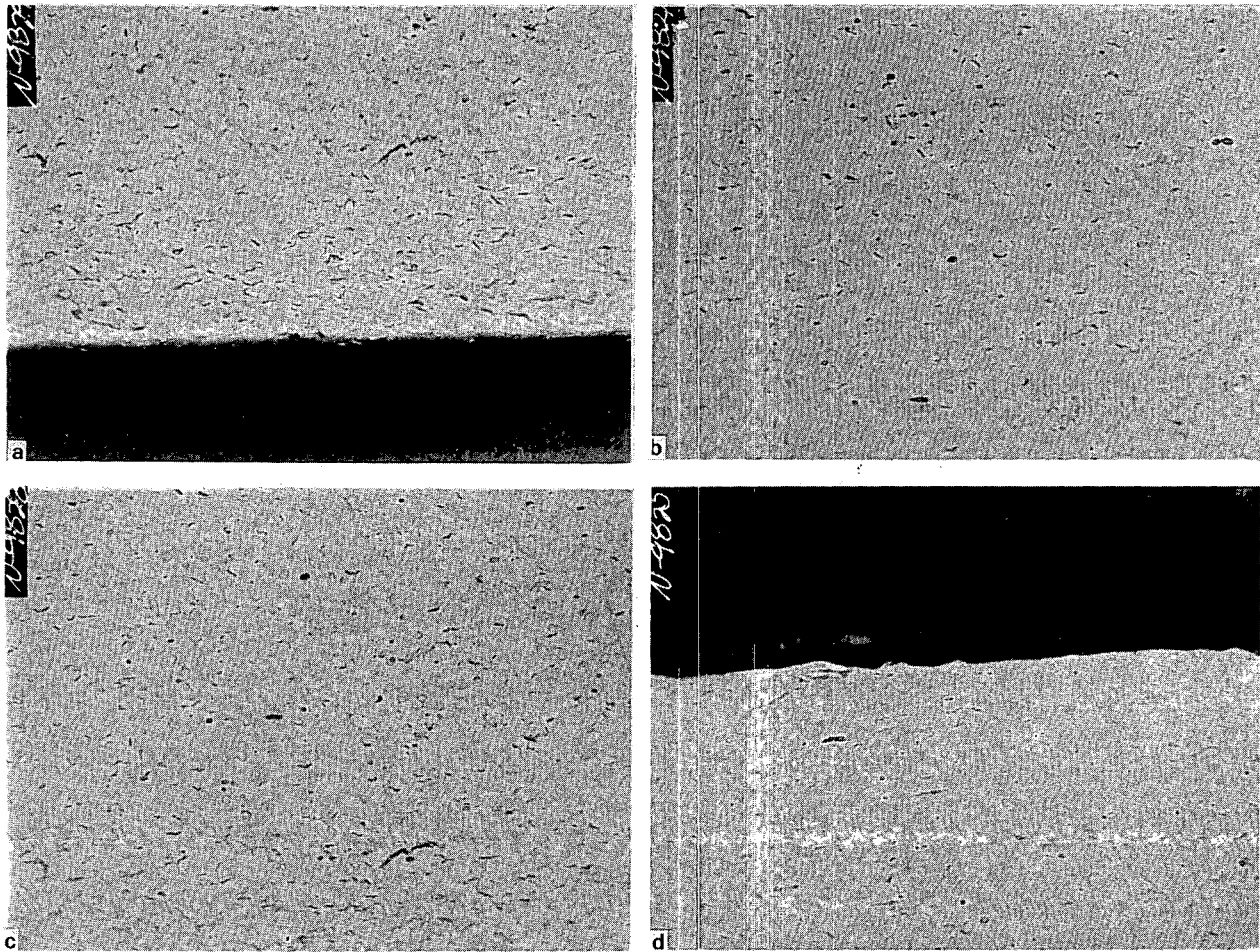
FIGURE 11.2. Micrographs of Fuel Element Adjacent to Failed Cladding

- a. Cracking of cladding at cladding fuel interface.
- b. Outer edge of inner fuel element cladding.
- c. Center of outer cladding.
- d. Inner section of outer cladding.

at the surface exposed to cooling water (Figure 11.2b), and less than 100 ppm in the center of the cladding and at the cladding-fuel interface. The micrographs shown in Figure 11.2 were taken near a breach in the cladding, and would be expected to contain a higher hydrogen concentration than the remainder of the cladding. It is evident from the observed levels of hydrogen

and the dispersed nature of the hydrides that these hydrides do not constitute a pyrophoricity problem.

Another cross-section of the cladding is shown in Figure 11.3. This cross-section was taken in an area away from any breaches, to estimate the overall hydrogen absorption in the cladding. The hydrogen content of this



~150x

FIGURE 11.3. Cross Section of Cladding in Non-Failed Area Showing Typical Hydride Distribution

- a. Cladding-water interface.
- b. Inner section of cladding.
- c. Inner section of cladding.
- d. Cladding-fuel interface.

cladding varies from approximately 200 ppm at the surface exposed to cooling water (Figure 11.3a) to considerably less than 100 ppm at the Zircaloy-fuel interface (Figure 11.3d).

The inner fuel element was examined at a cladding failure. The results of this examination are shown in Figure 11.4. Figure 11.4a shows the overall

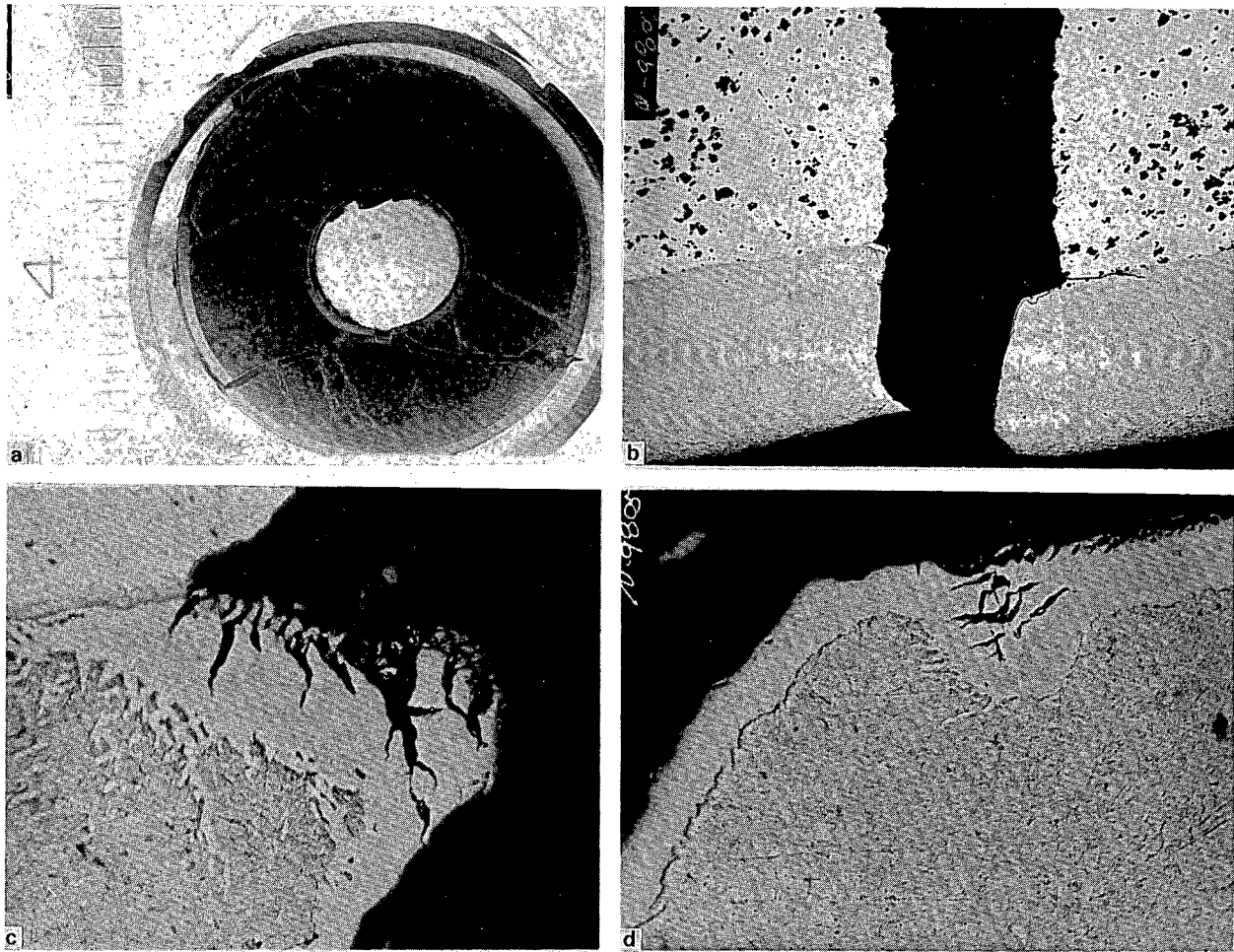


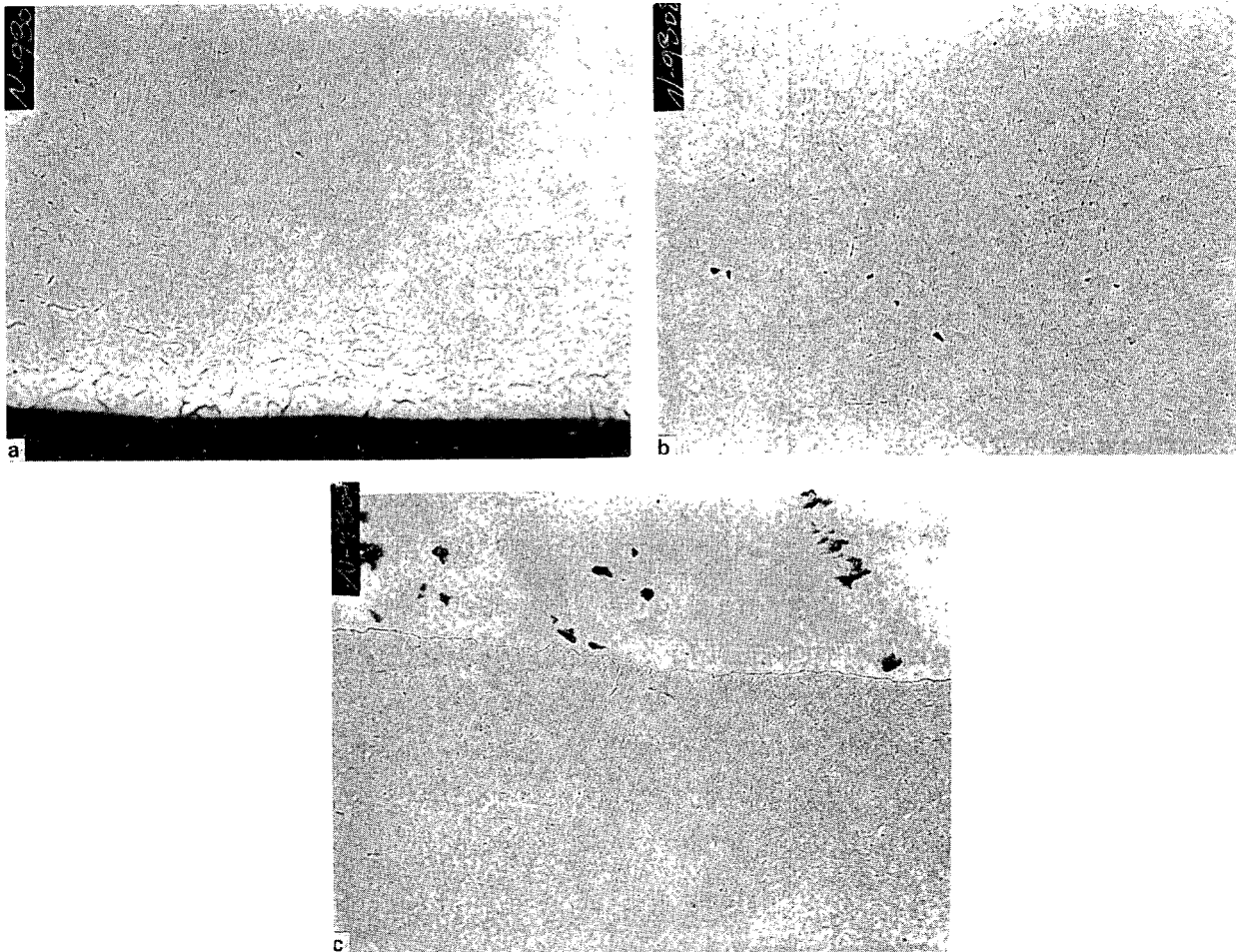
FIGURE 11.4. Micrographs of Outer Cladding at Cladding Failure

- a. Overall view of inner fuel element cross section. The outer ring is the metallographic mounting fixture.
- b. Crack in cladding, ~23x.
- c. Higher magnification of b., ~540x.
- d. Opposite side of crack from c., ~540x.

view of the inner fuel element cross-section. Cracks have occurred in both the cladding and the fuel. Distortion of the cladding is apparent, due to expansion of the fuel caused by oxide and hydride formation. The outer cladding-fuel interface is shown in Figure 11.4b. There is no evidence of hydride formation, except possibly in a small area at the fuel-cladding interface. However, this phase was examined in greater detail in Figures 11.4c and 11.4d, and was found to be zirconium oxide. Thus, no evidence of the existence of uranium hydride was found in this examination.

A thin uranium-zirconium diffusion zone can be seen in Figure 11.4b. Although this zone was too thin to be accurately measured, it is apparent that the epsilon phase was not present in sufficient quantity to cause a pyrophoricity problem, as was discussed in Section 9.

The outer cladding shown in Figure 11.4 was examined a short distance from a breach. The results of this examination are shown in Figure 11.5. Very little hydride formation was observed, except at the surface exposed to water. The hydrogen concentration near this surface was estimated to be approximately 200 ppm. The hydrogen is present in the form of dispersed hydrides, not as a distinct hydride zone.



~150x

FIGURE 11.5. Cross Section of Outer Cladding Near Cladding Failure

- a. Cladding-water interface.
- b. Inner portion of cladding.
- c. Cladding-fuel interface.

11.3 REFERENCES FOR SECTION 11.0

- Hartcorn, L. A., and R. E. Westerman. 1963. Quantitative Metallography of Hydride Phase in Zircaloy-2 Process Tubes. HW-74949, Hanford Atomic Products Operation, Richland, Washington.
- Hillner, E. 1980. Corrosion and Hydriding Performance Evaluation of Three Zircaloy-2 Clad Fuel Assemblies After Continuous Exposure in PWR Cores 1 and 2 at Shippingport, Pa. WAPD-TM-1412, Bettis Atomic Power Laboratory, Pittsburgh, Pennsylvania.
- Schulz, W. W. 1972. Shear-Leach Processing of N-Reactor Fuel--Cladding Fires. ARH-2351, Atlantic Richfield Hanford Company, Richland, Washington.
- Thomas, D. E., and F. Forscher. 1956. "Properties of Zircaloy-2." Journal of Metals 8.
- Wheeler, R. G. 1956. Quarterly Progress Report, Fuels Development Operation, July, August, September. HW-46091, Hanford Atomic Products Operation, Richland, Washington.

12.0 ACKNOWLEDGMENTS

The progress of this work benefitted greatly from the cooperation received from many people, spread over most of the contractors at the Hanford site. The work was funded by Rockwell Hanford Operations (RHO) as part of their Process Facility Modifications (PFM) activities for the Department of Energy. Special thanks are given to E. D. Waters, the principal RHO contact, for his cooperation and understanding as well as for his technical abilities. Other RHO people who participated in the development and execution of this project were R. M. Orme, A. L. Pajunen, J. D. Ludowise, and K. M. Hodgson. Our thanks to them as well.

Among the UNC Nuclear Industries people who were of special assistance were: W. D. Wittekind and G. A. Wolf for information regarding and assistance in obtaining the irradiated fuel; R. T. Johnson and J. W. Sharp for discussions regarding, and preparation of, the specimens of unirradiated fuel; and E. A. Weakley for discussions regarding current and past N-Reactor fuel fabrication procedures and materials.

Hanford Engineering Development Laboratory personnel contributed in the areas of irradiated fuel sample preparation and microprobe analysis and of chemical analysis. J. M. Lott and D. J. DesChane directed the irradiated fuel sectioning and specimen preparation activities. E. D. Jenson performed the electron microprobe analyses. A. C. Leaf performed many of the radiochemical analyses and M. C. Burt performed most of the acid analyses.

Pacific Northwest Laboratory contributors in addition to the authors included G. M. Richardson and A. D. Peoples, who performed most of the experimental work; C. O. Harvey, who performed most of the pulsed laser fluorimetric uranium analyses; J. E. Coleman, who performed the scanning electron microscopy analyses; D. H. Parks, who performed the optical microscopy on the unirradiated fuel; L. D. Maki and K. M. McCormack, who typed the report; and N. M. Sherer, who provided editorial assistance.

Special thanks are given to J. P. Duckworth, now of Westinghouse Idaho Nuclear Company but formerly of Nuclear Fuels Services (NFS) Company, for several informative discussions regarding equipment design, operating practices, and results at NFS.

DISTRIBUTION

No. of
Copies

No. of
Copies

OFFSITE

30 DOE Technical Information Center

J. P. Duckworth
WINCO
P.O. Box 4000
Idaho Falls, ID 83403

C. W. Forsberg
Oak Ridge National
Laboratory
P.O. Box X
Oak Ridge, TN 37831

ONSITE

2 DOE Richland Operations Office

J. D. Furubotten (2)

20 Rockwell Hanford Company

W. C. Alaconis
D. E. Ball
W. R. Dworzak
D. G. Harlow
E. W. Harris
J. P. Hinkley
K. M. Hodgson
J. O. Honeyman
E. J. Kosiancic
D. L. Lamberd
J. D. Ludowise
R. M. Orme
A. L. Pajunen
K. E. Plummer
R. C. Roal
W. W. Schulz
H. Spanheimer
J. A. Swenson
R. E. Van der Cook
E. D. Waters

4 UNC United Nuclear Industries

R. T. Johnson
E. A. Weakley
W. P. Wittekind
G. A. Wolf

2 Westinghouse Hanford Company

R. J. Cash
R. G. Cowan

50 Pacific Northwest Laboratory

L. A. Bray
W. F. Bonner
T. D. Chikalla
V. F. Fitzpatrick
M. D. Freshley
J. H. Haberman
A. B. Johnson
R. S. Kemper
H. E. Kjarmo
D. E. Knowlton
J. M. Latkovich
R. C. Liikala
C. L. Matsuzaki
L. G. Morgan/D. J. Bradley
J. M. Nielsen
R. E. Nightingale
A. D. Peoples
S. G. Pitman
G. M. Richardson
J. L. Ryan
J. L. Swanson (20)
C. L. Timmerman
R. E. Westerman
E. J. Wheelwright
Technical Information (5)
Publishing Coordination (2)